Langmuir probe and corpuscular plasma diagnostic

Milan Tichý, CU in Prague, FMP

The data used in presentation originated from cooperation of CU in Prague, FMP, EMA Universität Greifswald, Germany and University of South Bohemia in České Budějovice

The work is part of the research program MSM 0021620834, which is financed by MŠMT ČR

Overview-probes

- Basics of probe diagnostic, regimes of operation of Langmuir probe.
- Druyvesteyn method for estimation of EEDF in plasma.
- Space and time resolution of probe.
- Particularities of probe diagnostic of plasmas generated by RF energy.
- Special probes.
- Double and triple probe method.
- Probes in high-temperature plasma.

Overview – mass-spectrometry

- Principles of mass-spectrometers.
- Detectors for mass-spectrometers.
- Application of mass-spectrometry for diagnostic of low-temperature plasmas.
- Mass-spectra interpretation, examples, methods PTR-MS and EA-MS.
- Conclusions.

Basics of probe diagnostic

Probe shapes and manufacturing

Material: W, Ni, Pt
Isolated holder: glass, ceramics (Degussit ®)

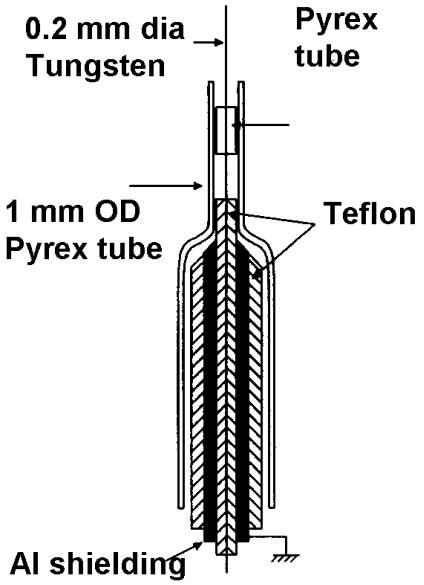

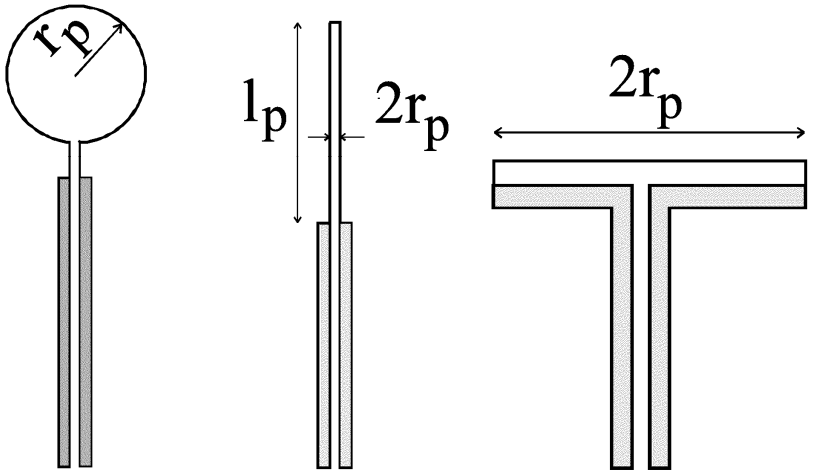

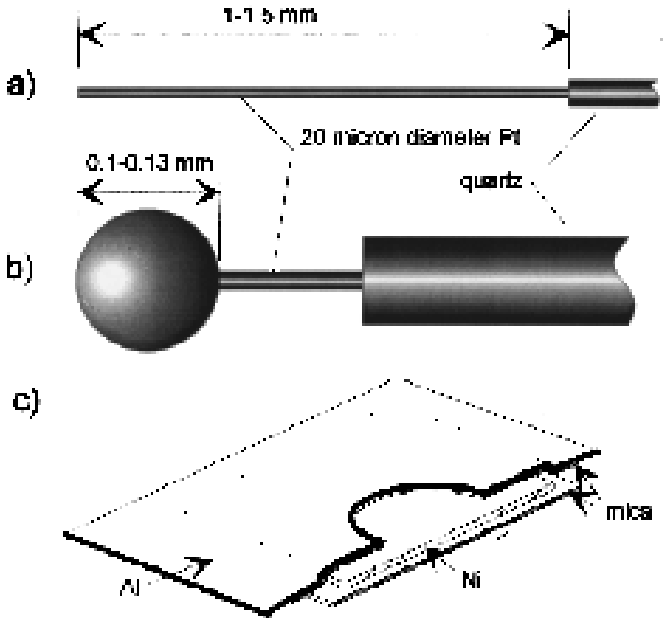

Basics of probe diagnostic

Probe circuit

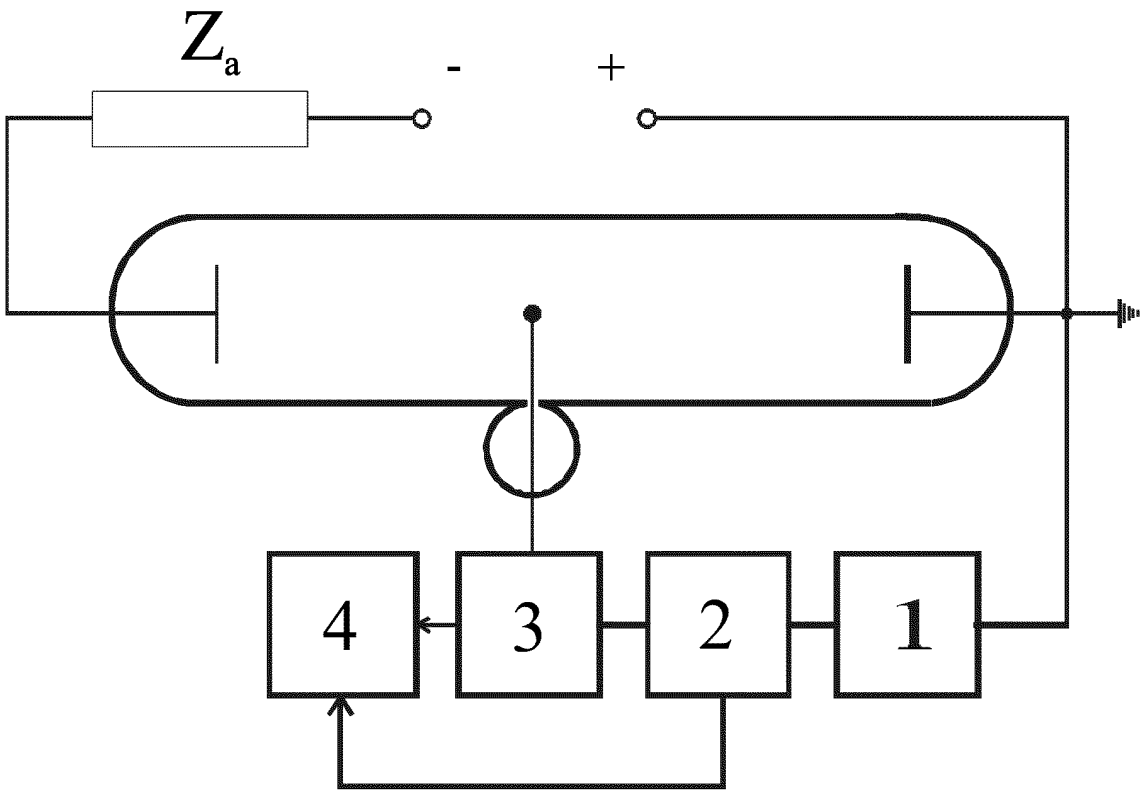

1 – dc bias

2 - generator of sawtooth (staircase) bias voltage

3 – current-voltage converter

4 –I_p-U_p data acquisition (computer)

Basics of probe diagnostic

Probe circuit with analog isolation amplifiers

T. Bindemann, M. Tichý, J.F. Behnke, H. Deutsch,
Rev. Sci. Instr. 69(1998)2037

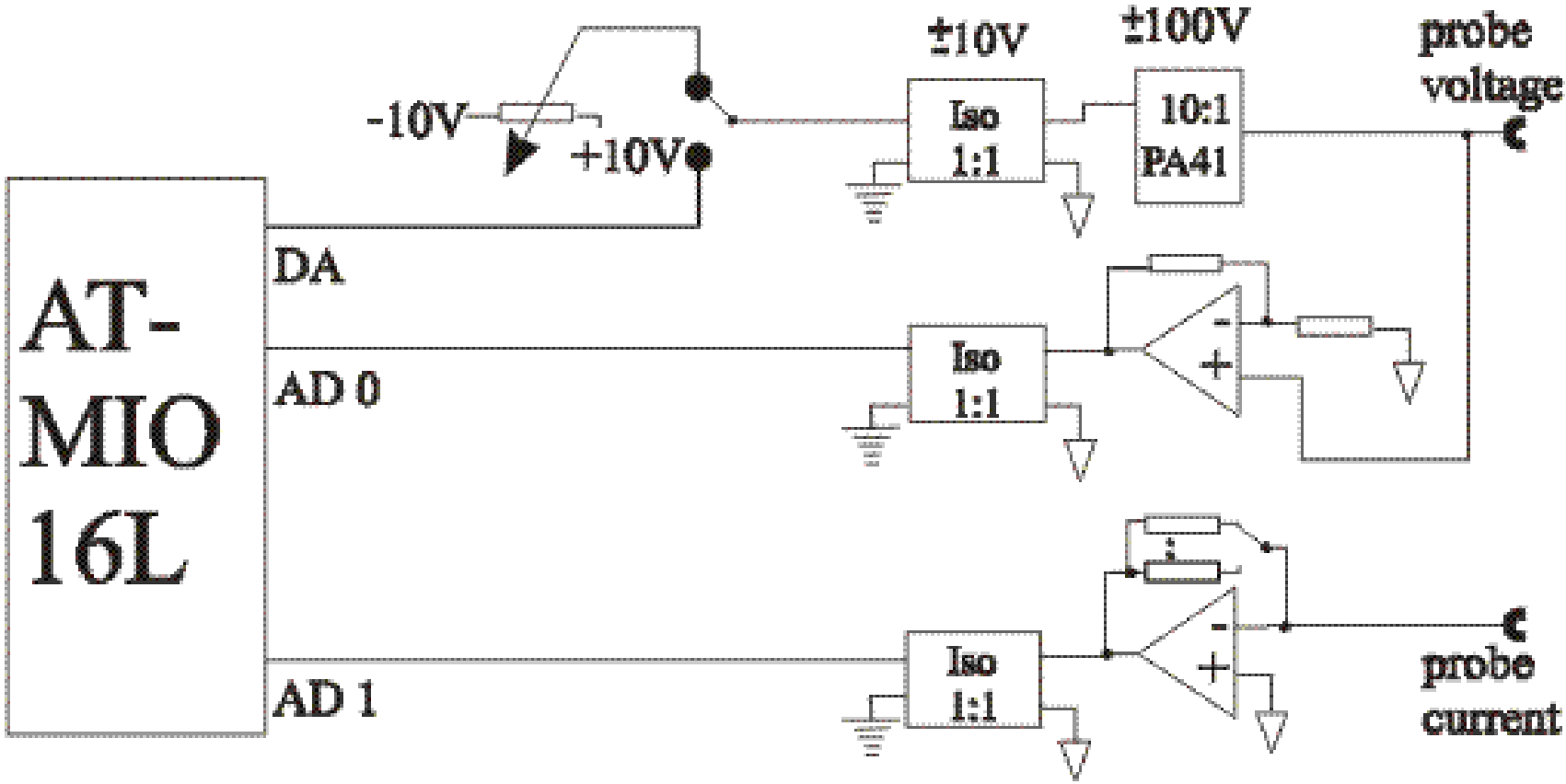

Basics of probe diagnostic

Probe circuit with isolated digital control

P. Špatenka, R. Studený, H. Suhr, Meas. Sci. Technol. 3(1992)704

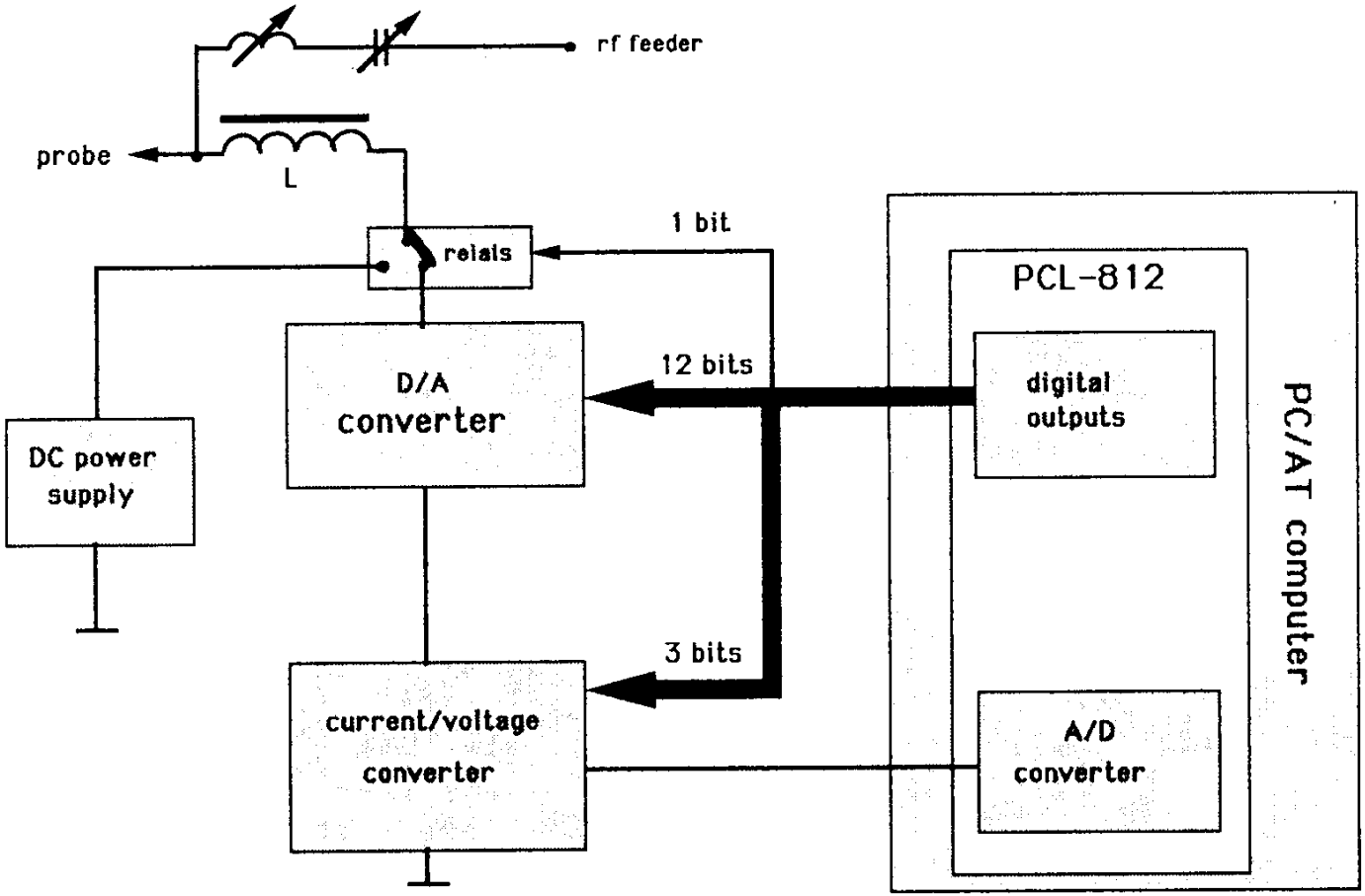

Basics of probe diagnostic

Example of probe characteristic

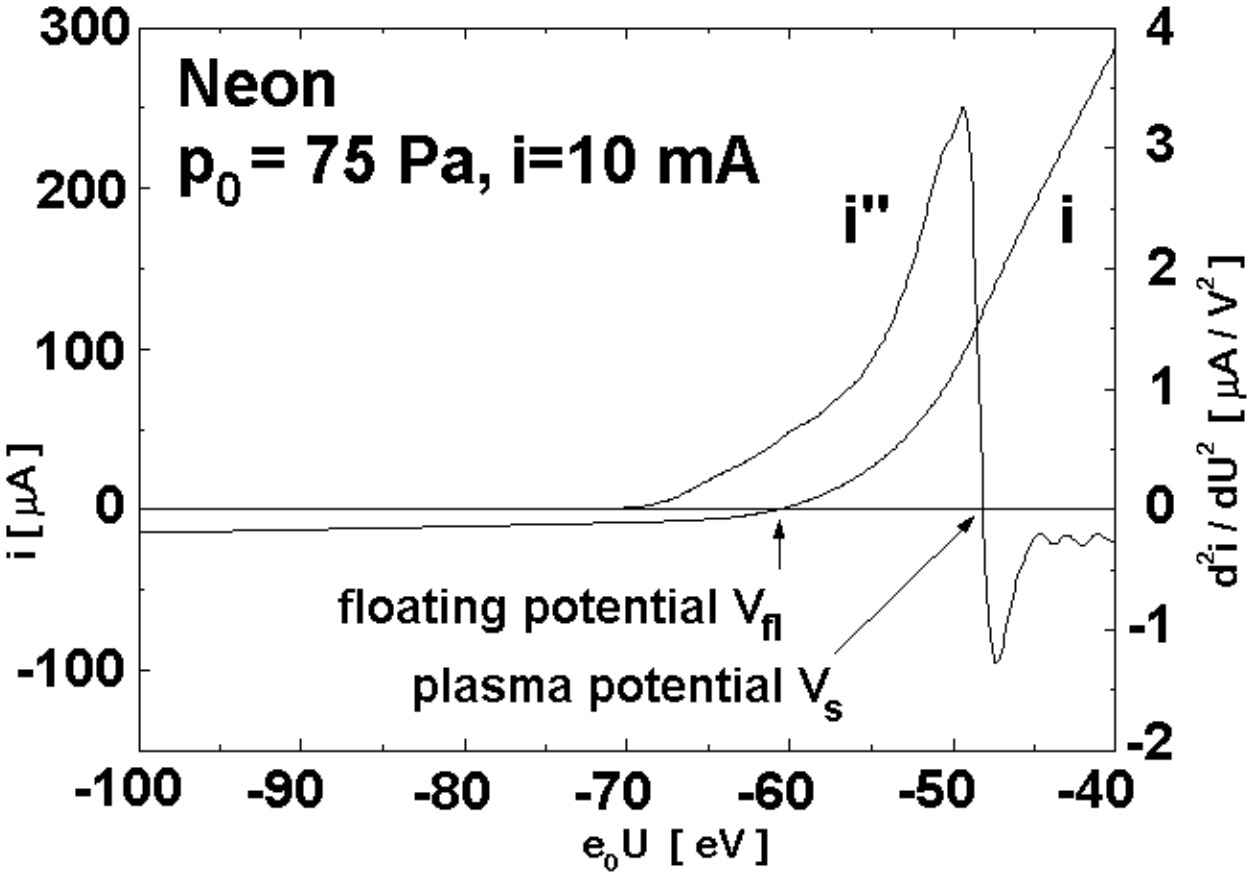

I. $U_p < 2U_{fl}$
$|i_i / i_e| >> 1$
Positive ion accelerating region

II. $2U_{fl} \leq U_p \leq 0$
$|i_i / i_e| <> 1$
Transition region

III. $0 \leq U_p$
$|i_i / i_e| << 1$
Electron accelerating region

Collection of particles by probe

We consider an element of the area of the wall of a chamber (or of a plane plasma probe, which can only collect particles from one side), in which there is gas or plasma of a density n. Perpendicular to this unit area there is the axis of a spherical coordinate system with the usual coordinates r, ϑ and φ, where $\vartheta = 0$ is exactly on the axis. The particle flux from the entire half-space in front of this unit area is given by :

$$\Gamma(\boldsymbol{r}) = \int v f(\boldsymbol{r}, \boldsymbol{v}) \mathrm{d}^3 v, \qquad (1.1)$$

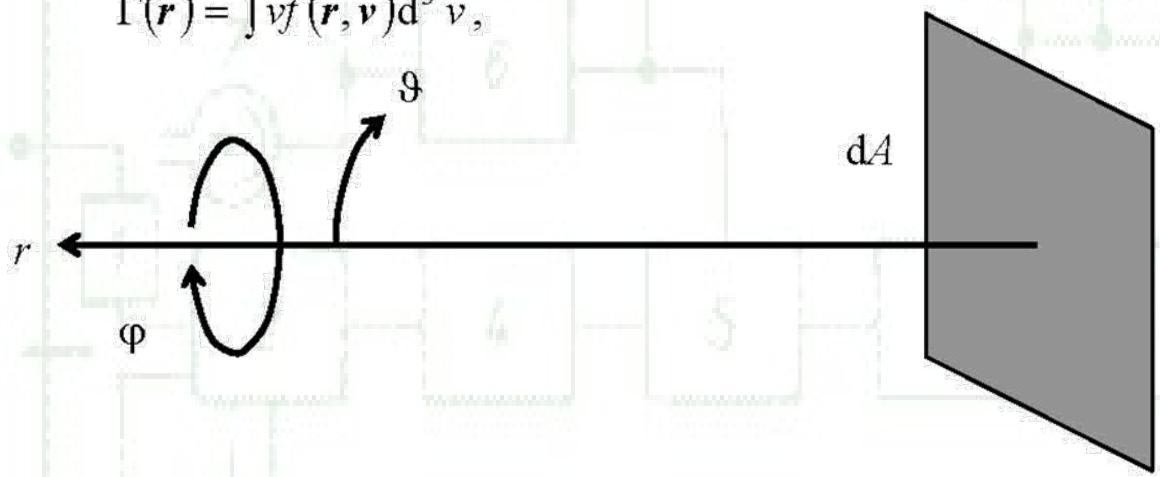

$\boldsymbol{v}$ is the respective particle velocity, $f(\boldsymbol{r},\boldsymbol{v})$ is the respective velocity distribution function (VDF) of the particles and $\mathrm{d}^3 v$ is the unit volume in the velocity space. Assuming a Maxwellian VDF, $f(\boldsymbol{r},\boldsymbol{v})$ is given by:

Collection of particles by probe

$$f(\boldsymbol{r},\boldsymbol{v}) = n(\boldsymbol{r})\left(\frac{m}{2\pi k_B T}\right)^{\frac{3}{2}} \exp\left(-\frac{m\boldsymbol{v}^2}{2k_B T}\right). \tag{1.2}$$

Here m is the mass of the particle and T the absolute temperature of the gas or of the plasma. k_B is of course the Boltzmann constant. We remember that VDF is that of the magnitude of the velocity. Therefore, from the entire particle density $n(\boldsymbol{r})$ we may take only one half, i.e., $n(\boldsymbol{r})/2$, since $n(\boldsymbol{r})$ comprises all particles, whereas a single-sided unit area "see" only particles, which have a velocity component *towards* the area. Taking this into account, we obtain from Eq. (1.1):

$$\Gamma(\boldsymbol{r}) = \frac{n(\boldsymbol{r})}{2}\left(\frac{m}{2\pi k_B T}\right)^{\frac{3}{2}} \int v \exp\left(-\frac{m\boldsymbol{v}^2}{2k_B T}\right) \mathrm{d}^3 v\,, \tag{1.3}$$

where $\mathrm{d}^3 v$ can be transformed with the help of the differential unit solid angle in spherical coordinates $\mathrm{d}^2\Omega = \sin\vartheta\ \mathrm{d}\vartheta\ \mathrm{d}\varphi$:

$$\mathrm{d}^3 v = v^2\ \mathrm{d}v\ \mathrm{d}^2\Omega = v^2\ \mathrm{d}v \sin\vartheta\ \mathrm{d}\vartheta\ \mathrm{d}\varphi. \tag{1.4}$$

Collection of particles by probe

Taking into account the correct limits of integration, Eq. (1.3) becomes:

$$\Gamma(\boldsymbol{r}) = \frac{n(\boldsymbol{r})}{2}\left(\frac{m}{2\pi k_B T}\right)^{\frac{3}{2}} \int_0^{\infty} v^3 \exp\left(-\frac{mv^2}{2k_B T}\right) \mathrm{d}v \int_0^{2\pi} \mathrm{d}\varphi \int_0^{\pi/2} \sin\vartheta \,\mathrm{d}\vartheta\,, \tag{1.5}$$

$= 2\pi$ $= 1$

This leads to:

$$\Gamma(\boldsymbol{r}) = \pi n(\boldsymbol{r})\left(\frac{m}{2\pi k_B T}\right)^{\frac{3}{2}} \int_0^{\infty} v^3 \exp\left(-\frac{mv^2}{2k_B T}\right) \mathrm{d}v = \tag{1.6}$$

$$= \pi n(\boldsymbol{r})\left(\frac{m}{2\pi k_B T}\right)^{\frac{3}{2}} \frac{1}{2}\left(\frac{2k_B T}{m}\right)^2$$

By resolving the terms in the brackets, the above already mentioned formula can eventually be derived:

$$\Gamma(\boldsymbol{r}) = \frac{n(\boldsymbol{r})\overline{v}}{4}, \tag{1.7}$$

Collection of particles by probe

$$\bar{v} = \sqrt{\frac{8k_B T}{\pi m}} \tag{1.8}$$

is the mean value of the particle velocity, which is well known from statistical physics.

Once again we emphasise that Eq. (1.7) is valid only for the particle flux towards a *one-sided* unit area from a *three-dimensional* gas or plasma (i.e., a medium with three degrees of freedom) and that $\bar{v}$ is the corresponding mean velocity.

For a plasma and by multiplying this particle flux with the electric charge transported, we obtain the current density $j_{i,e}$ of the electrons or ions towards this unit area:

$$j_{i,e} = \pm \frac{q_0 n_{i,e} \bar{v}_{i,e}}{4}, \tag{1.9}$$

where $\bar{v}_{i,e}$ is the respective mean velocity of the ions and electrons. As we will see, especially the mean velocity of the ions is not always given by Eq. (1.8), but we have to take into account the actual conditions of every situation and every configuration, to be able to calculate the real mean velocity of the particles.

Working regimes of Langmuir probe

$$\lambda_D = \sqrt{\frac{\varepsilon_0 k_B T_e}{q_0^2 n_e}}$$

Parameters:

- *Characteristic probe dimension r_p,*
- *Mean free path for ions, electrons, λ_i, λ_e,*
- *Debye shielding length λ_D,*
- *Degree of plasma anisothermicity $\tau = T_e / T_i$.*

The thickness of the probe sheath is of the order of several λ_D's. We distinguish the following working regimes:

1. $\lambda_{i,e} >> r_p >> \lambda_D$ Collision-free movement of charge carriers in thin sheath (space charge limit).
2. $\lambda_{i,e} >> \lambda_D >> r_p$ Collision-free movement of charge carriers in thick sheath (orbital motion limit, OML).
3. $\lambda_D >> \lambda_{i,e} >> r_p$ Probe current is determined by collisions of charged and neutral particles in space-charge sheath around the probe.

Working regimes of Langmuir probe comment to the Debye length

The well-known formula is derived under several restrictions; most important is the assumption of frozen ions, i.e. $T_i \approx 0$:

$$\lambda_D = \sqrt{\frac{\varepsilon_0 k_B T_e}{q_0^2 n_e}}$$

Assuming that none of the ion/electron temperature is negligible (electrolytes) we arrive at the formula:

$$\lambda_D = \sqrt{\frac{\varepsilon_0 k_B}{q_0^2 n_e} \frac{T_i T_e}{T_i + T_e}}$$

Or, if both temperatures are the same:

$$\lambda_D = \sqrt{\frac{\varepsilon_0 k_B T_e}{2 q_0^2 n_e}}$$

This is not a mistake !!!

Working regimes of Langmuir probe

With reasonably thin probes in many technologically used low-pressure plasmas the following case applies:

- $\lambda_e >> \lambda_D >> r_p$ Collision-free movement of charge carriers in thick sheath (orbital motion limit, OML).

Note just λ_e in the expression. It is obvious that $\lambda_e >> \lambda_i$.

Hence at such conditions and at very low pressures holds the relation $\lambda_{i,e} >> \lambda_D$, in so-called „transition“ region of pressures $\lambda_e > \lambda_D >\approx \lambda_i$. I.e. ions incur collisions while electrons may be assumed collisionless. Moreover, in high-density plasmas it is impossible to drive the probe up to the plasma potential in order to determine the electron density and it is therefore desirable to get that information from the ion current part of the probe characteristic. Therefore a great effort has been devoted to the theoretical description of the positive ion collection by a Langmuir probe.

Determination of electron temperature and density from probe data

Mott-Smith, H.M., Langmuir I., *Phys. Rev.* **28** (1926) 727

retarding regime

$$i_e = J_e \exp(-|\eta|)$$

$$i_i = J_i \exp(-\tau\eta)$$

accelerating regime

$$i_e \cong J_e \frac{2}{\sqrt{\pi}} \sqrt{\eta}$$

$$i_i \cong J_i \frac{2}{\sqrt{\pi}} \sqrt{\tau|\eta|}$$

$$J_{i,e} = \frac{1}{4} q_0 A_p n_{i,e} \sqrt{\frac{8 k_B T_{i,e}}{\pi m_{i,e}}}$$

$$\eta = \frac{q_0 (U_p - V_{pl})}{k_B T_e}$$

Electron temperature

$$T_e = -\frac{q_0}{k_B} \frac{d}{dU_p} \ln(|i_e|)$$

$i_i = i_{i0}(1+\eta)^{\kappa}$

B. Nuhn, G. Peter, Proc. XIII. ICPIG Berlin (1977), p. 999.

Determination of electron temperature and density from probe data

When determining the electron temperature we have to keep in mind that we measure the SUM of electron and positive ion currents. While for the determination of T_e we need the slope of the semilogarithmic plot of i_e only.

The original procedure how to eliminate i_i consists in linear extrapolation of i_i using the „saturated“ part of the probe characteristic back to plasma potential. However, except in the case of spherical probe we do no have theoretical basis for linear extrapolation. For the double-logarithmic approximation using the Nuhn and Peter formula we need to know the T_e since the formula uses probe potential normalized to T_e (and, in addition, knowledge of the plasma potential is also necessary).

The way out offers the use of second derivative of the probe characteristics with respect to the probe potential; if it is possible to obtain it either directly by measurement or off-line using numerical differentiation. Since the derivative of an exponential function is again exponential function, the slope in semilogarithmic scale of the second derivative yields immediately the electron temperature.

Determination of electron temperature and density from probe data

Assuming the Maxwellian EEDF we have for the determination of electron density two possibilities:

1) the obvious one is making use of the electron probe current at plasma potential i_{e0}:

Since $i_e = J_e \exp\left(-|\eta|\right)$ with $J_{i,e} = \frac{1}{4} q_0 A_p n_{i,e} \sqrt{\frac{8 k_B T_{i,e}}{\pi m_{i,e}}}$ at

plasma potential holds $i_{e,0} = J_{e,0} = \frac{1}{4} q_0 A_p n_e \sqrt{\frac{8 k_B T_{i,e}}{\pi m_{i,e}}}$ from which the n_e is easily calculated.

Determination of electron temperature and density from probe data

2) Provided that we are able to measure in the electron accelerating region (typically in the afterglow plasma, but also in lower density active plasma) and that the OML model for electrons holds, we can estimate the n_e from so-called i^2 vs V plot. Since in this region $i_e \cong J_e \frac{2}{\sqrt{\pi}} \sqrt{\eta}$ we arrive at the following expression for i_e^2:

$$i_e^2 = 2 \frac{q_0^3 A_p^2 n_e^2}{\pi^2 m_e} \left(U_p - V_{pl} \right)$$

The i^2 vs V plot is therefore linear and its slope yields the (squared) electron density. Note that in this method we need to estimate neither the electron temperature nor the plasma potential prior to this procedure. However, especially in dense plasmas we are unable to measure within enough voltage range into the electron accelerating region.

Langmuir probe in a homogeneous magnetic field

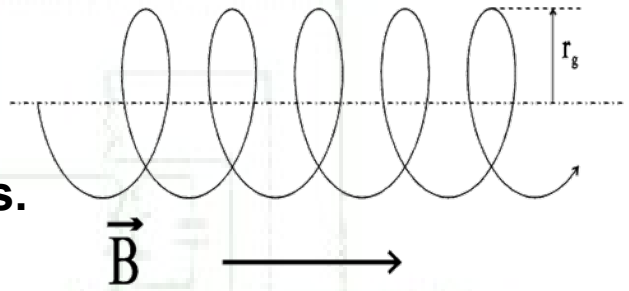

Magnetic field $\vec{B}$, Lorentz force $\vec{F} = e\left(\vec{v} \times \vec{B}\right)$

The charged particles move along helical trajectories.

$$r_g = \frac{m_p v}{e_p B} \qquad \bar{r_g} = \frac{1}{eB}\sqrt{\frac{\pi m_{e,i} k T_{e,i}}{2}}$$

Important ratio: $\beta = \dfrac{r_p}{\bar{r_g}}$.

Probe potential: V_p
Electron temperature: T_e
Electron current at the
Plasma potential V_s: I_{Vpl}
Boltzmann constant: k_B
Normalised probe voltage:

$$\eta_p = \frac{e(V_p - V_s)}{k_B T_e}$$

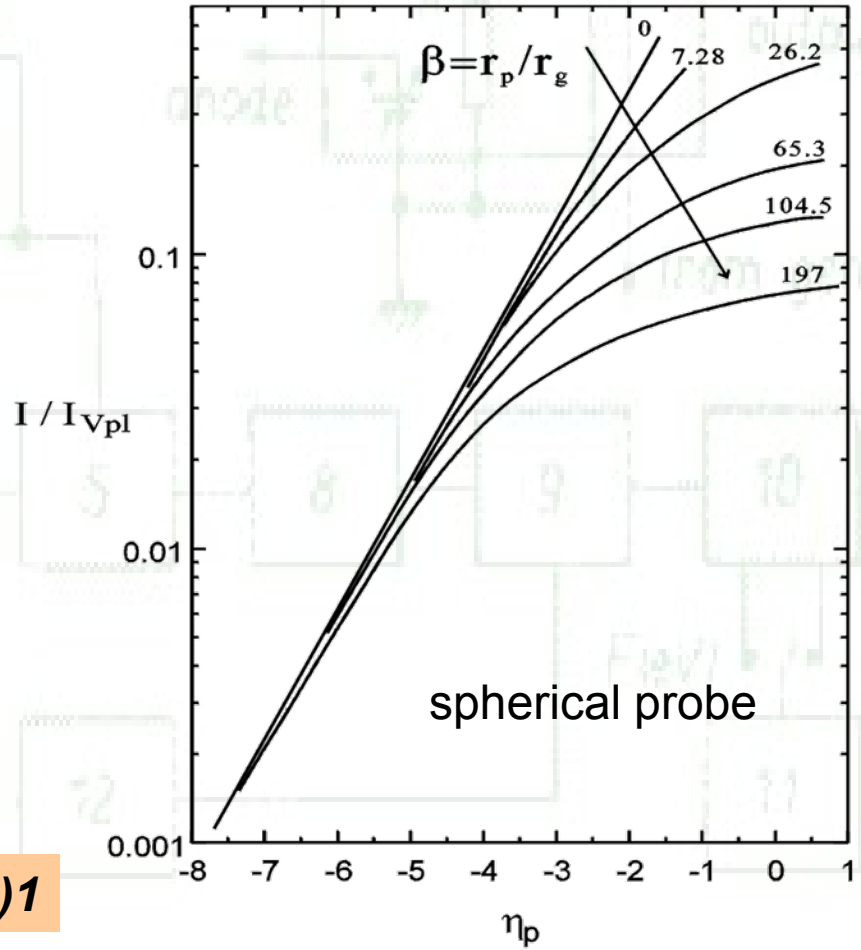

Sanmartin, J.R., Phys.Fluids 13(1970)1

Langmuir probe in a homogeneous magnetic field

Cylindrical probe; infinitely large λ_D

Important parameter: angle Θ between the probe axis and the vector of the magnetic field

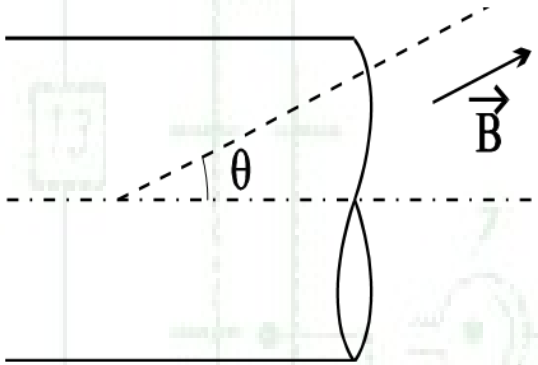

Consequence: Effect of magnetic field on the probe is **smallest** when the probe is oriented **perpendicular** to magnetic field.

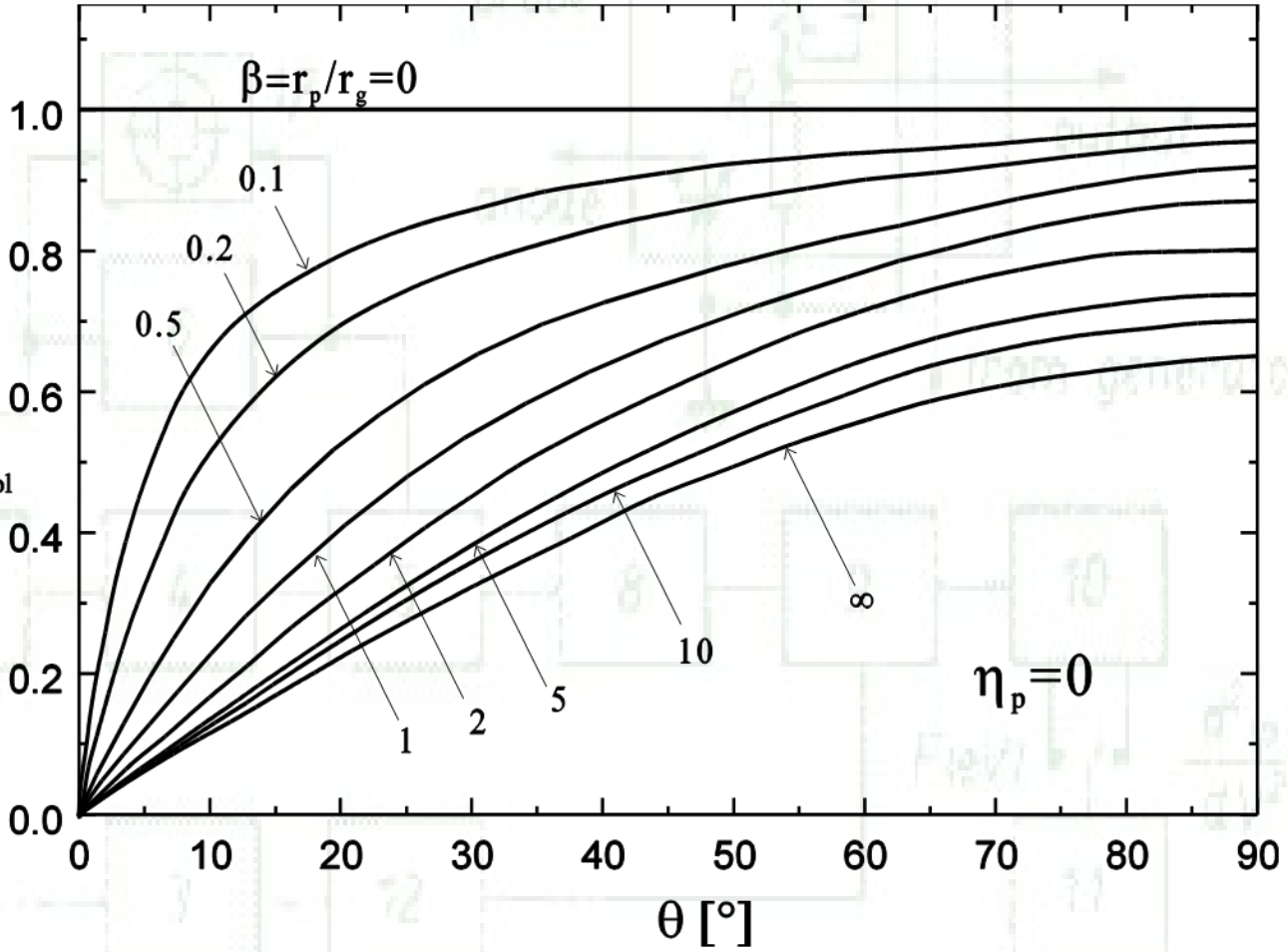

Laframboise, J.G., Rubinstein, J., Phys. Fluids 19(1976)1900

Druyvesteyn method for determination of EEDF in plasma

M.J. Druyvesteyn, *Z. Physik* **64**(1930)781

$$\int_0^\infty \bar{f}(u_p)\, u_p^{\frac{1}{2}} du_p = 1$$

$$n_e = \left(\frac{2}{q_0}\right)^{\frac{3}{2}} \frac{m_e^{\frac{1}{2}}}{A_p} \int_0^\infty U_p^{\frac{1}{2}} \frac{d^2 i_e}{dU_p^2} dU_p$$

$$q_0 u_m = \frac{q_0 \int_0^\infty U_p^{\frac{3}{2}} \frac{d^2 i_e}{dU_p^2} dU_p}{\int_0^\infty U_p^{\frac{1}{2}} \frac{d^2 i_e}{dU_p^2} dU_p}$$

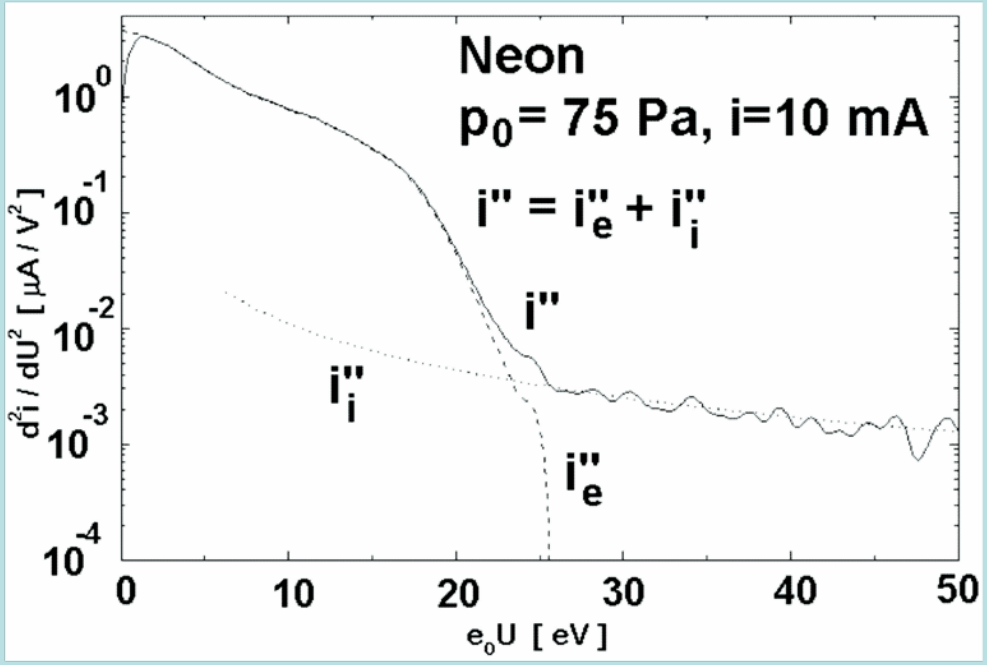

$$\frac{d^2 i_e}{dU_p^2} = \frac{q_0^{\frac{3}{2}}}{2^{\frac{3}{2}}} m_e^{-\frac{1}{2}} n_e A_p \bar{f}(u_p)$$

Druyvesteyn method for determination of EEDF in plasma

The second derivative necessary for the estimation of the EEDF can be either directly measured (on-line methods) or computed numerically from the experimental data (off-line methods).

Experimental set-ups for on-line measurement of the second derivative of the total probe current work on following principles:

- **use of the non-linearity of the probe characteristic, i.e. the relation between the „curvature“ of the characteristic and second harmonic generation [*G.R. Branner, E.M. Friar, G. Medicus, Rev. Sci. Instr. 34(1963)231*], mixing [*S.C.M. Luijendijk, J. Van Eck, Physica 36(1967)49*], detection of the modulated signal [*N.A. Vorobjeva, J.M. Kagan, V.M. Milenin, Zhurnal tekhnicheskoi fiziki (J.Tech.Phys. USSR) 34(1964)2079*] etc.,**
- **direct analog differentiators using operational amplifiers and sawtooth-like probe voltage [*V.A. Godyak, R.B. Piejak, B.M. Alexandrovich, Plasma Sources Sci. Technol. 1(1992)36*],**
- **analog difference amplifiers and stepwise-like probe voltage [*B. Saggau, Zeitschrift für angewandte Physik 32(1972)324*].**

Druyvesteyn method for determination of EEDF in plasma

The off-line differentiating methods are either based on algorithms of the numerical analysis or on direct numeric solution of the integral equation [*L.M. Volkova, A.M. Devyatov, G.A. Kralkina, N.N. Sedov, M.A. Sherif: Vestnik Mosk.Univ.(fizika, astronomija) 16(1957)502*]

or on the non-recursive digital filtering of a dependence given as a set of data [*M. Hannemann, INP-Report VII. Institute for Low-Temperature Plasma Physics, Greifswald, 1995, D. Trunec, Contrib. Plasma Phys. 32(1992)523, J.I. Fernández Palop, J. Ballesteros, V. Colomer, M.A. Hernández, Rev. Sci. Instr. 66(1995)4625*].

It is important to note that the Druyvesteyn formula includes second derivative of just electron current. To replace the electron by the total probe current is permissible only when the ion current can be approximated by linear relation. Since that is not always the case the residual influence of the second derivative of the ion current leads to lower dynamics of the estimated EEDF (2-3 orders of magnitude compared to 4 orders of magnitude when I_i“ is eliminated.

Druyvesteyn method for determination of EEDF in plasma

The most common procedure for differentiation of noisy experimental data is the „sliding polynomial approximation“. This represents approximation of the selected odd number $M=2m+1$ ($m=1,2,...$) adjacent data points around selected x_l by a second order polynomial $p(x)=a_0+a_1x+a_2x^2$ (for $x_l-m*h \le x \le x_l+m*h$). The second derivative at x_l is hence $y_l^{(2)}(x_0)=2a_2$

Since the coefficient a_2 is a weighted sum of the ordinates y_i (for $l-m \le i \le l+m$) this method may be regarded as the digital filtering where the weights are the filter coefficients $c_i / (h^2)$. Tables of such coefficients are given by Savitzky and Golay *[i] and formulae for the evaluation of these filter coefficients in [ii]. Computer programs that make use of this procedure have already been constructed and reported [iii].*

[i] A. Savitzky, M.J.E. Golay, *Anal. Chem.* **36**(1964)1627.
[ii] H. Madden, *Anal. Chem.* **50**(1978)1383.
[iii] M. Tichý, P. Kudrna, J.F. Behnke, C. Csambal, S. Klagge, *Journal de Physique IV France* **7**(1997)C4-397.

Druyvesteyn method for determination of EEDF in plasma

Generally, one has to be careful in the choice of the degree of smoothness in any of the methods mentioned above. Secondary maximums or local deficits on the EEDF due to elementary processes that create or require electrons at a certain range of energies that do come from the nature of the investigated plasma should not be suppressed. When in doubt whether a particular irregularity on the EEDF is due to the plasma processes or due to noise the best recommendation is to process one set of data with different kinds of differentiating methods and compare the results with theoretical expectations.

Also, practice has shown that in order to get EEDF's that are close to reality it is a better way to enhance the signal-to-noise ratio of the measured signal from the probe than to try to process numerically the data with a bad signal-to-noise ratio.

Space and time resolution of Langmuir probe method

- Space resolution of probe method is given by Debye length λ_D or by probe dimensions depending on what is greater. Measurements with space resolution require *movable* Langmuir probe position with respect to the discharge volume.
- Due to the necessity of space-charge sheath creation is the time resolution given approximately as $t_r \cong 2\pi / \omega_{pi}$, where ω_{pi} is the ion plasma frequency given by relation

For argon and $n_i \approx n_e = 10^{16}$ m^{-3} is $\omega_{pi} \approx 3{,}16$ MHz and $t_r \cong 2$ μs.

$$\omega_{pi} = \sqrt{\frac{q_0^2 n_i}{\varepsilon_0 m_i}}$$

Space-resolved probe method

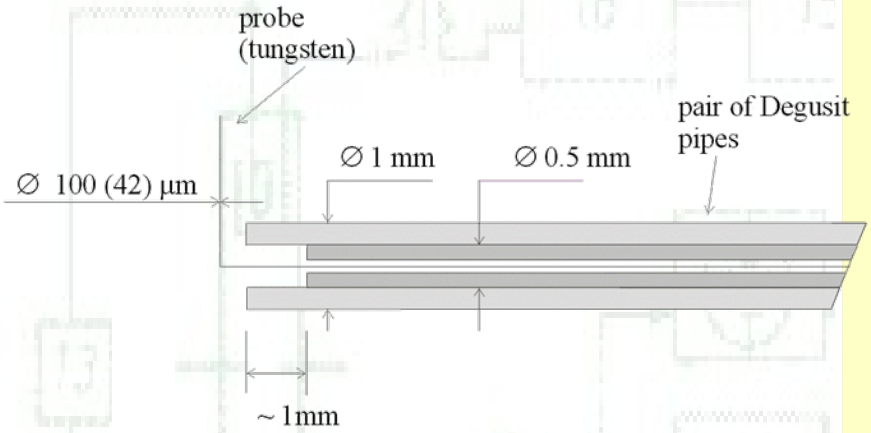

Example of the system for space-resolved probe measurements. The very thin probe is in magnetron radially driven by a manual/motorized vacuum feed-through with linear motion.

Passoth, E., Kudrna, P., Csambal, C., Behnke, J.F., Tichý, M., Helbig,V., J. Phys. D: Appl. Phys. 30(1997)1763-1777.

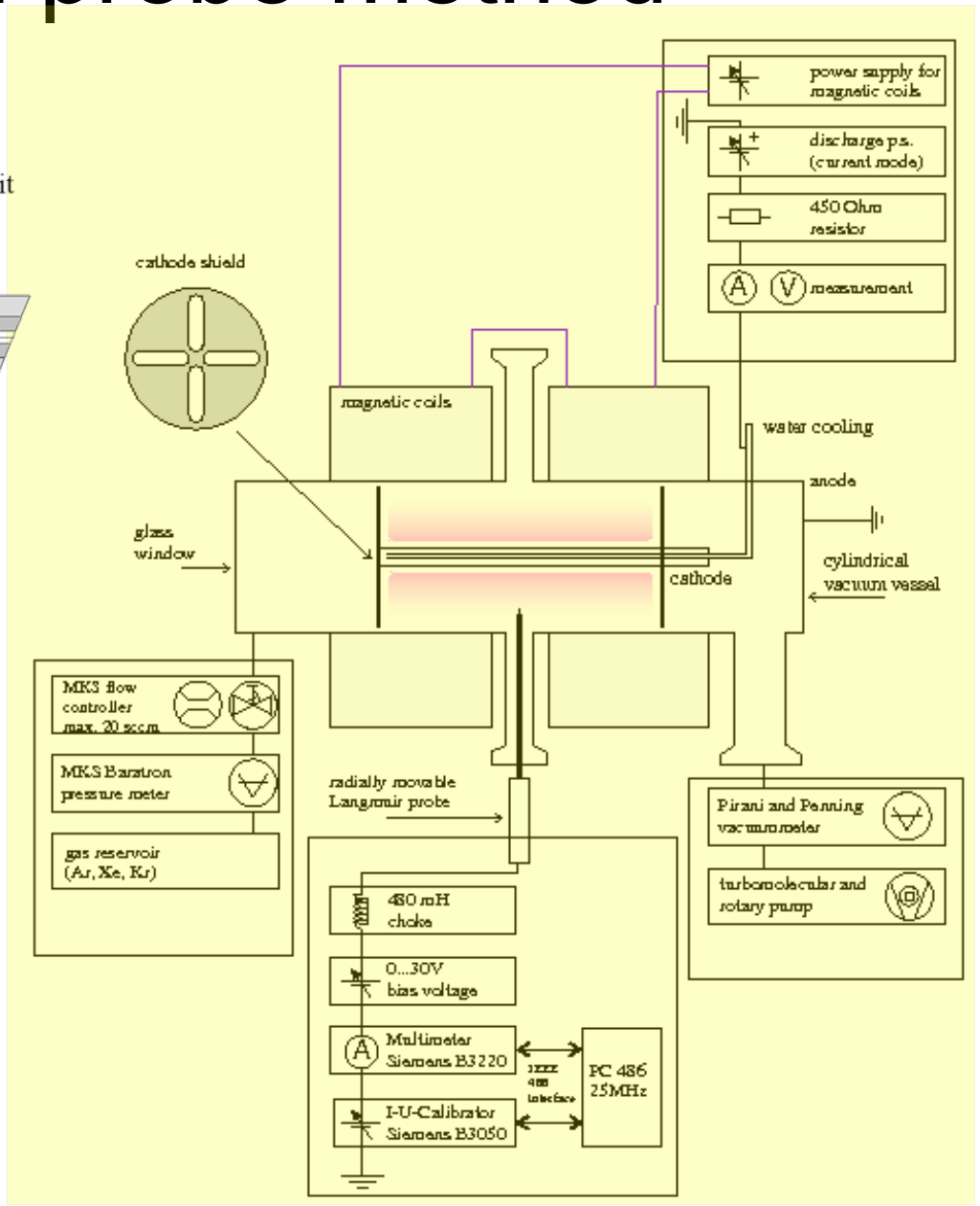

Space-resolved probe method

Measured EEDF‘s in dependence on the radial coordinate. With increasing distance from the cathode to the anode the EEDF changes shape from Maxwellian with higher electron temperature to „double temperature“ EEDF with very low temperature of the EEDF body.

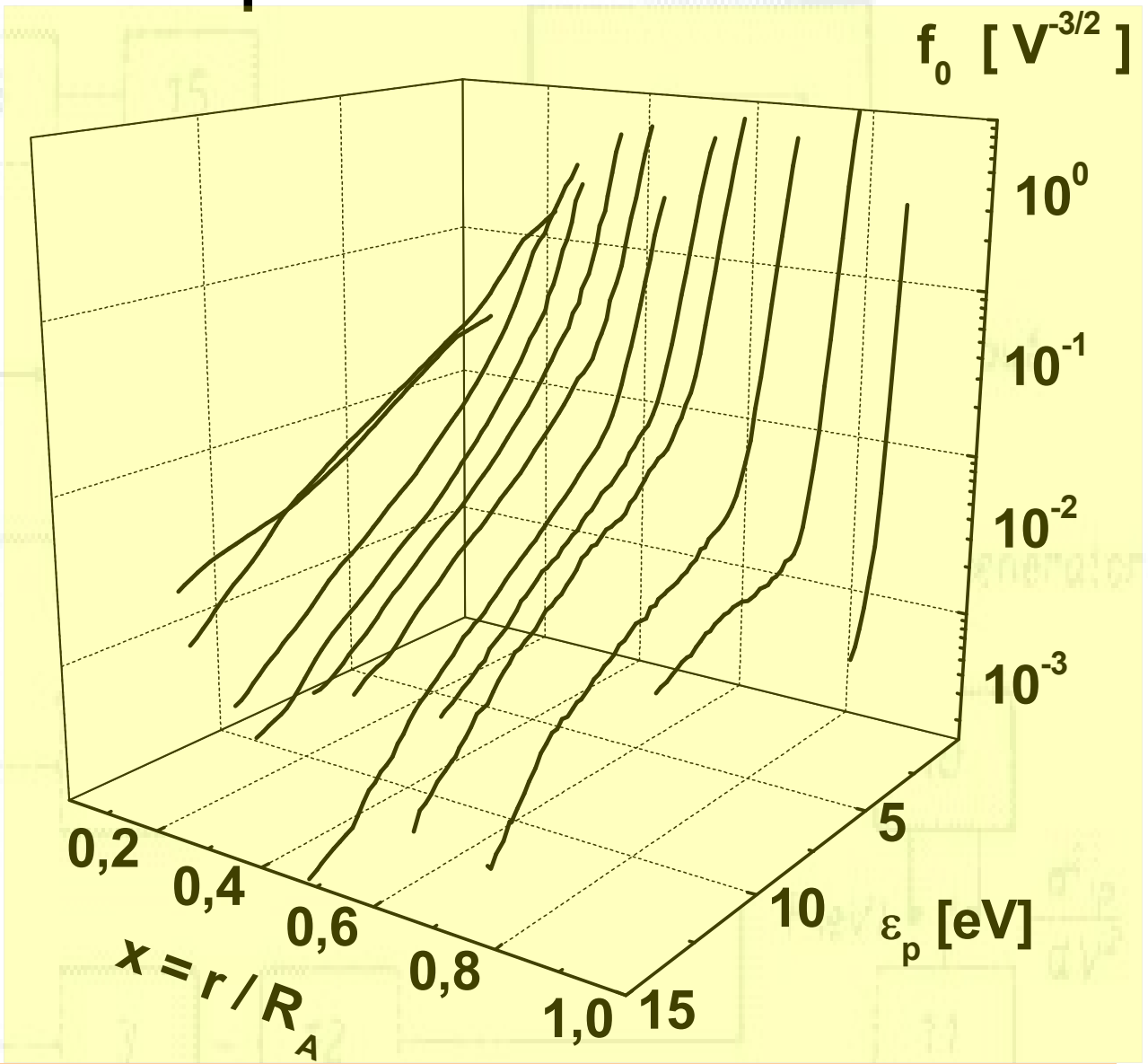

J.F. Behnke, E. Passoth, C. Csambal, M. Tichý, P. Kudrna, D. Trunec, A. Brablec, Czechoslovak Journal of Physics B 49(1999)483-498 .

Time-resolved probe method

Example of the apparatus for the time-resolved measurements -
M. Tichý, Czech.J.Phys B22(1972)264

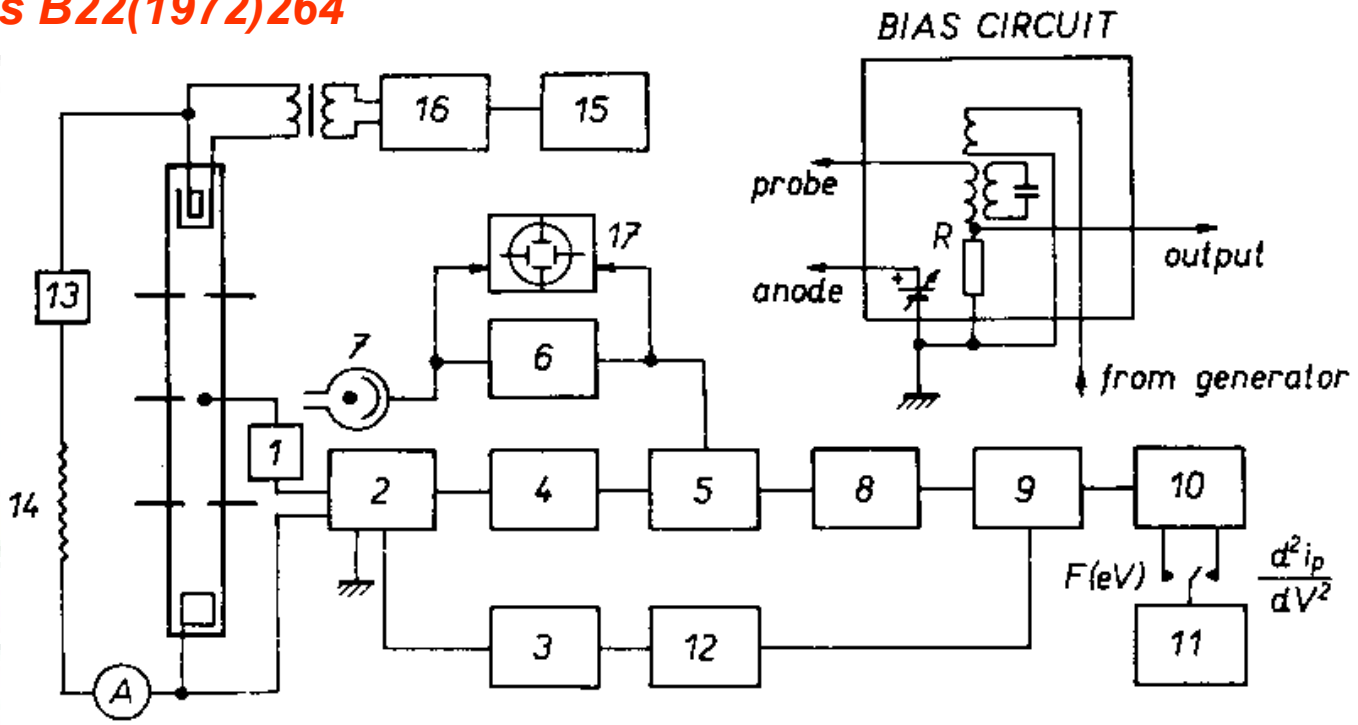

Two approaches to the time resolved measurements:

1. Gated probe signal; avoids the transitional effects that arise by application of the square-wave-like voltage to the probe:

a) U_p independent variable, probe signal sampled at a specified time τ => $I_p(U_p)$ at τ_1, τ_2, τ_3, ...

b) τ independent variable, probe signal sampled at specified U_p => $I_p(\tau)$ at U_{p1}, U_{p2}, U_{p3}, ...

2. Gated probe bias; avoids the over-current to the probe if there exists a large change of plasma potential along the studied time period, e.g. when measuring in the periodically switched discharge.

Direction-resolved Langmuir probe method

THE MEASUREMENTS OF THE ANISOTROPY OF THE ELECTRON ENERGY DISTRIBUTION FUNCTION USING LANGMUIR PROBE

Usage: In plasmas where a preferred direction exists (electric field, magnetic field, plasma jets etc.)
Method (see e.g. *S. Klagge, A. Lunk J. Appl.Phys. 70 (1991) 99*) :
Measurements with planar Langmuir probe with the normal to the probe plane in three or five different orientations to the preferred direction (*rotable* probe).
Three orientations:

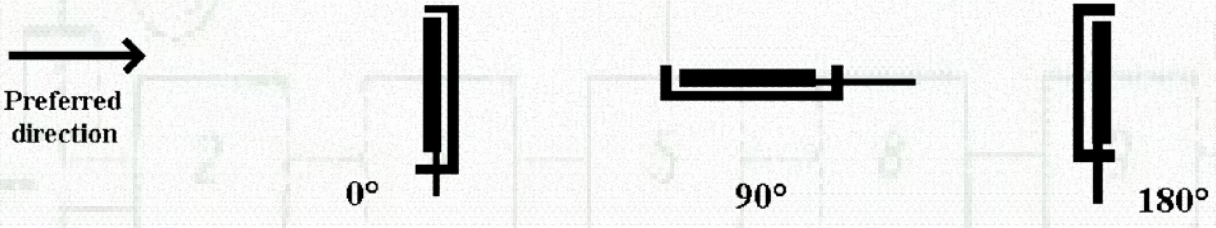

Five orientations:

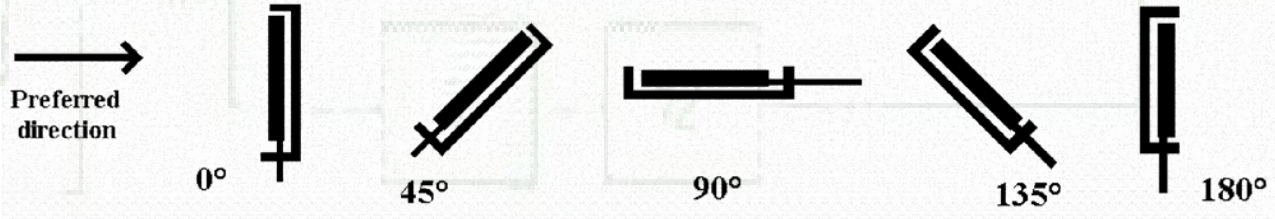

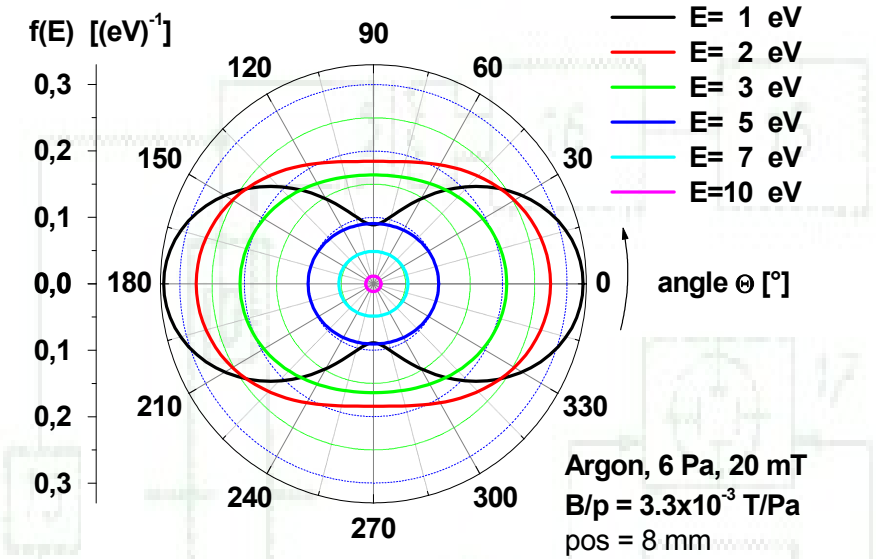

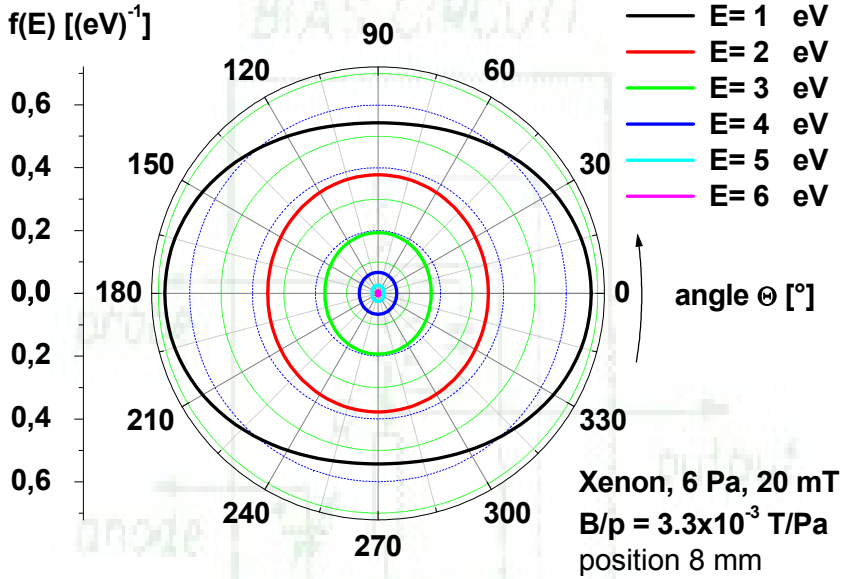

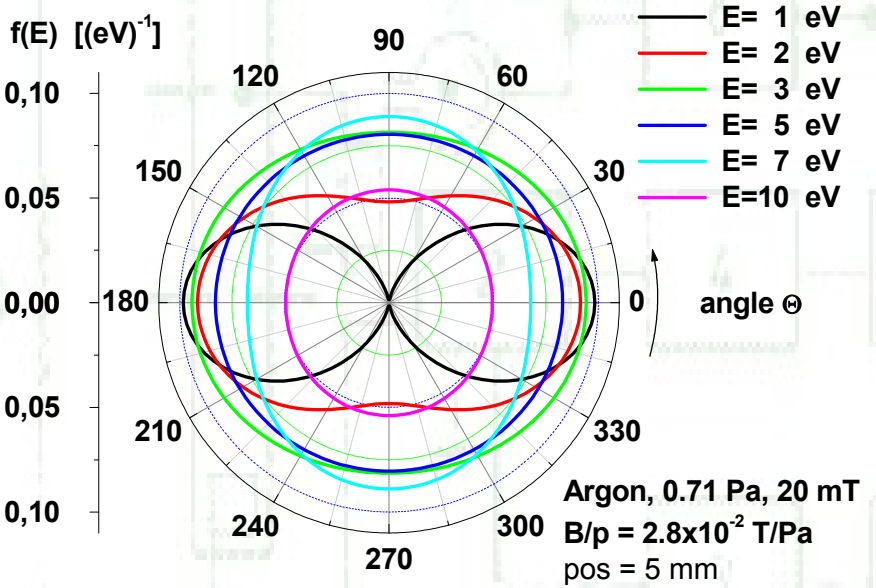

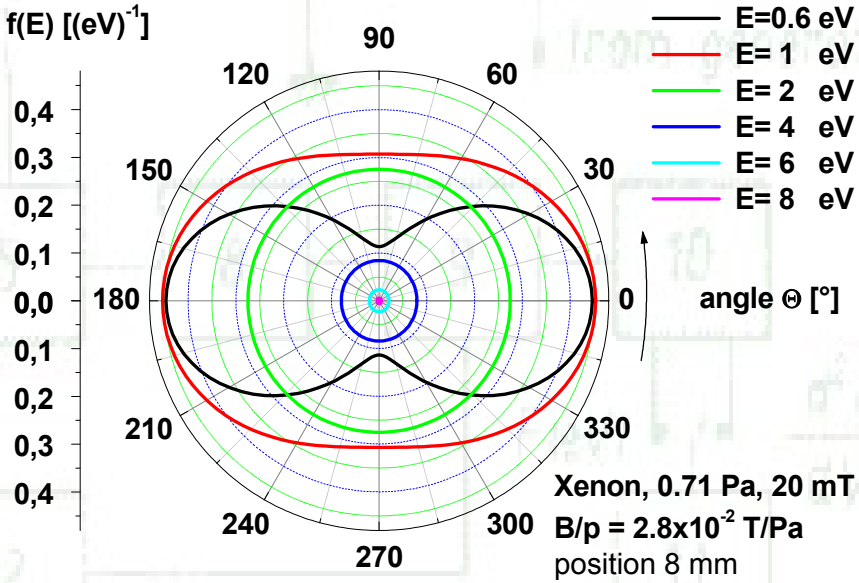

J.F. Behnke, E. Passoth, C. Csambal, M. Tichý, P. Kudrna, D. Trunec, A. Brablec, Czechoslovak Journal of Physics B 49(1999)483-498 .

Particularities of probe diagnostic of plasma generated by RF energy

What is meant by the notion „radio-frequency“?

$$\omega_{pi} = \sqrt{\frac{q_0^2 n_i}{\varepsilon_0 m_i}} \langle \omega \langle \sqrt{\frac{q_0^2 n_e}{\varepsilon_0 m_e}} = \omega_{pe}$$

For argon and $n_i \approx n_e = 10^{16}$ m^{-3} we arrive at $\omega_{pi} \approx 3.16$ MHz and $\omega_{pe} \approx 1$ GHz. At standard frequency 13.56 MHz the ions are basically in stillstand and only electrons follow changes of applied RF field.

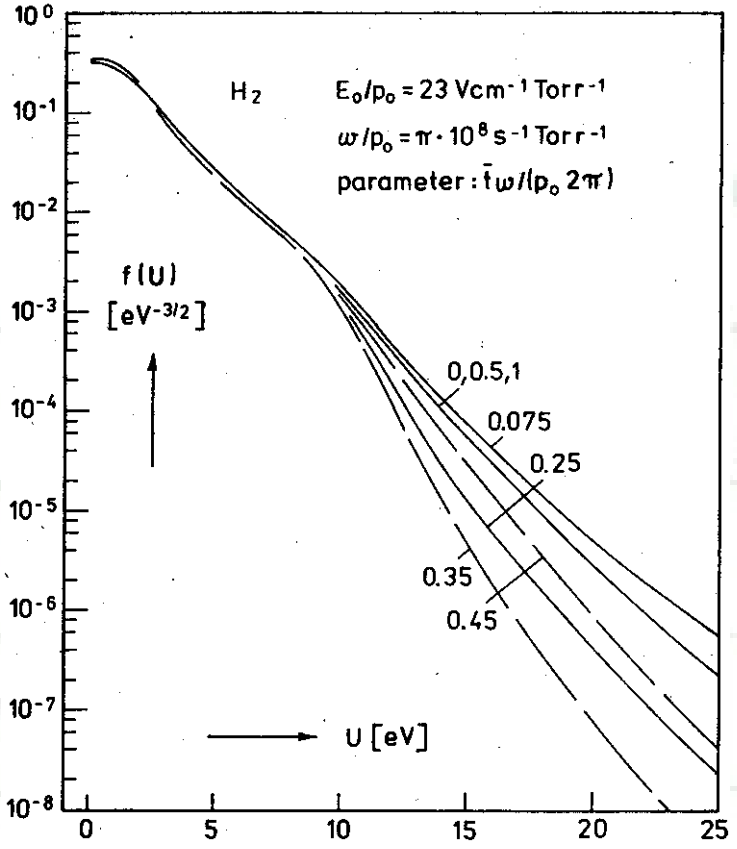

R. Winkler, J. Wilhelm, A. Hess, Annalen der Physik 42(1985)537

Particularities of probe diagnostic of plasma generated by RF energy

Plasma potential oscillates in synchronism with applied frequency. => Probe bias contains AC component with amplitude A_{RF}, which is „rectified“ by the probe, and for bias U_p-$V_0 \leq -A_{RF}$ arises „shift“ with magnitude

$$\Delta U_p = \left(k_B T_e / q_0\right) \ln I_0 \left(\frac{q_0 A_{RF}}{k_B T_e} \right)$$

=> Probe characteristic is deformed ans its slope does not yield any longer T_e (temperature is overestimated).

In order to minimize this effect it is necessary to *compensate* the probe. There exist two basic methods of RF probe compensation: active a passive (and their combinations).

Particularities of probe diagnostic of plasma generated by RF energy

DISTORTION OF THE SECOND DERIVA TIVE CAUSED BY RF VOLTAGE (SINUS SHAPED)

A) LINEAR SCALE

A is the amplitude of the disturbing RF voltage normalized to the electron temperature, $A=q_0A_{rf}/k_BT_e$

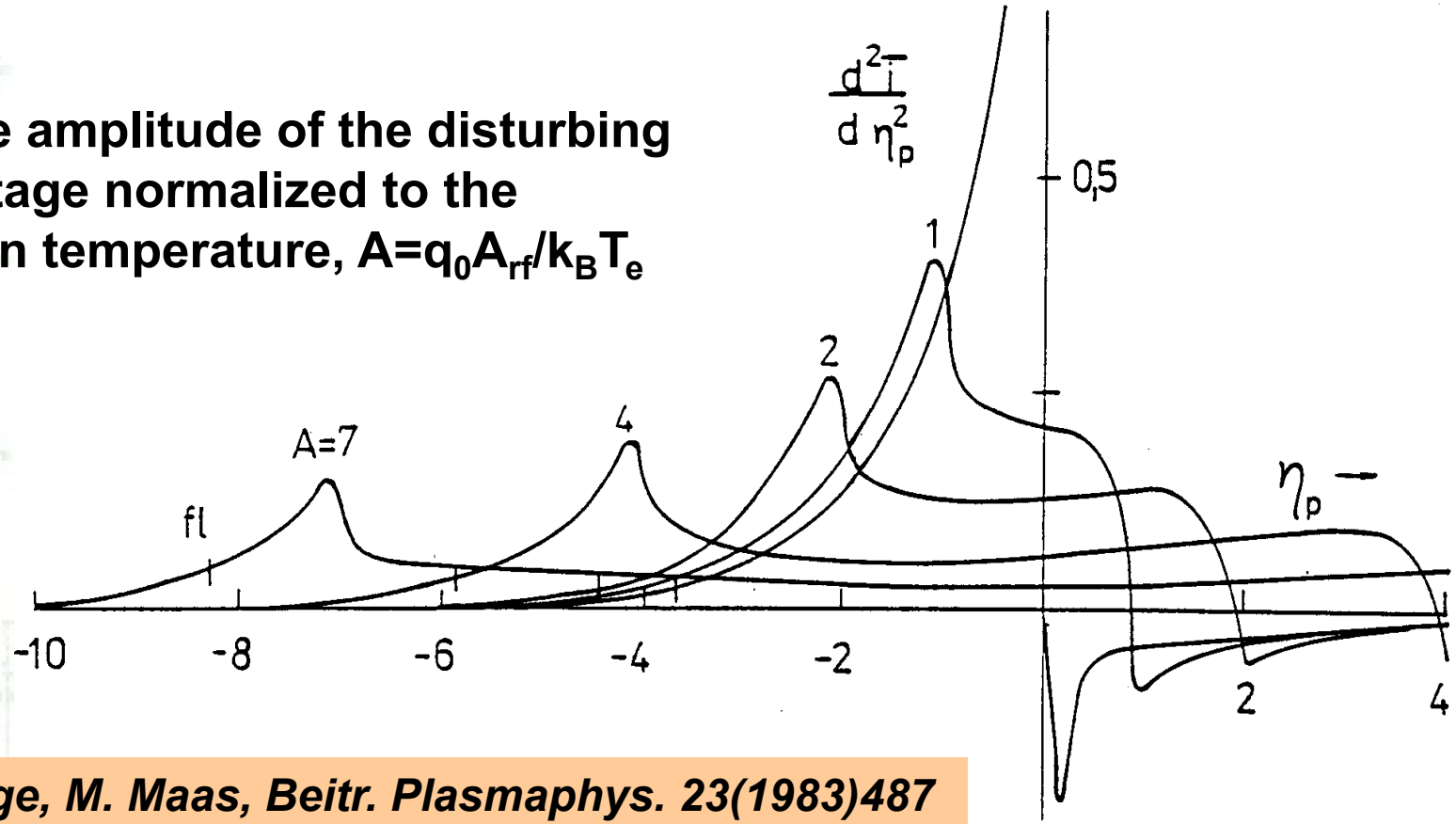

S. Klagge, M. Maas, Beitr. Plasmaphys. 23(1983)487

Particularities of probe diagnostic of plasma generated by RF energy

DISTORTION OF THE SECOND DERIVATIVE CAUSED BY RF VOLTAGE (SINUS SHAPED)

A) SEMILOGARITHMIC SCALE

Since ΔUp is constant with respect to η, RF distortion does not affect T_e **if estimated from the slope of second derivative** of electron current.

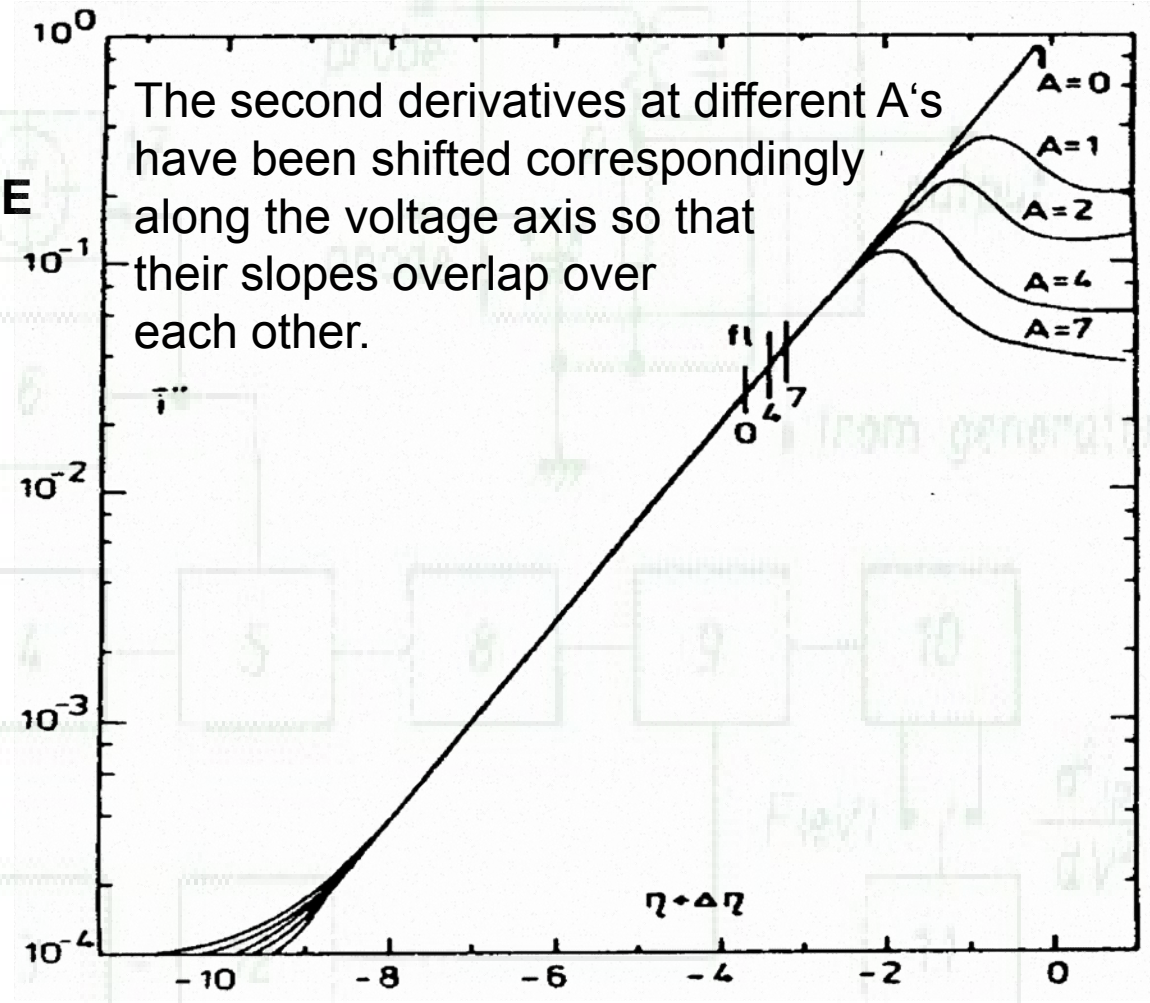

H. Sabadil, S. Klagge, M. Kammayer, Plasma Chemistry and Plasma Processing 8(1988)425

Methods of probe RF compensation

Active compensation:

N.St.J. Braithwaite, N.M.P. Benjamin,
J.E. Allen, J.Phys. E Sci. Instr. 20(1987)1046

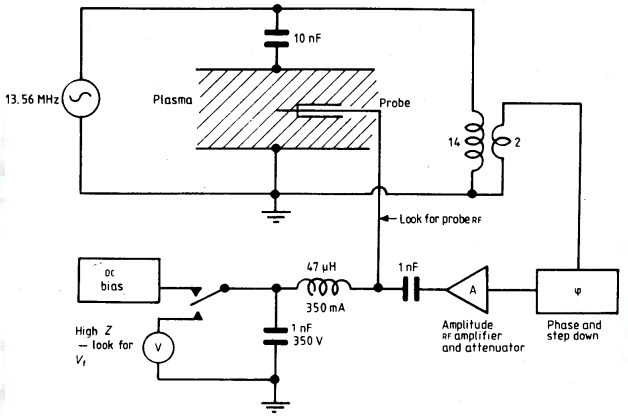

Passive compensation:

V.A. Godyak, R.B. Piejak,
B.M. Alexandrovich,
Plasma Sources Sci. Technol. 1(1992)36

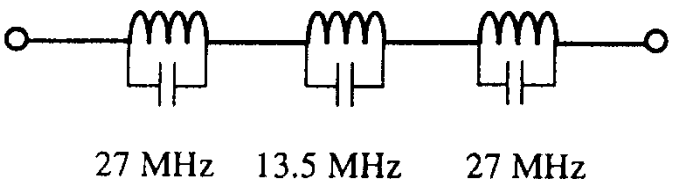

Combined compensation:

P.A. Chatterton, J.A. Rees,
W.L. Wu, K. Al-Assadi,
Vacuum 42(1991)489

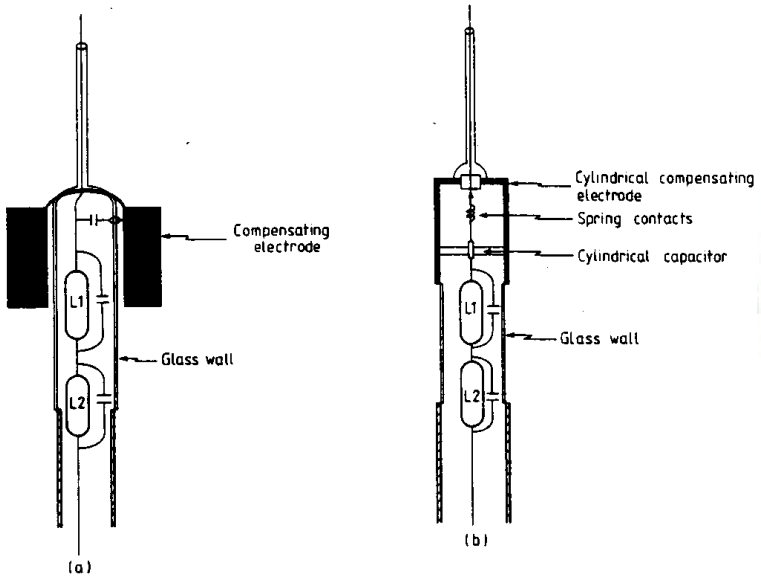

Methods of probe RF compensation

Combined compensation:
(LC + active)

W. Kasper, Proc. XXII. ICPIG Hoboken, New Jersey (USA), July, 31-August, 4, 1995, K.H. Becker, W.E. Carr, E.E. Kunhardt, Eds., Contributed Papers, Vol. 2, p. 171.

Question:
Do you see the active part of the probe compensation?

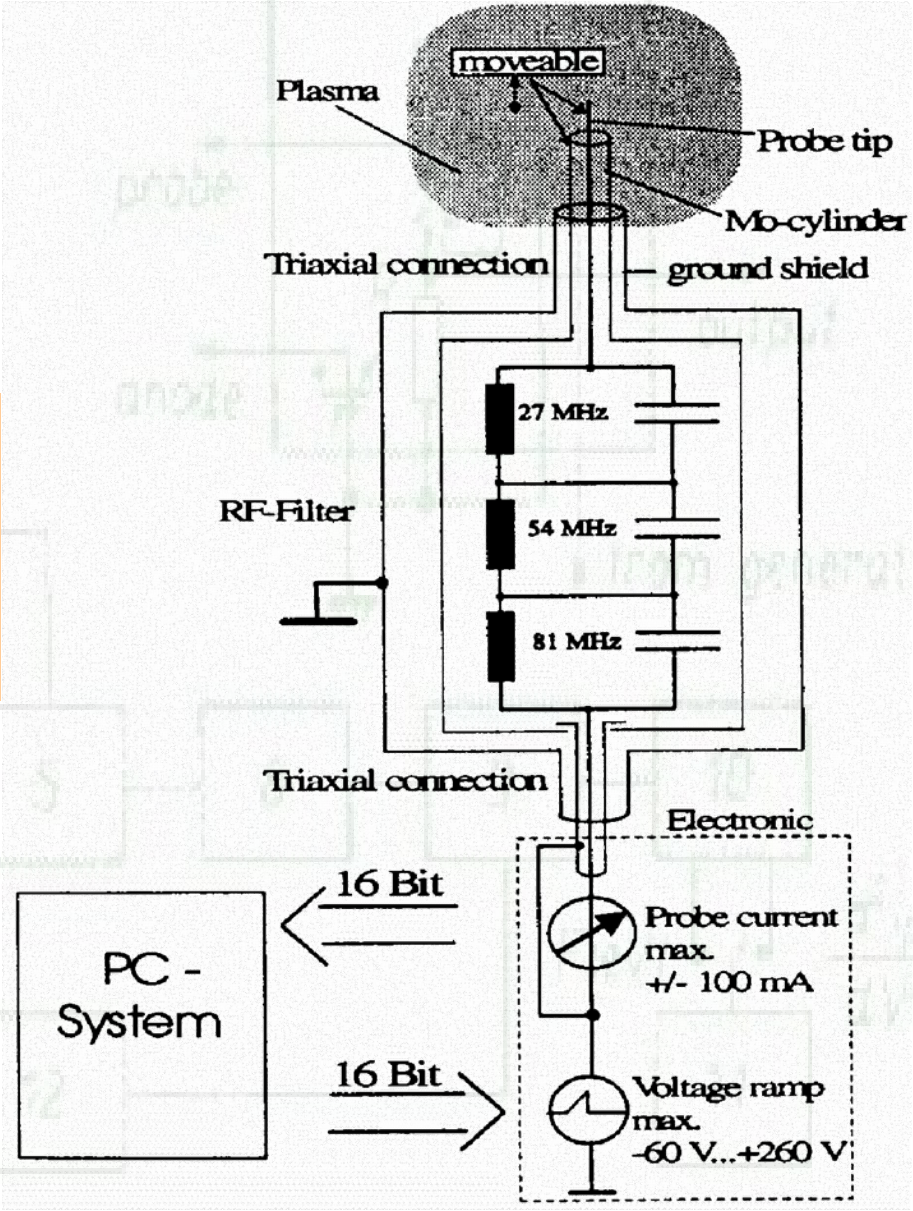

Methods of probe RF compensation

Combined compensation (RC circuits+LC circuits+ active):

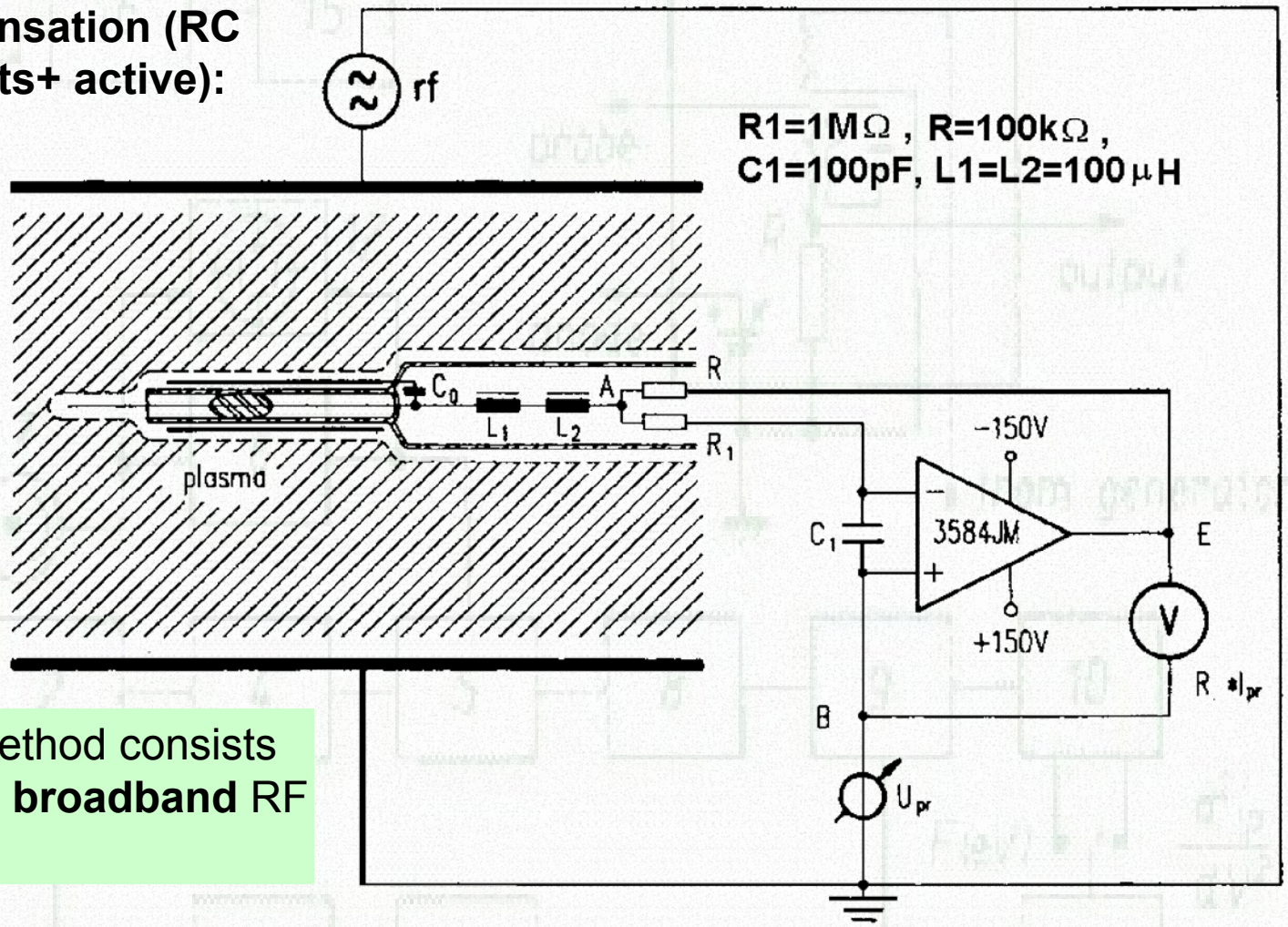

Note: This method requires larger DC power supply for probe bias since a large resistor is inserted into the probe current path.

Advantage of this method consists in the fact that it is a **broadband** RF compensation.

U. Flender, B.H. Nguyen Thi, K. Wiesemann, N.A. Khromov, N.B. Kolokolov, Plasma Sources Sci. Technol. 5(1996)61

Comparison of RF probe compensation methods

Comparison is performed in the article:

B.M. Annaratone, N.St.J. Braithwaite, Meas. Sci. Technol. 2(1991)795

Table 1. Comparison of active and passive probes.

	Passive	Active
Frequency range	Broadband	Fundamental only
Fidelity	More certain	Less certain
Intrusion	Significantly more than standard DC probe	As for standard DC probe
Manoeuverability or localization	Poor	As for standard DC probe
Complexity	Standard filter components in modified probe design	Standard probe with external amplifier
Additional data	Nil	Measures local RF potential

Criteria od RF probe compensation

How to set up the compensation circuit?

H. Sabadil, S. Klagge, M. Kammayer, Plasma Chemistry and Plasma Processing 8(1988)425

S. Klagge, Plasma Chemistry and Plasma Processing 12(1992)103

Criteria:

1. Floating potential reaches its maximum positive value with respect to the reference electrode.
2. Maximum and minimum of the second derivative reach their maximum ordinate value.
3. Beteween maximum and minimum of the second derivative appears the smallest potential difference (the difference $\left|U_p\left(I''_{max}\right)-U_p\left(I''_{min}\right)\right|$ is roughly equal to the double of the disturbing RF amplitude).
4. The difference $\left|U_p\left(I''_{max}\right)-V_{fl}\right|$ attains its maximum value.

Special probes

EXAMPLES OF HEATED PROBES

A) Directly heated probes by DC or AC current (warm and/or emissive)

J. Kalčík, Czech. J. Phys. 45(1995)241

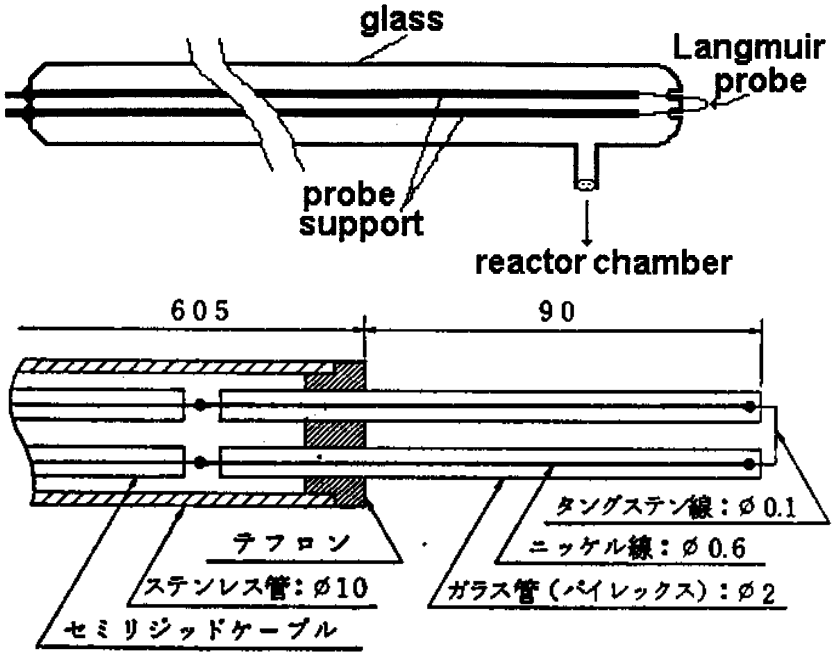

Y. Kobayashi, T. Ohte, M. Katoh, M. Sugawara, Trans. IEE of Japan 109-A(1989)69 (In Japanese)

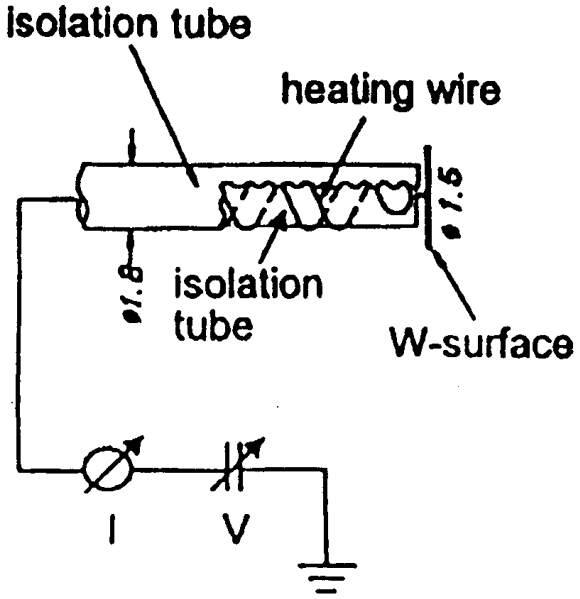

B) Indirectly heated probes

C. Winkler, D. Strele, S. Tscholl, R. Schrittwieser, Proc. 12th SAPP, Liptovský Ján (Slovakia), February, 9-13, 1999, J.D. Skalný, M. Černák, Eds., p 121

Special probes

Emissive probes:

S. Klagge, Thesis Dr. sc. nat., Ernst-Moritz-Arndt-University Greifswald, Germany, (1988)

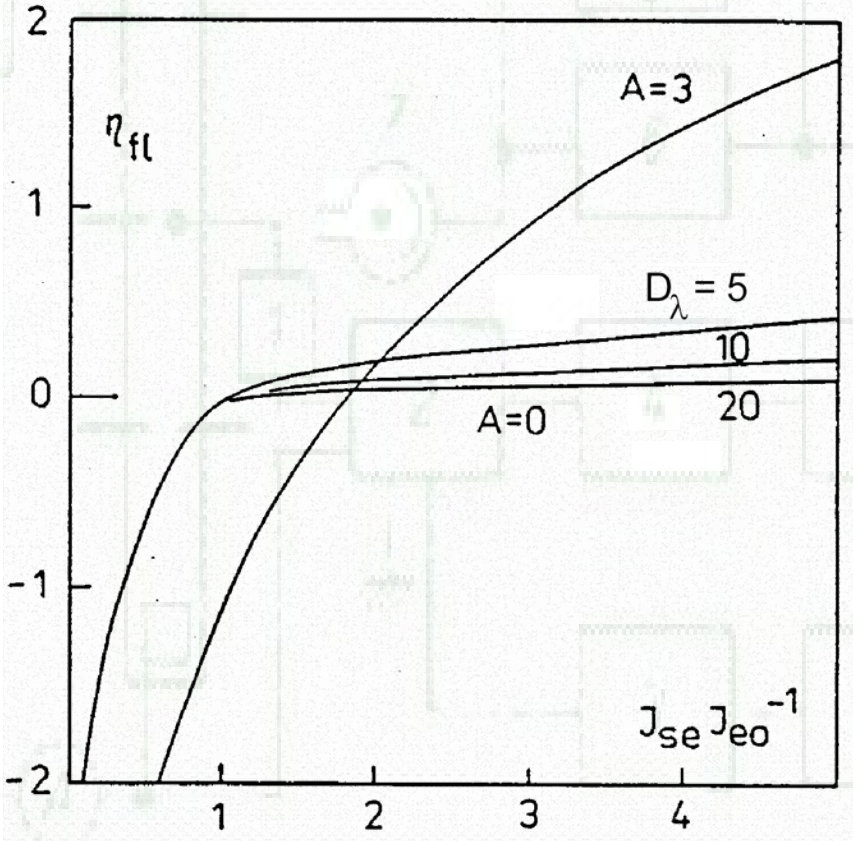

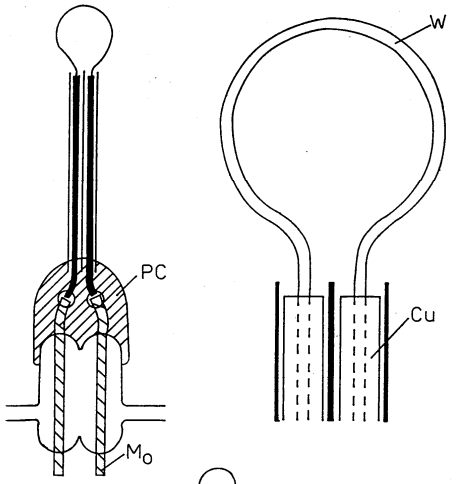

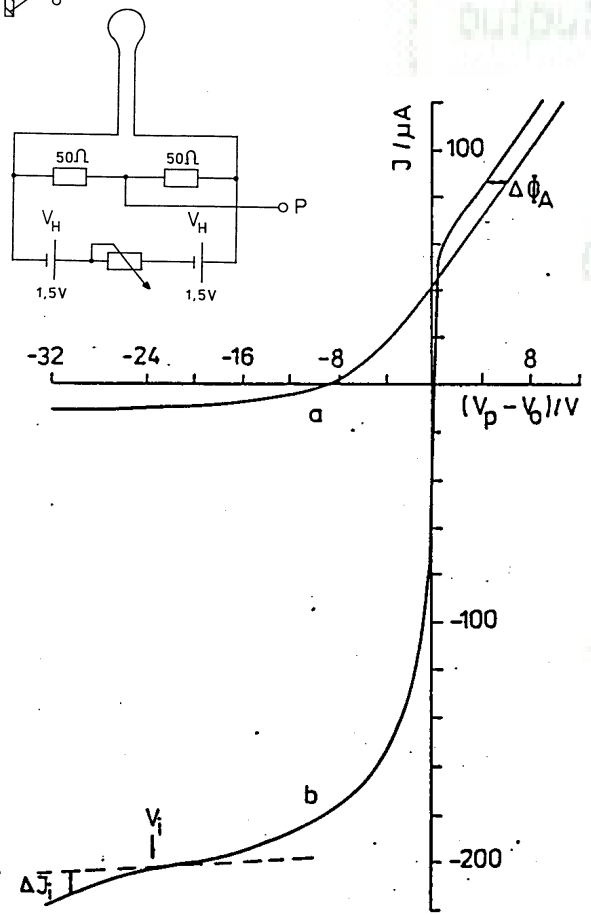

Special probes

Emissive probes –
laser heated emissive probe:

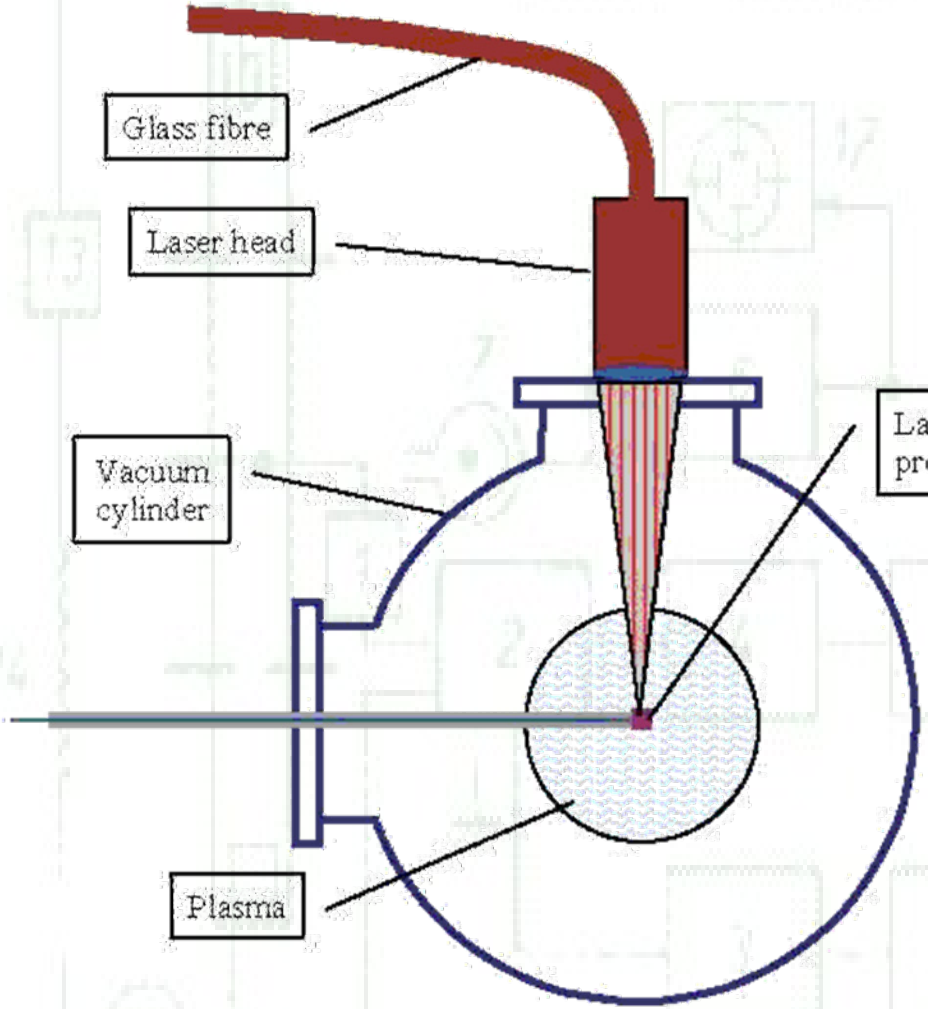

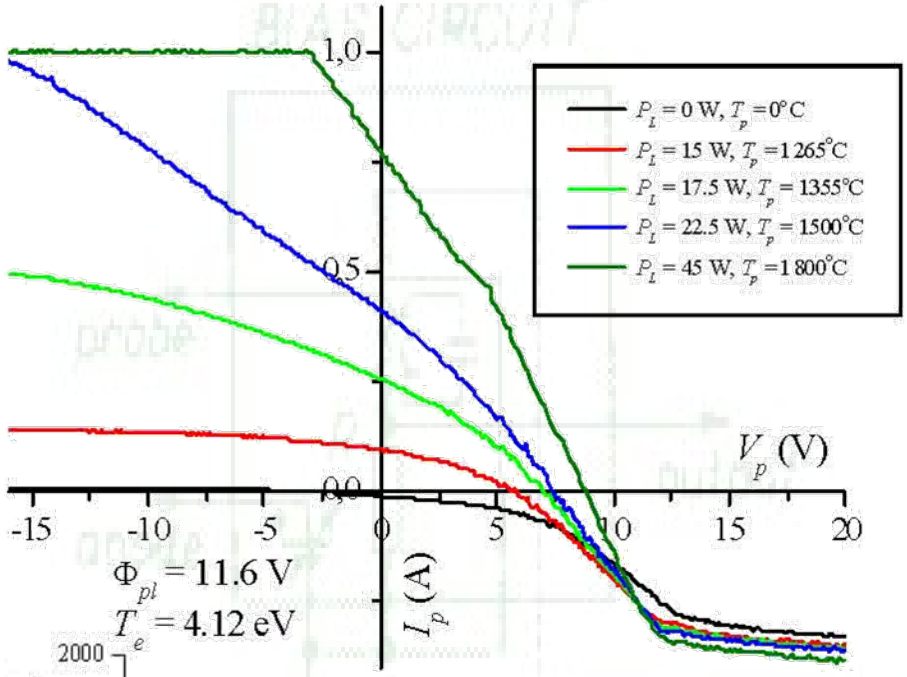

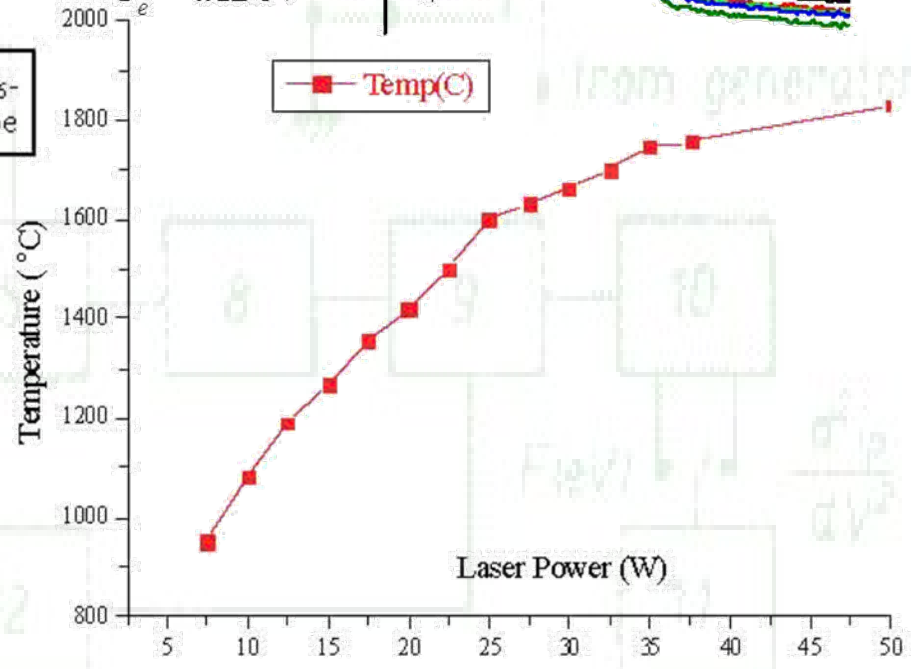

R. Schrittwieser et al., PHYSICA SCRIPTA T123(2006) 94-98

Special probes

Emissive probes –
laser heated emissive probe:

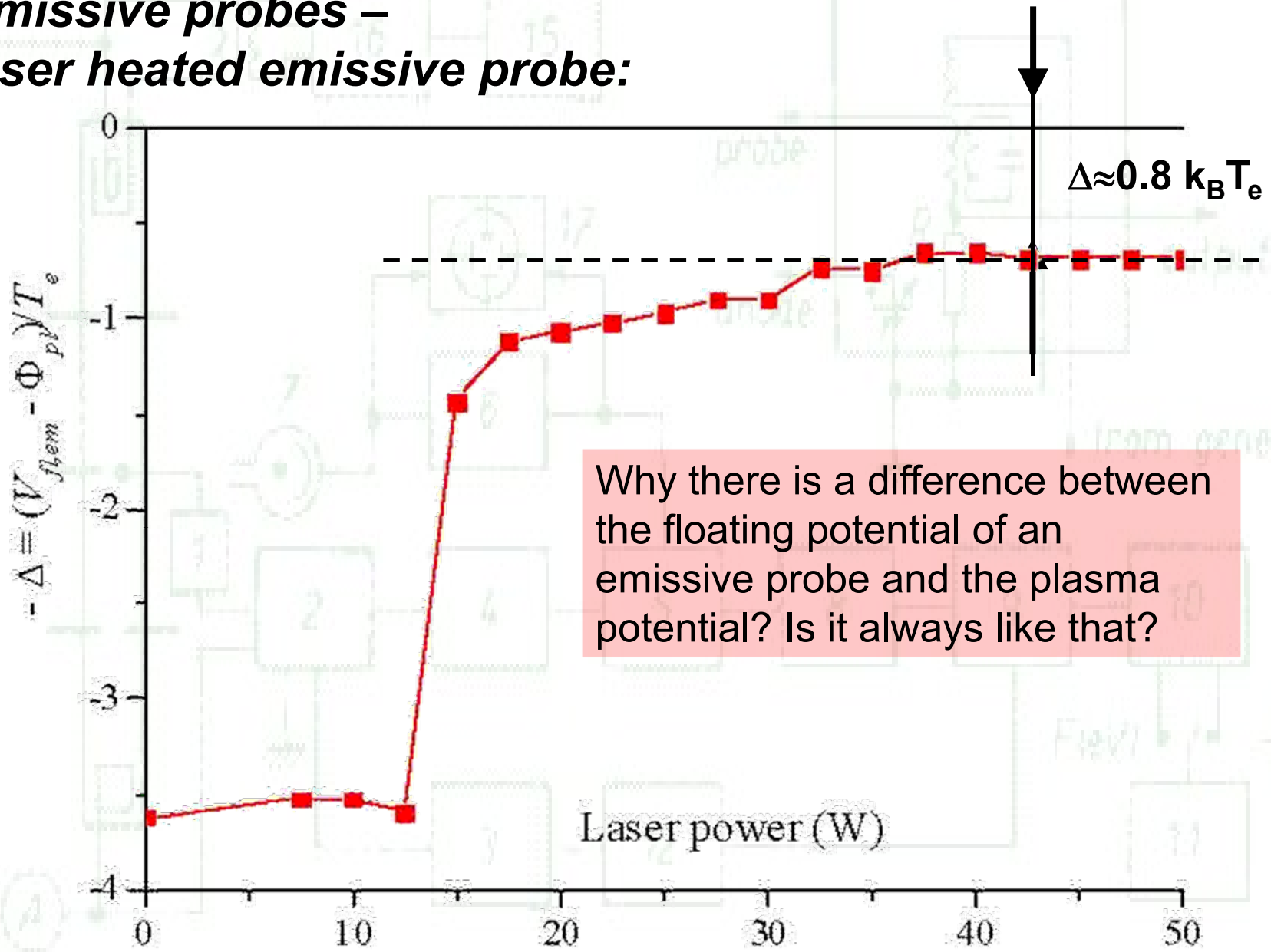

Why there is a difference between the floating potential of an emissive probe and the plasma potential? Is it always like that?

Special probes

Emissive probe – creation of negative potential barrier due to emitted electrons – 1D model by S. Takamura et al.

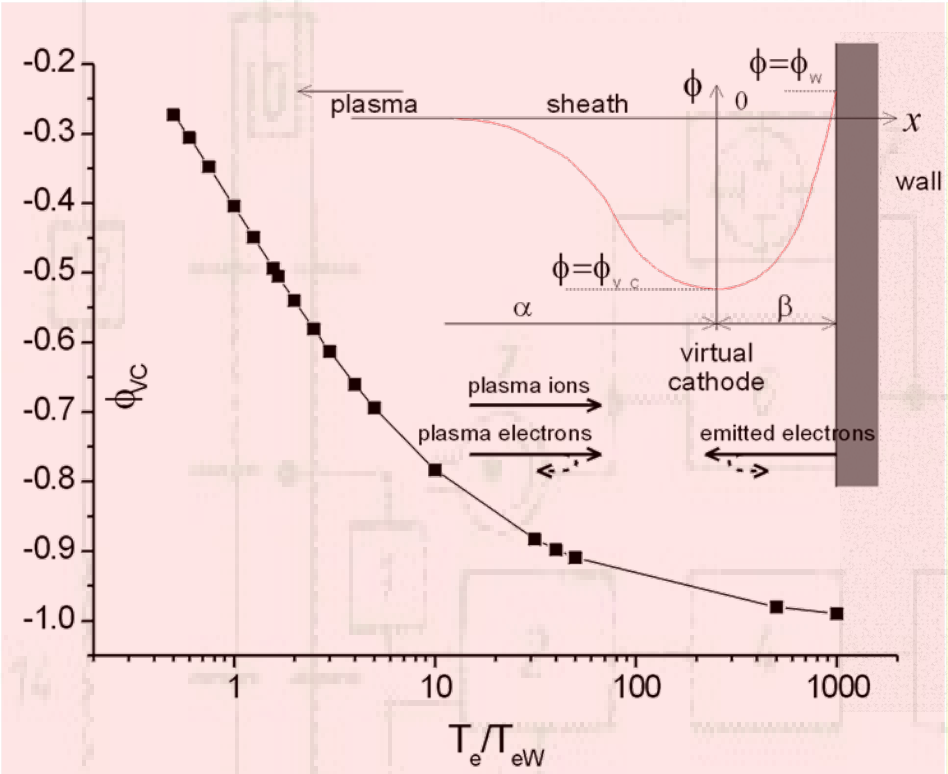

Difference between plasma potential and virtual cathode potential in dependence on T_e/T_{eW}.

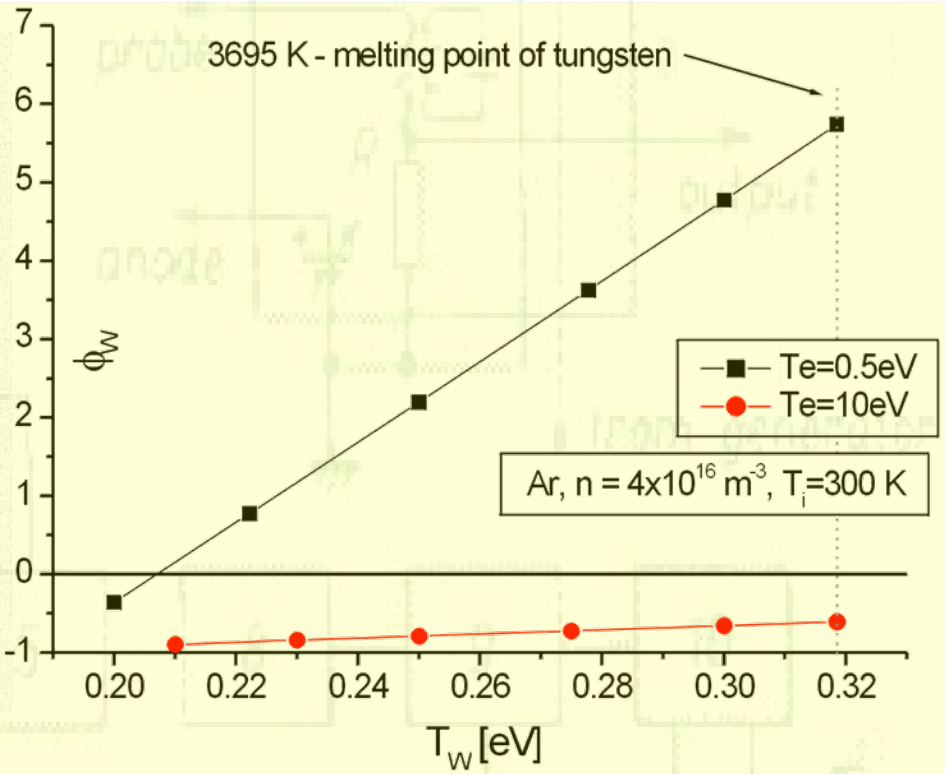

Potential on the plasma-facing emitting wall for case of tungsten and Maxwellian distribution of emitted electrons.

S. Takamura et al, Contrib. Plasma Phys., 44, 126-137, (2004)

Special probes

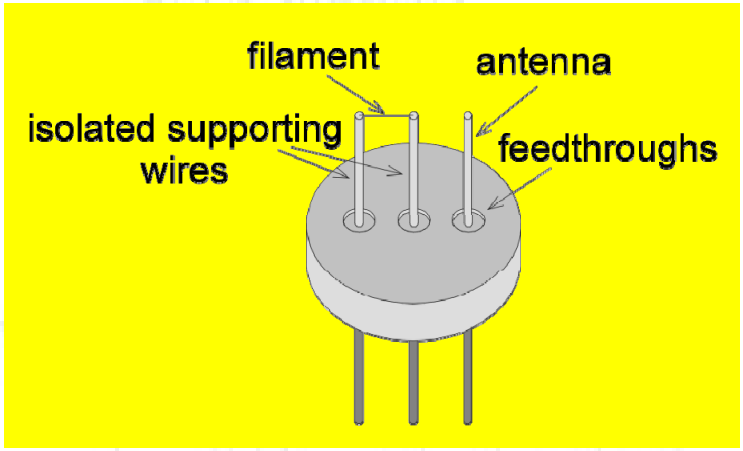

Oscillating probe:

A. Brockhaus, A. Schwabedissen, Ch. Soll, J. Engemann, Proc. Frontiers in Low Temperature Plasma Diagnostic III, Saillon (Switzerland), 15-19 February 1999, p. 89

$$\omega_{pe} = \sqrt{\frac{q_0^2 n_e}{\varepsilon_0 m_e}}$$

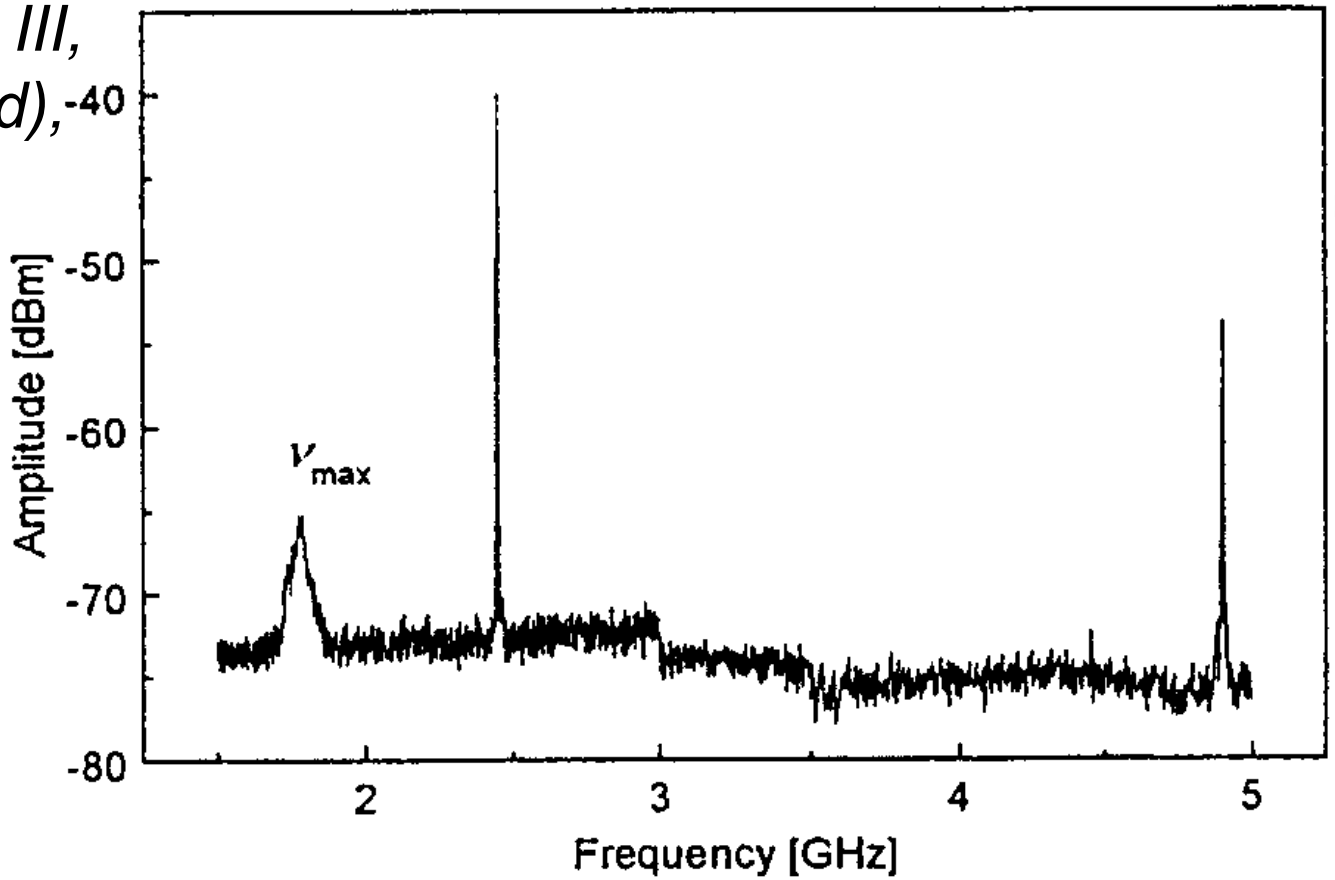

Special probes

ION FLUX RF PROBE

N. St.J. Braithwaite, J.P. Booth, G. Cunge, Plasma Sources Sci. Technol. 5(1996)677

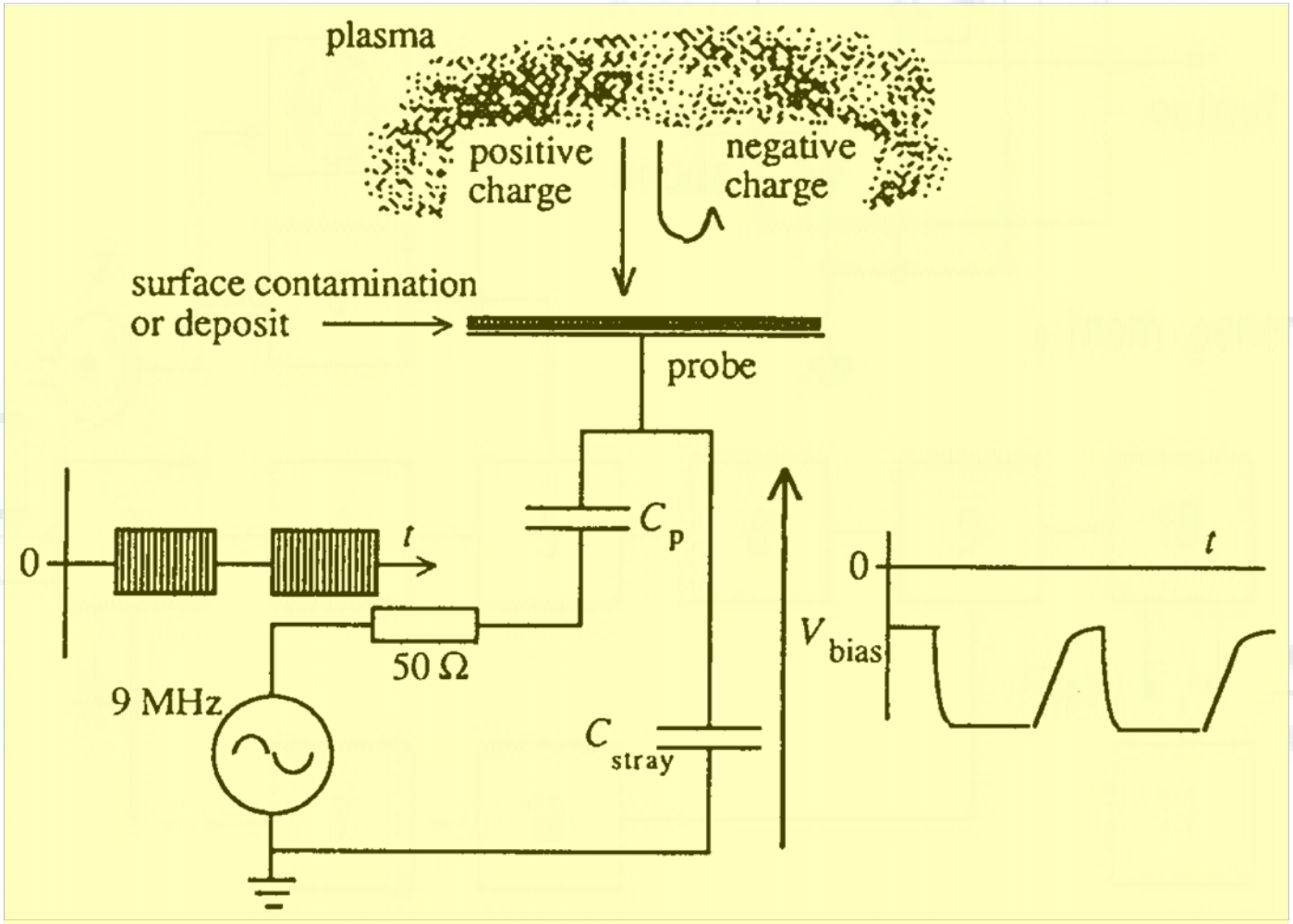

Special probes

HAIRPIN (MICROWAVE RESONATOR) PROBE

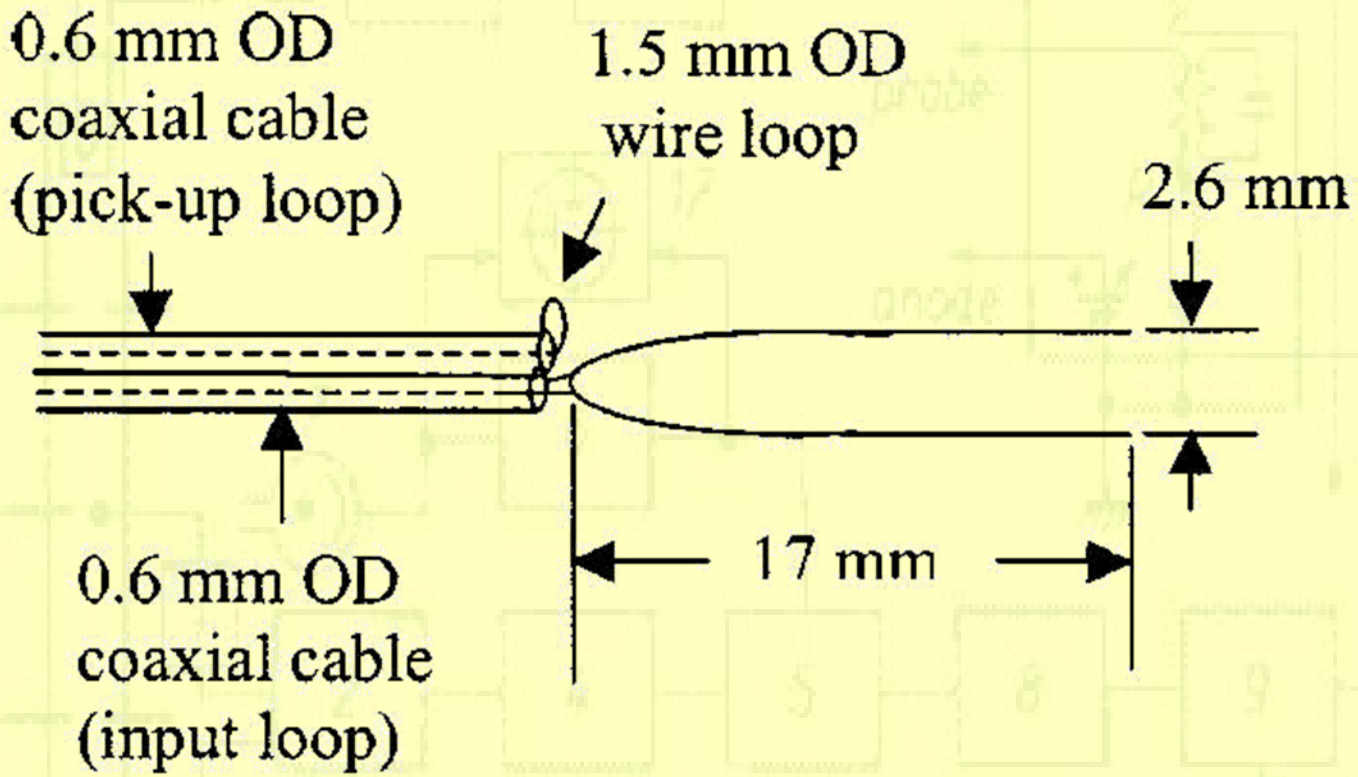

A schematic diagram of a transmission type hairpin resonator.

R. L. Stenzel, Rev. Sci. Instrum. 47 (1976) 603
Piejak R.B., et al., J. Appl. Phys., Vol. 95 (2004) 3785

Special probes

HAIRPIN (MICROWAVE RESONATOR) PROBE

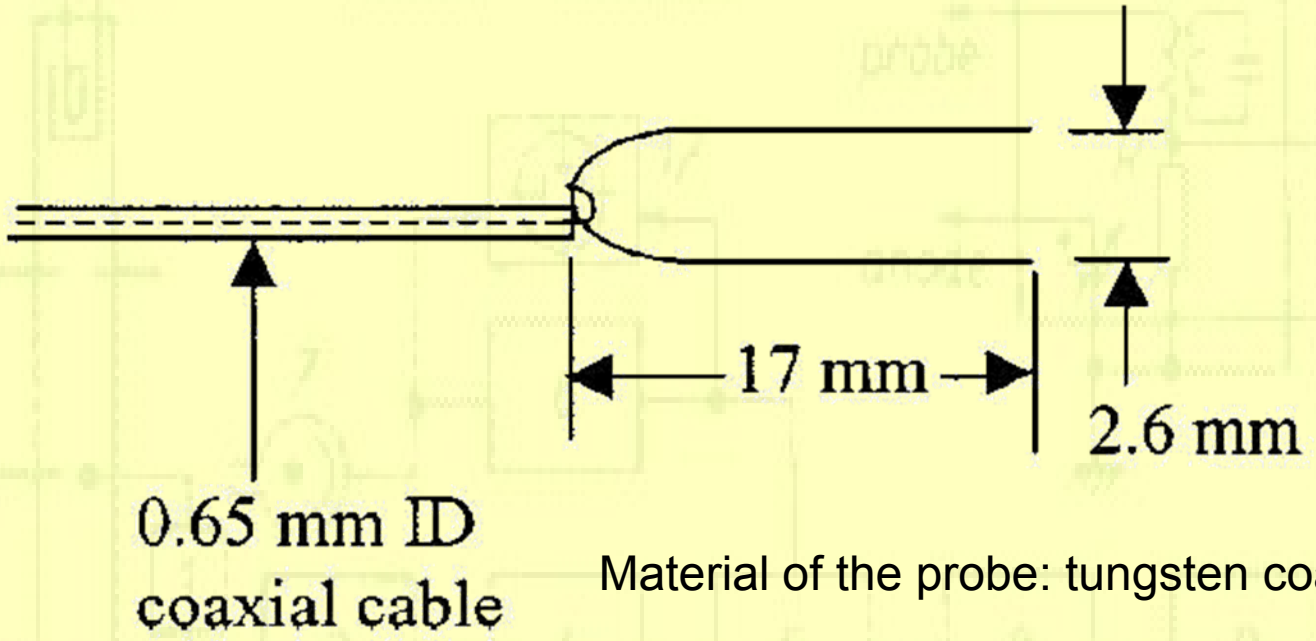

Material of the probe: tungsten coated with silver

A schematic diagram of a reflection type hairpin resonator.

Piejak R.B., et al., J. Appl. Phys., Vol. 95 (2004) 3785

Special probes

HAIRPIN (MICROWAVE RESONATOR) PROBE

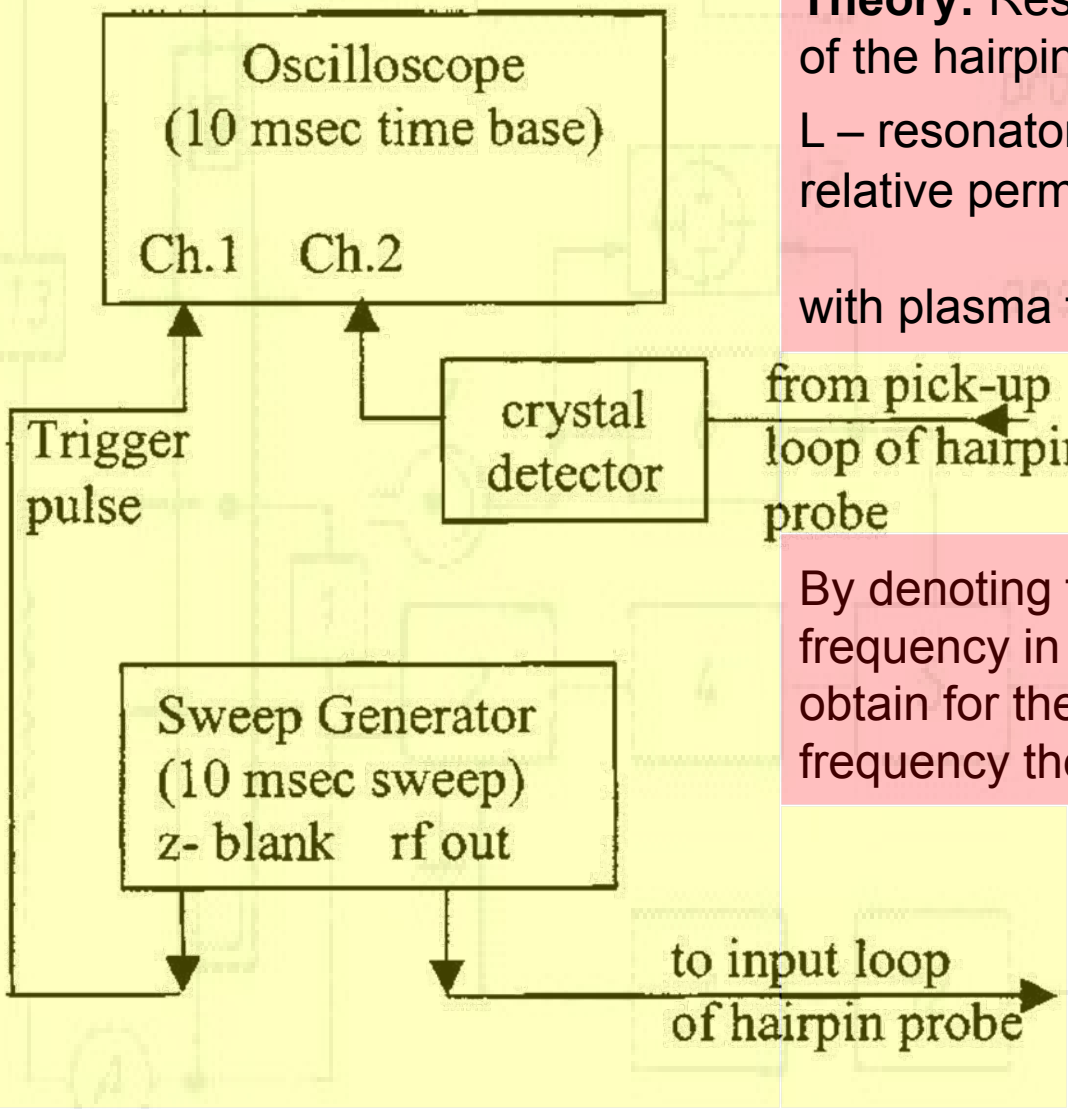

Theory: Resonant frequency of the hairpin is:

$$f_r = \frac{c}{4L\sqrt{\varepsilon}}$$

L – resonator length, ε relative permittivity given by:

$$\varepsilon = 1 - \frac{f_p^2}{f^2}$$

with plasma frequency

$$f_p = (e^2 n / \pi m)^{1/2}$$

By denoting f_0 the resonant frequency in vacuum we obtain for the resonator frequency the expression:

$$f_r^2 = f_0^2 + f_p^2$$

From this follows for the plasma density

$$n = \frac{f_r^2 - f_0^2}{0.81}$$

(n in x10^{10} cm^{-3}, f in GHz)

Double probe method

E.O. Johnson, L. Malter, Phys. Rev. 80(1950)58

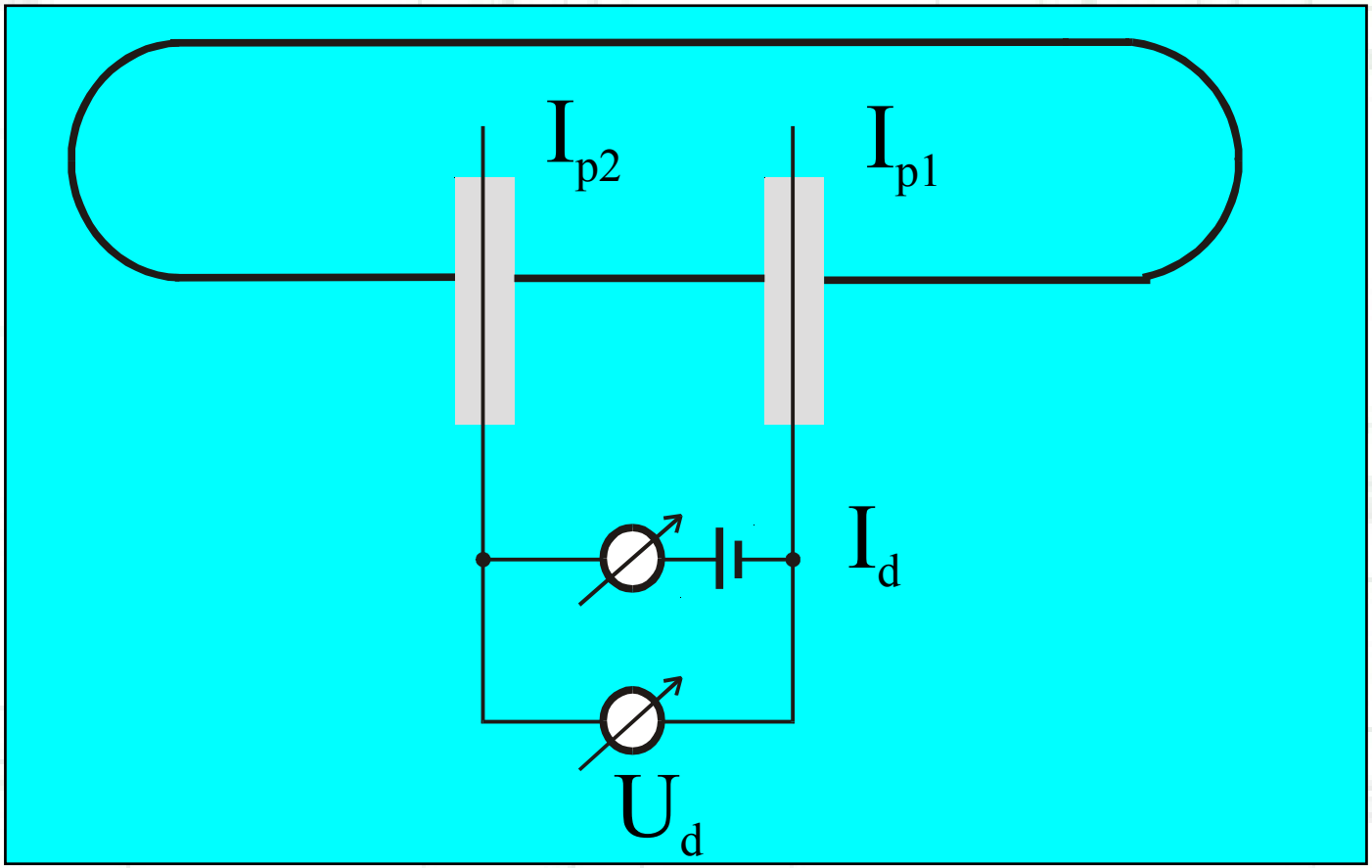

Double probe method

Characteristic of double probe (for two probes with the same collecting surface area)

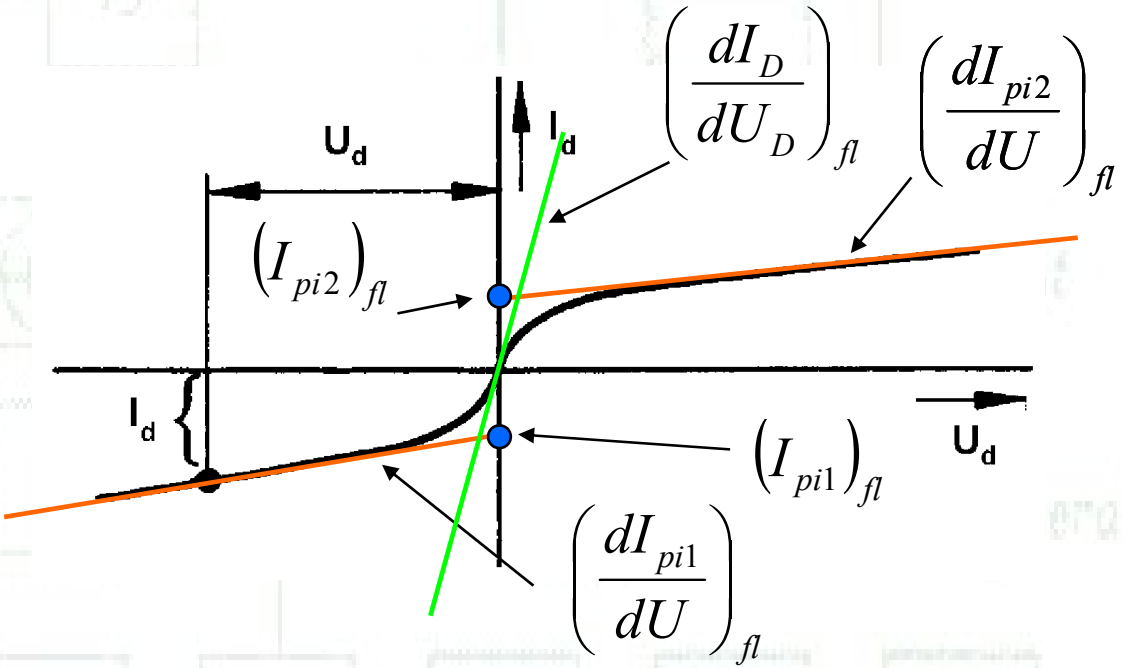

Determination of T_e from double probe characteristic

$$\frac{k_B T_e}{q_0} = \frac{1}{2\left(\frac{dI_D}{dU_D}\right)_{fl} - \frac{1}{2}\left(\frac{dI_{pi1}}{dU} + \frac{dI_{pi2}}{dU}\right)_{fl}} \frac{2(I_{pi1})_{fl}(I_{pi2})_{fl}}{(I_{pi1})_{fl} + (I_{pi2})_{fl}}$$

Triple probe method

Principle (floating system of three probes):

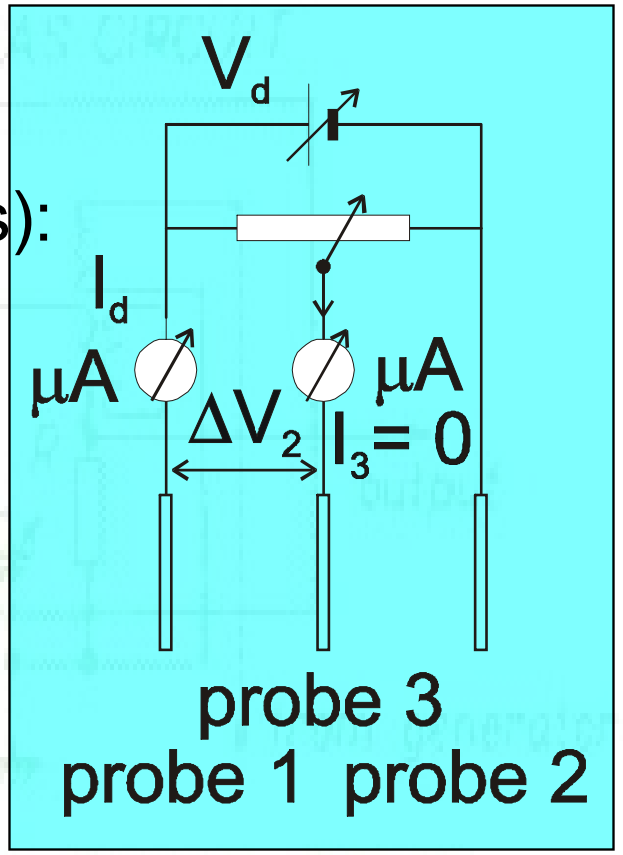

K. Yamamoto, T. Okuda,
J.Phys. Soc. Japan 11(1956)57
T. Okuda, K. Yamamoto, J. Appl. Phys. 31(1960)158
S. Aisenberg, J.Appl.Phys. 35(1964)130.
S. Chen, T. Sekiguchi, J. Appl. Phys. 36(1965)2363
J.S. Chang, G.L. Ogram, R.M. Hobson, S. Teii,
J.Phys.D: Appl. Phys. 13(1980)1083

Probes 1 and 3 may be asymmetrical.

In the collisionless case it is possible to evaluate the electron temperature from one measured point ΔV_2 at constant V_{12} (assumption $\left(\eta_{fl} + \Delta\eta_2\right) \rangle\rangle \eta_{12}$) from the relation

$$\left[1 - \exp\left(\frac{-\Delta V_2}{k_B T_e}\right)\right] = \frac{1}{2}\left[1 - \exp\left(\frac{-V_{12}}{k_B T_e}\right)\right]$$

(*S. Chen, T. Sekiguchi*, see above)

PROBE DIAGNOSTICS IN HIGH-TEMPERATURE PLASMA

Types of probes used in CASTOR tokamak edge plasma:

- Langmuir probes
- Mach probe
- Gundestrup probe
- Katsumata probe
- Ion sensitive probe
- Tunnel probe
- Ball-pen probe.

Measurement of:

- concentrations of charged particles
- temperatures of charged particles (parallel, perpendicular)
- flows of charged particles, etc.

PROBE DIAGNOSTICS IN HIGH-TEMPERATURE PLASMA

Examples of probe arrays (CASTOR)

Brotánková, PhD disser.

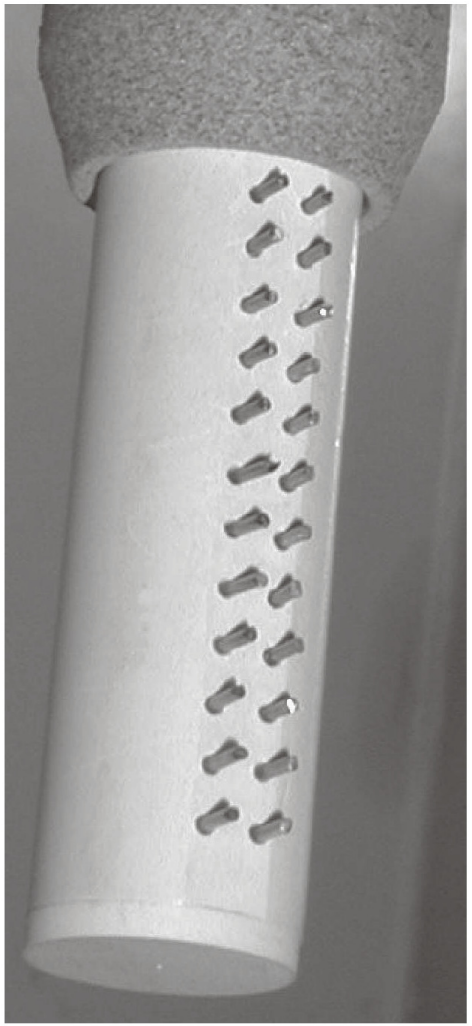

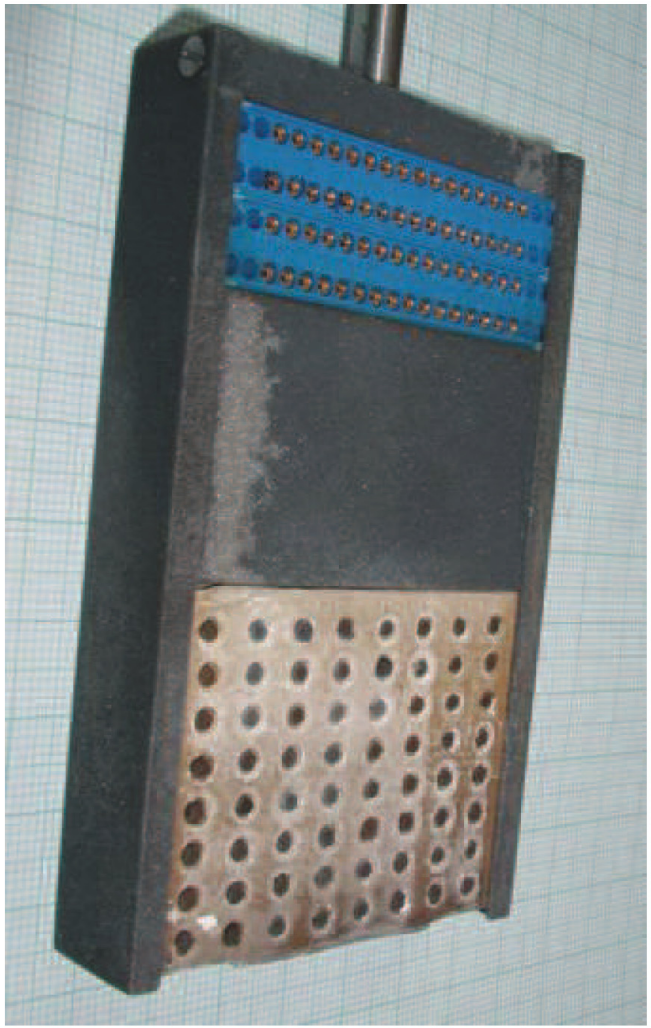

PROBE DIAGNOSTICS IN HIGH-TEMPERATURE PLASMA

Examples of probe arrays (poloidal ring of probes, CASTOR)

Brotánková, PhD disser.

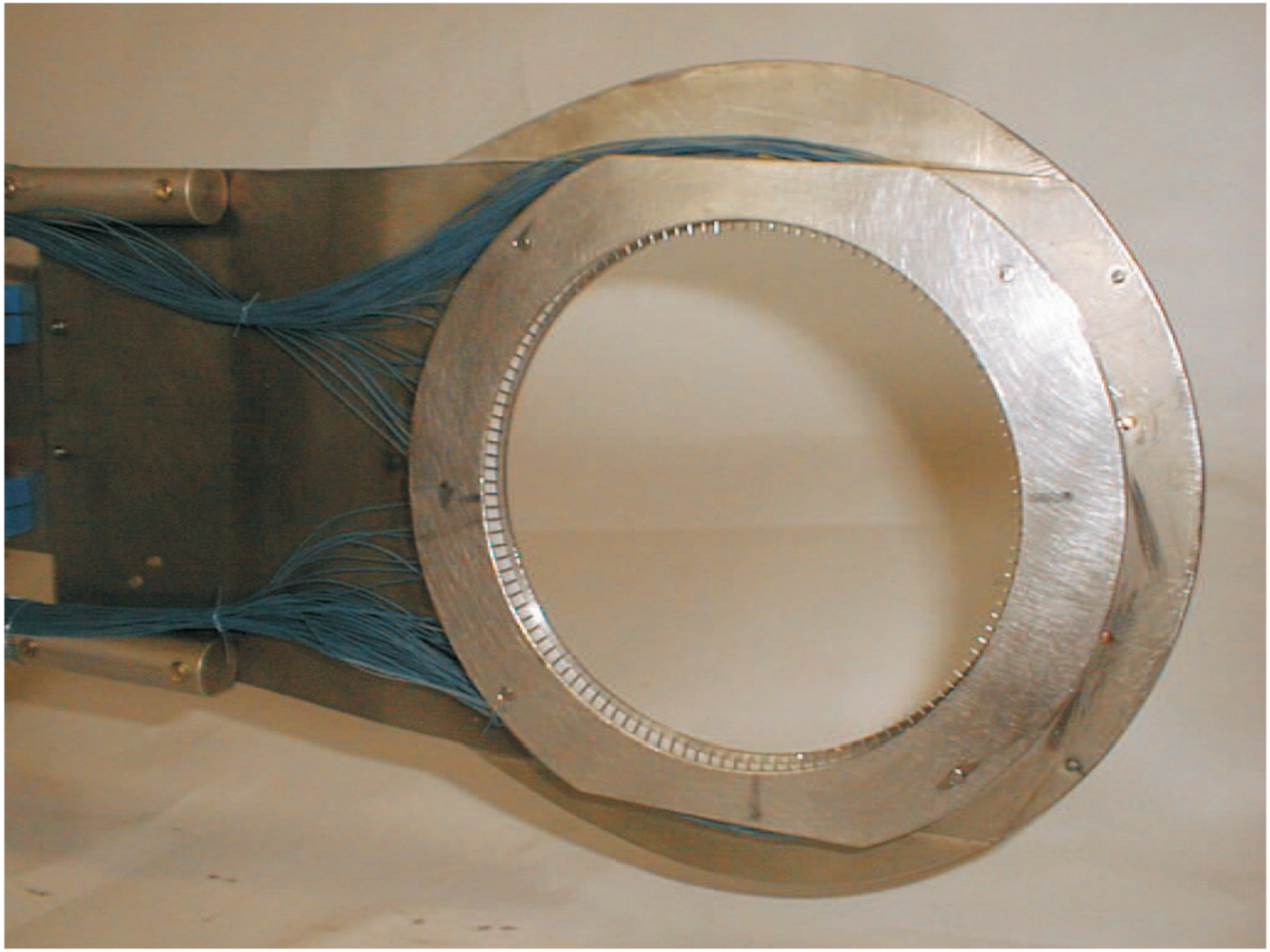

PROBE DIAGNOSTICS IN HIGH-TEMPERATURE PLASMA

Examples of probe arrays (poloidal ring of probes with magnetic pick-up coils, CASTOR)

Brotánková, PhD disser.

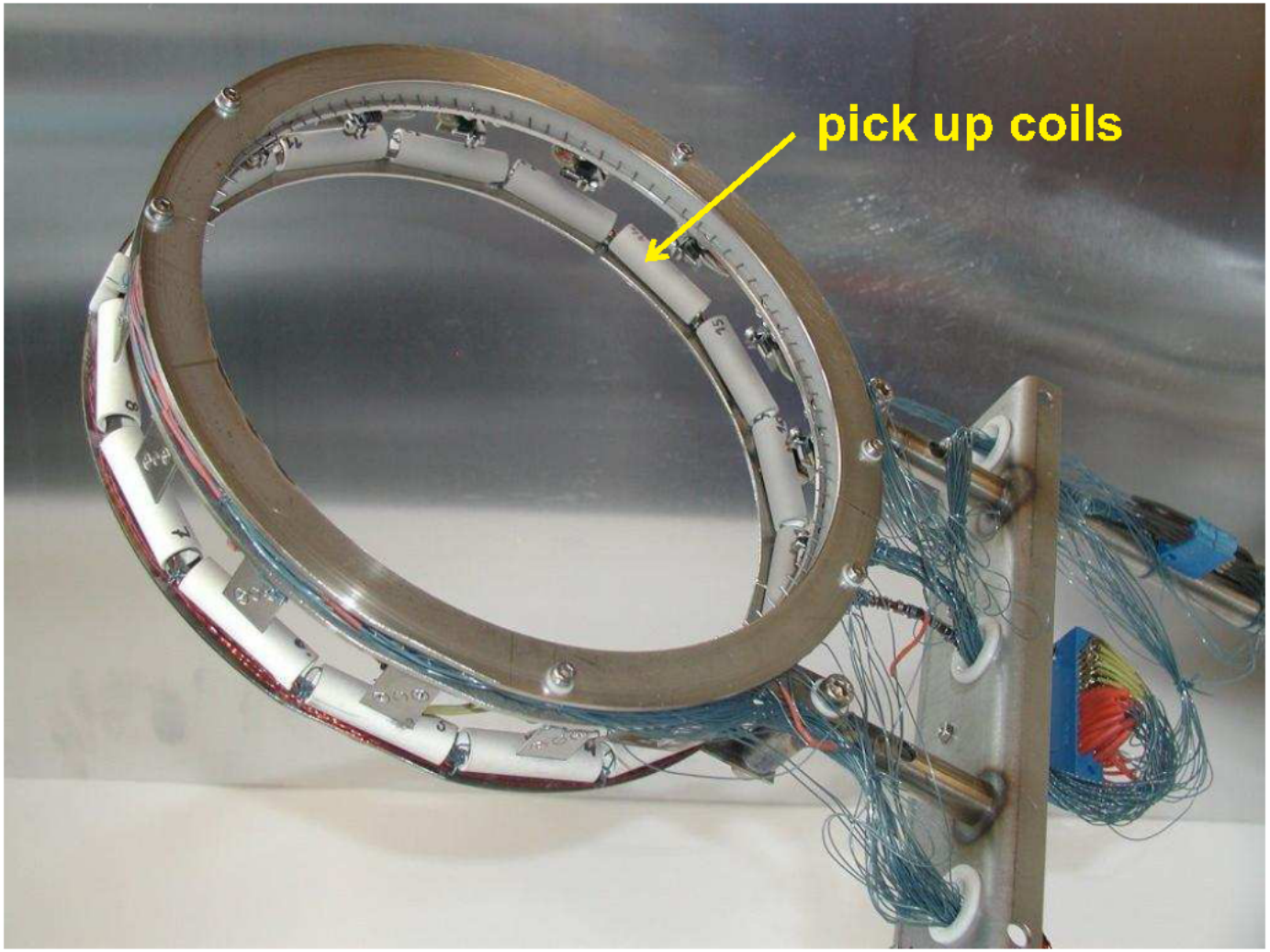

PROBE DIAGNOSTICS IN HIGH-TEMPERATURE PLASMA

Langmuir probes

2D matrix of cylindrical Langmuir probes

64 tips arranged in matrix 8 x 8.

Mach probe

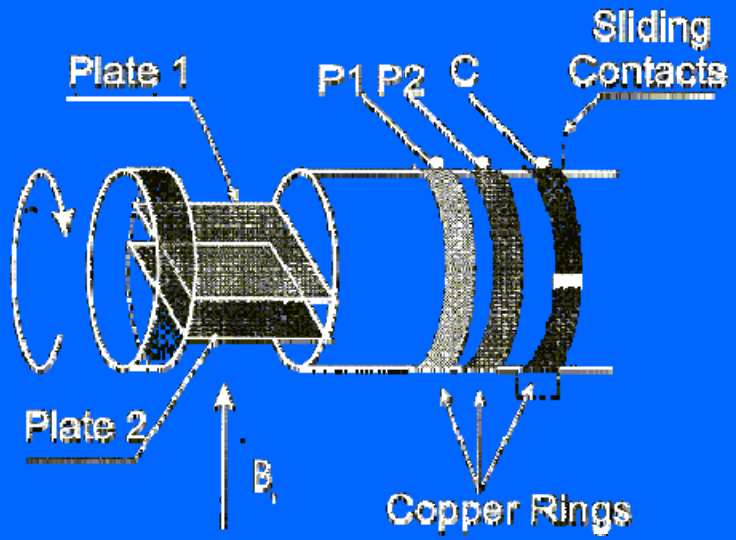

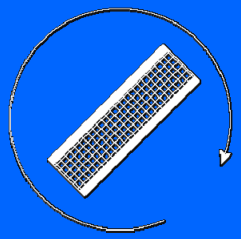

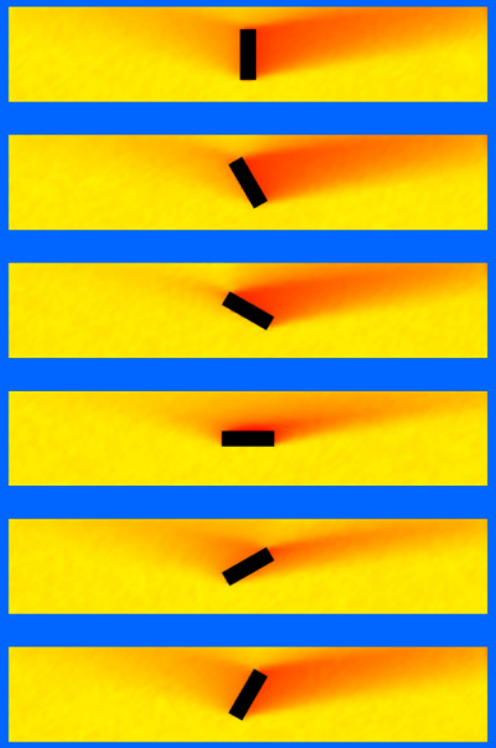

PROBE DIAGNOSTICS IN HIGH-TEMPERATURE PLASMA

Reciprocating Mach probe

SOL – scrape off layer

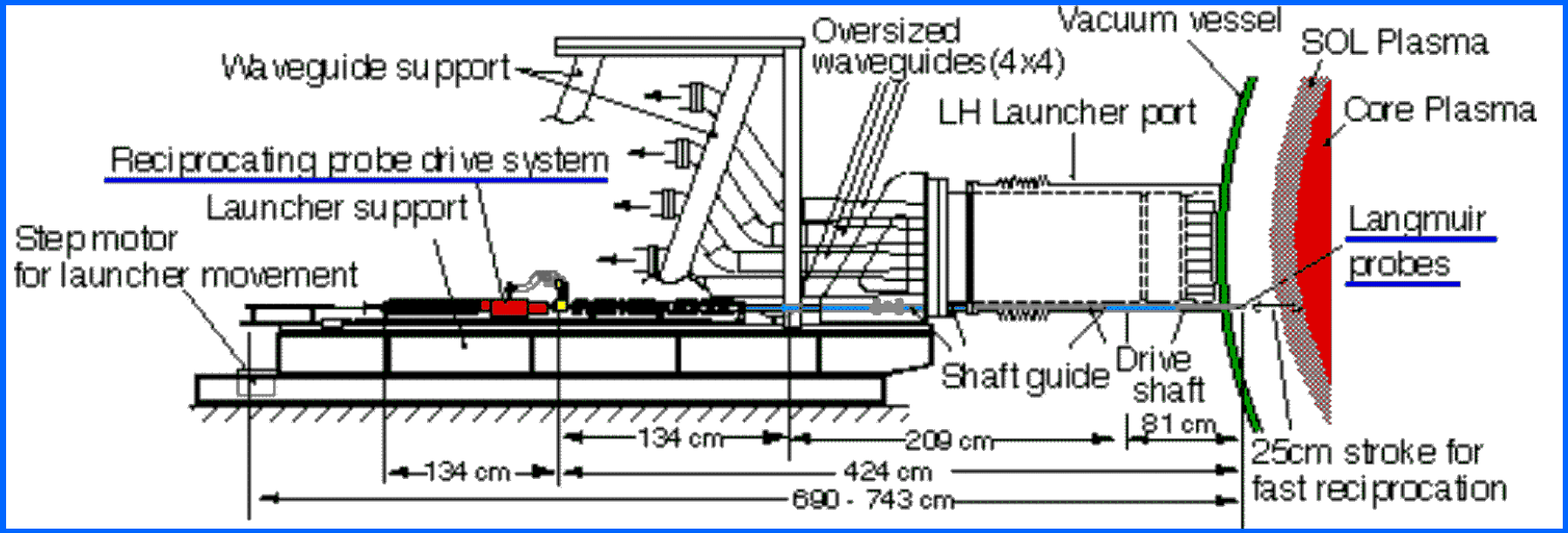

LH – lower hybrid frequency

At JET 3.7 GHz, λ=10cm, 12 MW

$$\omega = \left[\left(\Omega_i \Omega_e \right)^{-1} + \omega_{pi}^{-2} \right]^{-1/2}$$

PROBE DIAGNOSTICS IN HIGH-TEMPERATURE PLASMA

Gundestrup cauldron **is the largest known example of European Iron age (1st century BC) silver work (diameter 69 cm, height 42 cm).**

What does it have to do with probes?

PROBE DIAGNOSTICS IN HIGH-TEMPERATURE PLASMA

Gundestrup probe

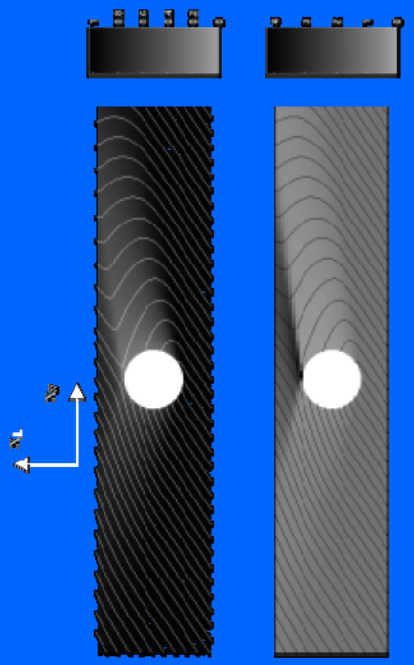

Ion density Ion temperature

Magnetized plasma
Mach numbers $M_{||}$= 0.4 and $M_{\perp}$= 0.3.

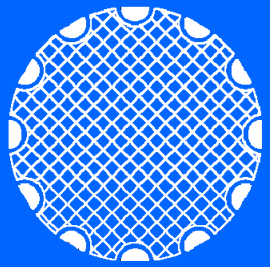

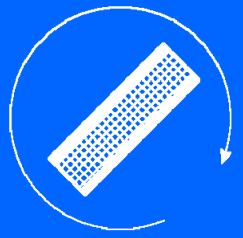

Gundestrup probe Mach probe

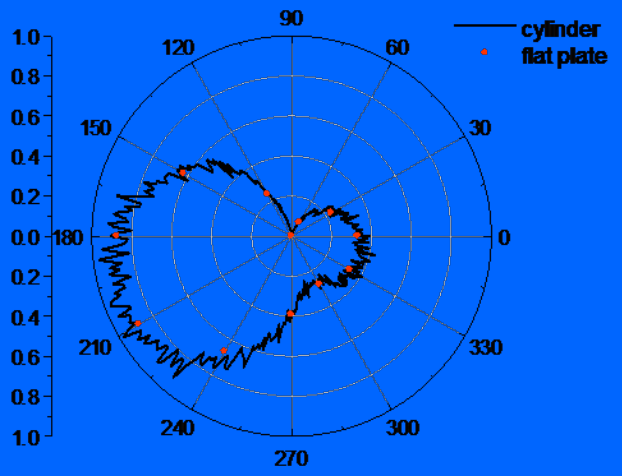

Angular distribution of ions measured
by Gundestrup probe (points) and Mach probe (line).

PROBE DIAGNOSTICS IN HIGH-TEMPERATURE PLASMA

Real Gundestrup probe (Castor)

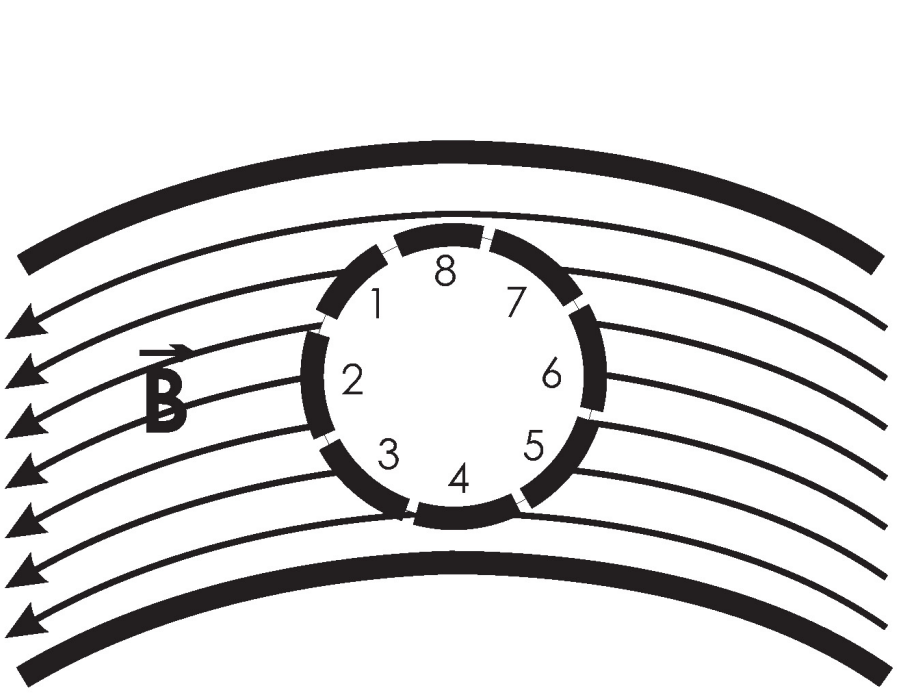

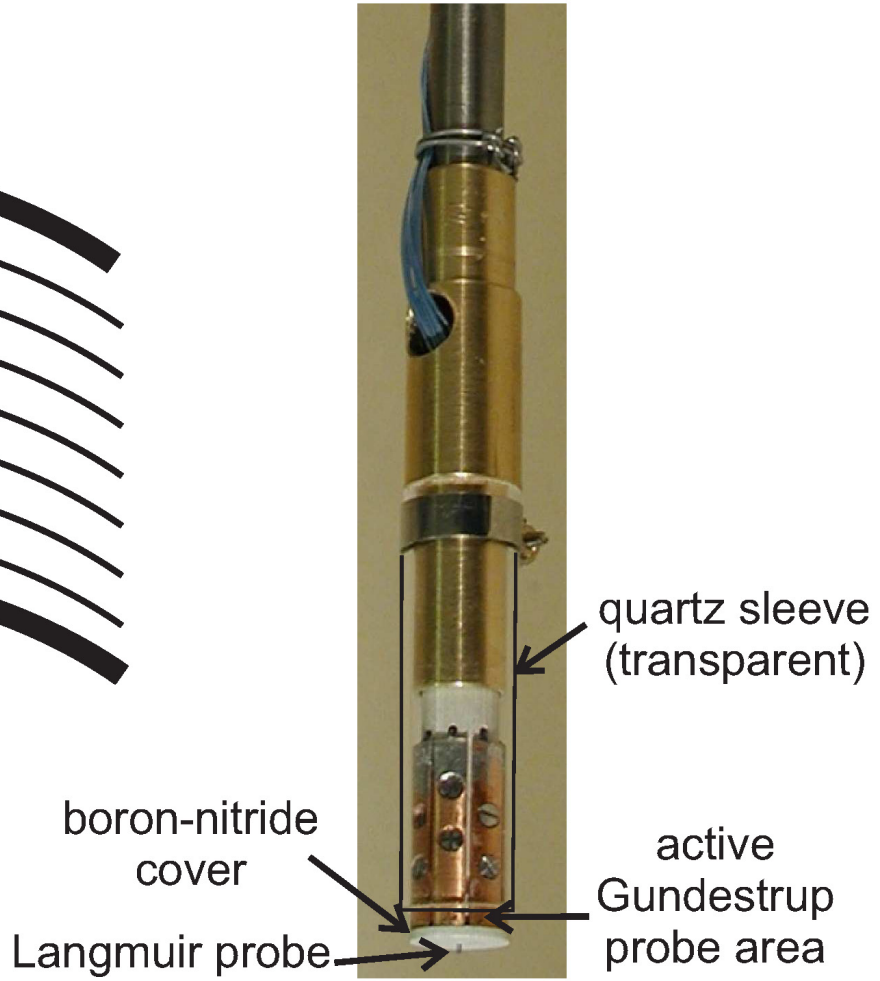

PROBE DIAGNOSTICS IN HIGH-TEMPERATURE PLASMA

Real Gundestrup probe

PROBE DIAGNOSTICS IN HIGH-TEMPERATURE PLASMA

Tunnel probe

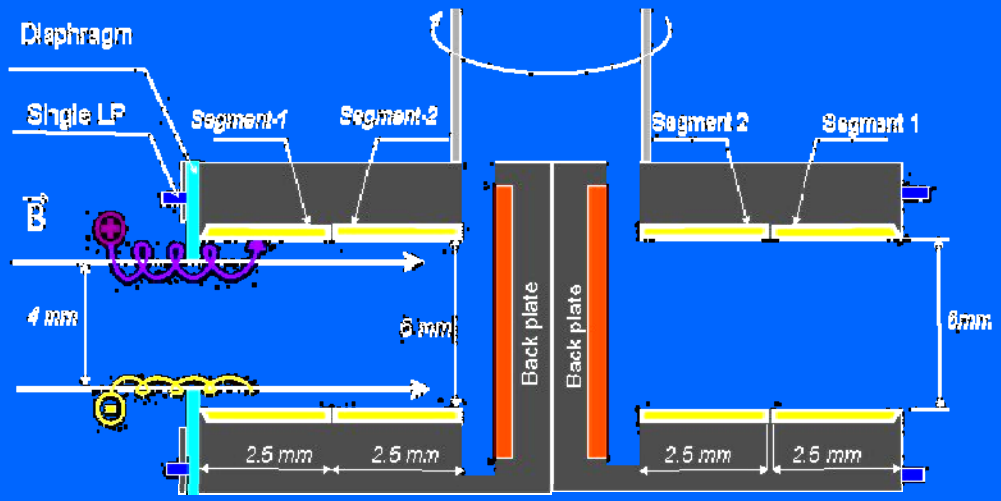

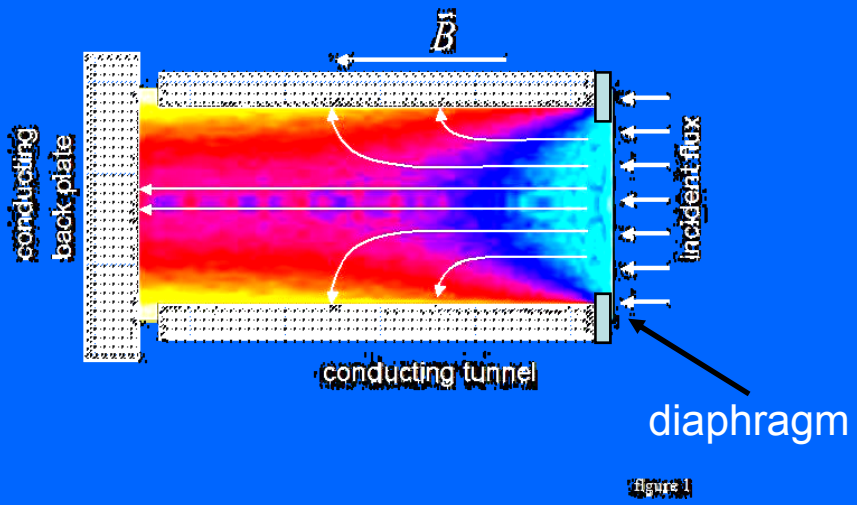

Last three types of probes are based on various Larmor radii or electrons and ions in magnetic field.

Tunnel probe consists of tunnel electrodes shielded by diaphragm.

For better resolution the electrodes can be divided into 2-3 parts: back plate and 1-2 cylindrical segments.

PROBE DIAGNOSTICS IN HIGH-TEMPERATURE PLASMA

Real tunnel probe

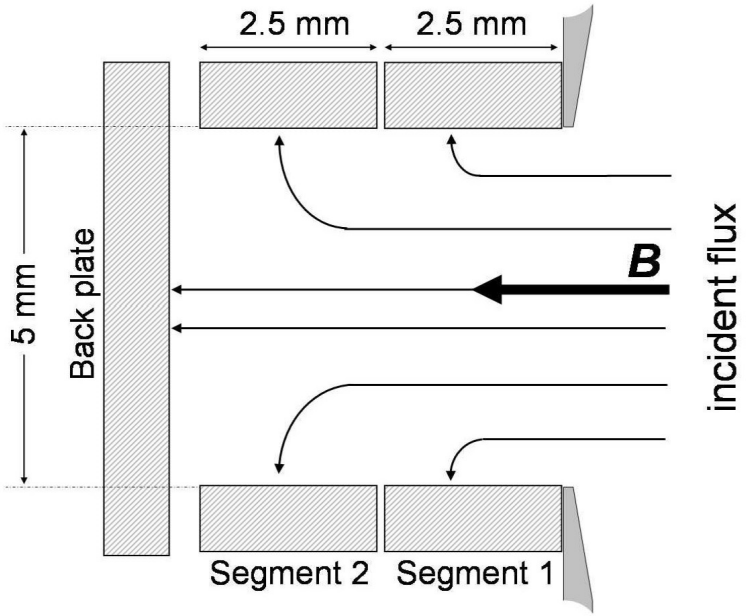

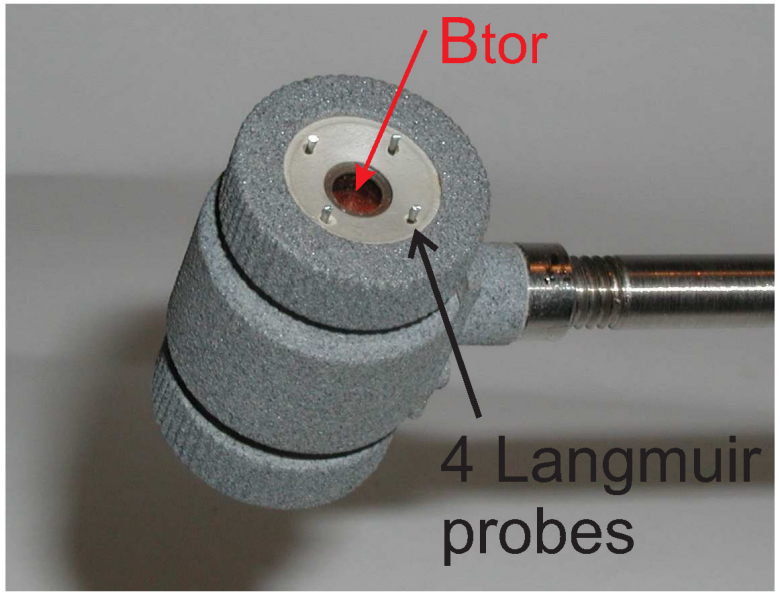

PROBE DIAGNOSTICS IN HIGH-TEMPERATURE PLASMA

Ion sensitive (Katsumata) probe

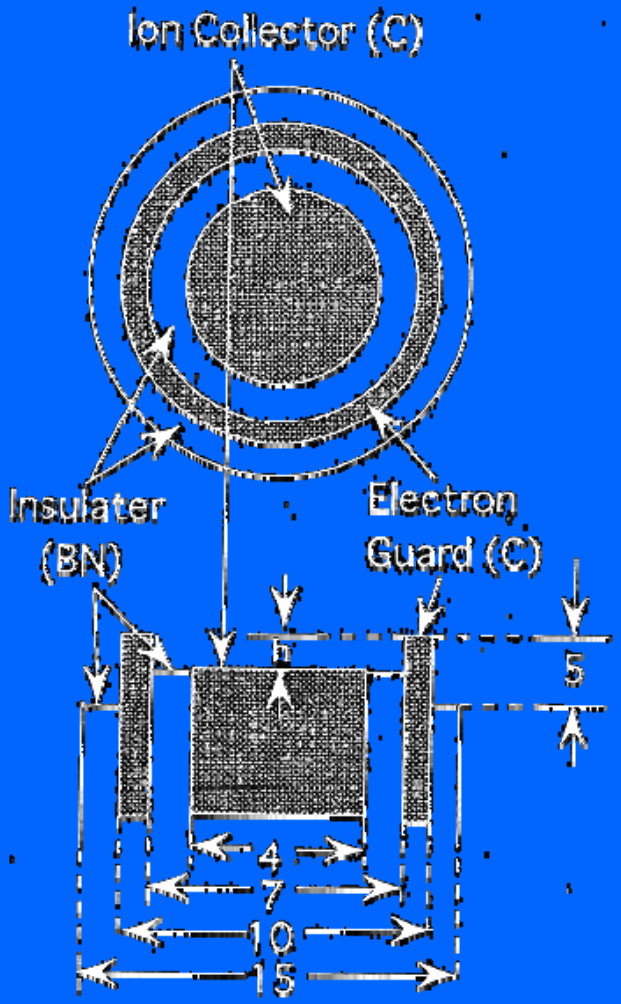

Tunnel probe

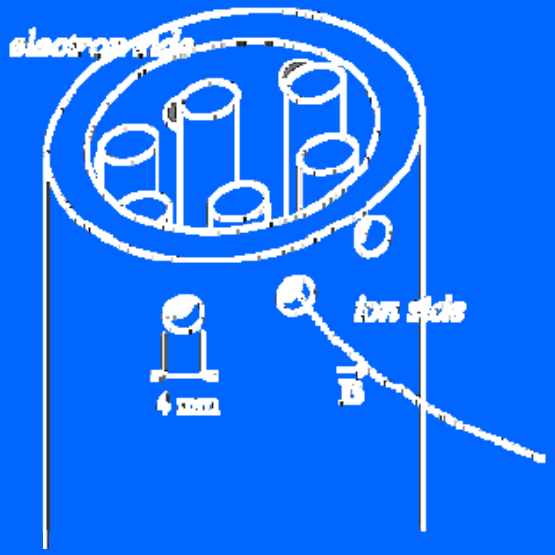

PROBE DIAGNOSTICS IN HIGH-TEMPERATURE PLASMA

Ball-pen probe – direct estimation of plasma potential in strongly magnetized plasma

$$V_{fl} = \Phi - \left(\frac{kT_e}{e} \right) \ln(R)$$

R is the ratio of the electron and ion saturated currents, $R=I_{sat}^{-}/I_{sat}^{+}$

For emissive probe $R=I_{sat}^{-}/(I_{sat}^{+}+I_{ee}^{-})$, I_{ee}^{-} is the emitted current (adjustable by probe heating). When $I_{sat}^{-} \approx I_{ee}^{-}$ the ln(R) is close to zero.

Alternative approach, which can be used only in magnetized plasmas, is a concept of the Ball-pen probe.

PROBE DIAGNOSTICS IN HIGH-TEMPERATURE PLASMA

Ball-pen probe – direct estimation of plasma potential in strongly magnetized plasma

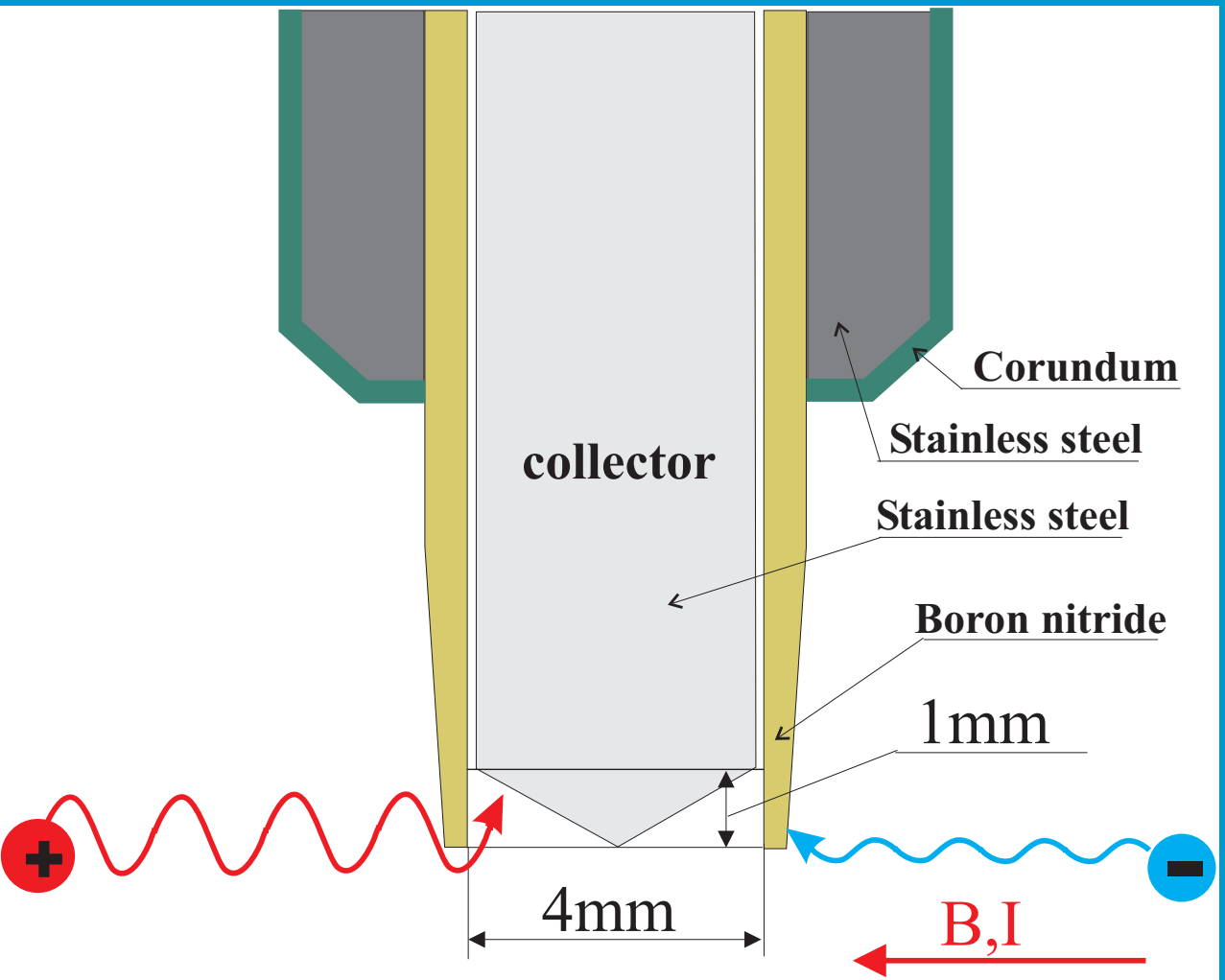

The collector does not have to be movable => probe has robust construction => great prospect for application.

PROBE DIAGNOSTICS IN HIGH-TEMPERATURE PLASMA

Ball-pen probe – direct estimation of plasma potential in strongly magnetized plasma

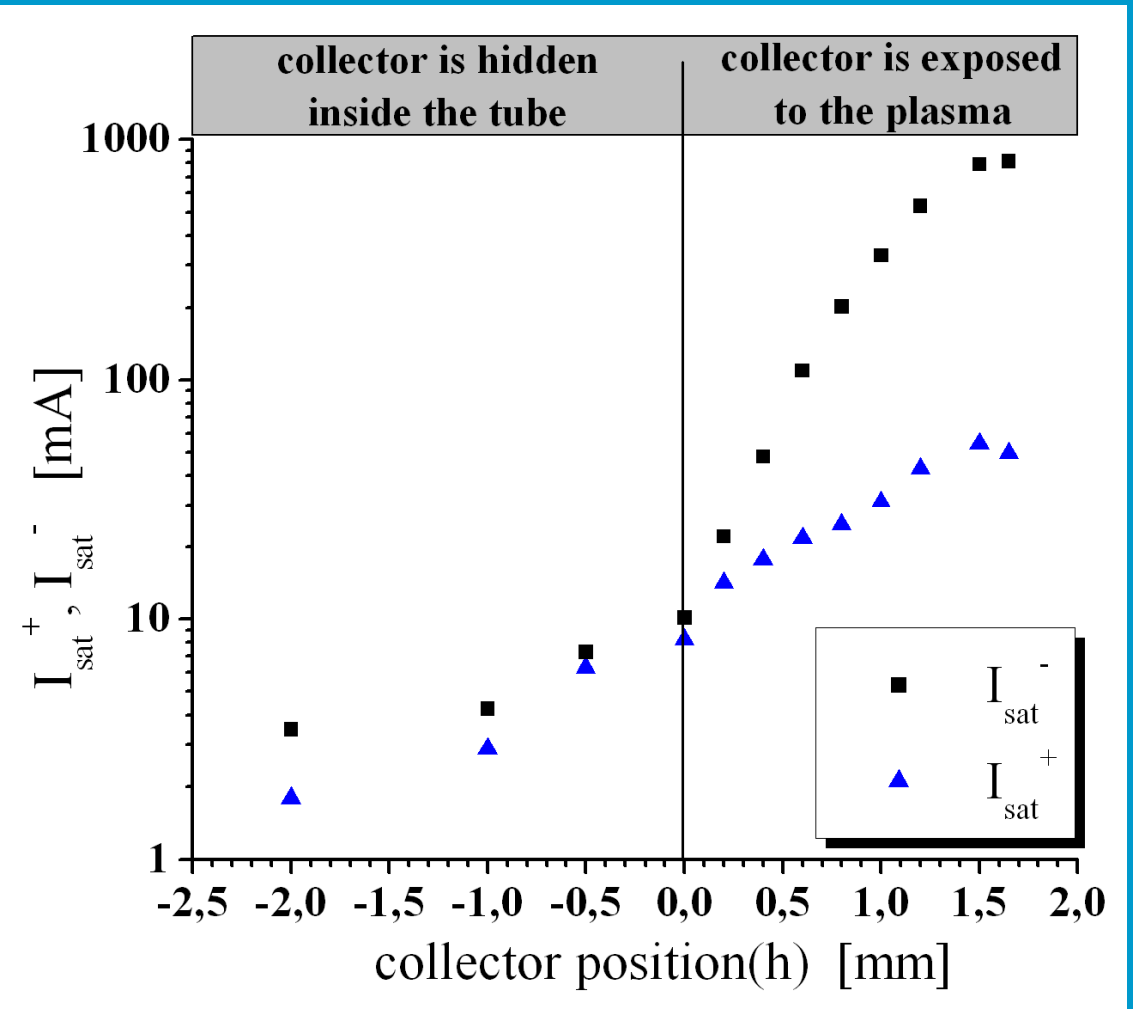

Dependence of the electron and ion saturated current on the collector position. When the collector is retracted both saturated currents are similar => R->0 !!!

PROBE DIAGNOSTICS IN HIGH-TEMPERATURE PLASMA

Ball-pen probe – direct estimation of plasma potential in strongly magnetized plasma

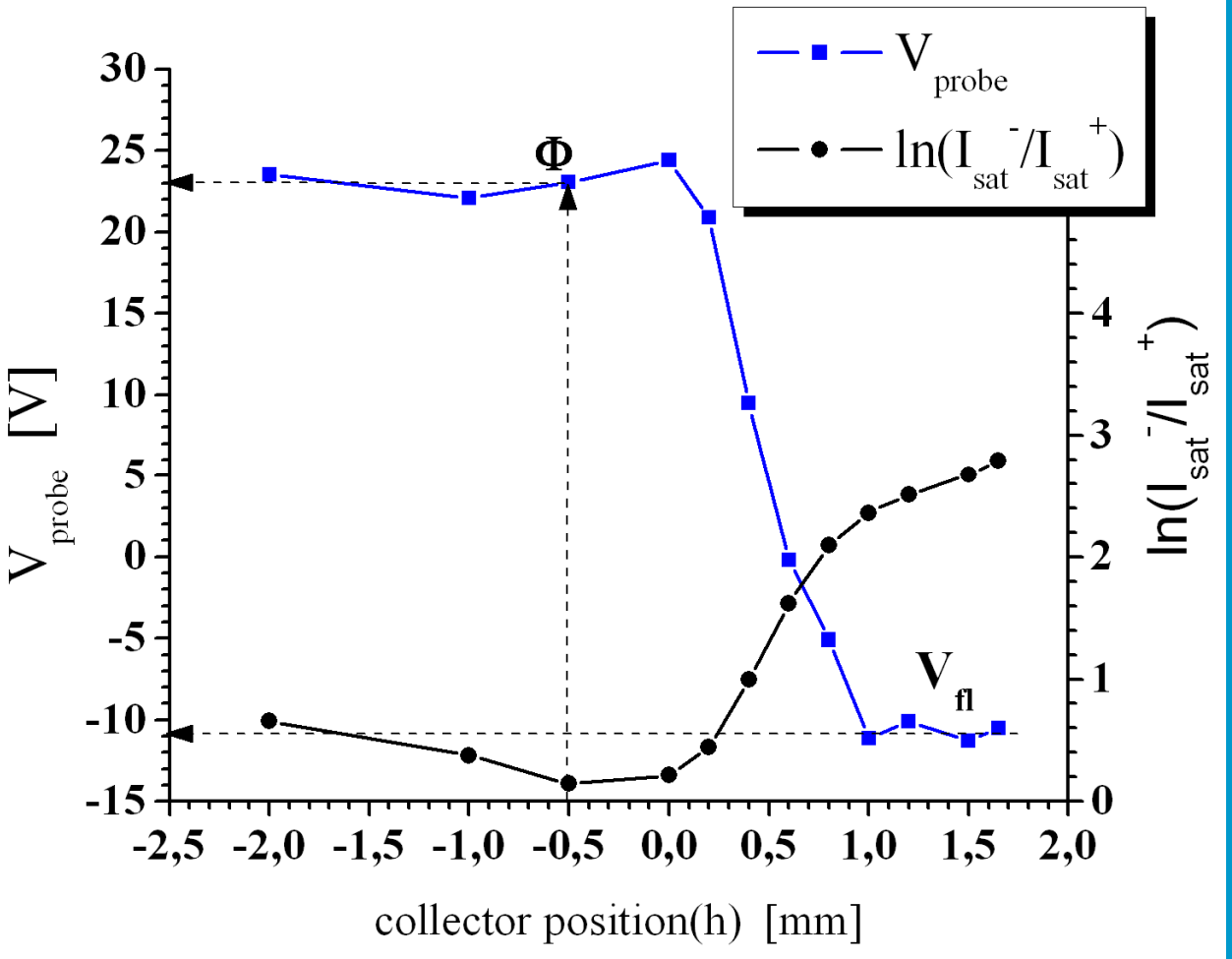

Dependence of the floating potential of the BPP on the collector position. When the collector is retracted, R->0 and Φ approaches to plasma potential !!!

PROBE DIAGNOSTICS IN HIGH-TEMPERATURE PLASMA

Ball-pen probe – direct estimation of plasma potential in strongly magnetized plasma

Construction of ball-pen probe in CASTOR tokamak.

J. Adámek et al., Czech.J.Phys. 54(2004)C95

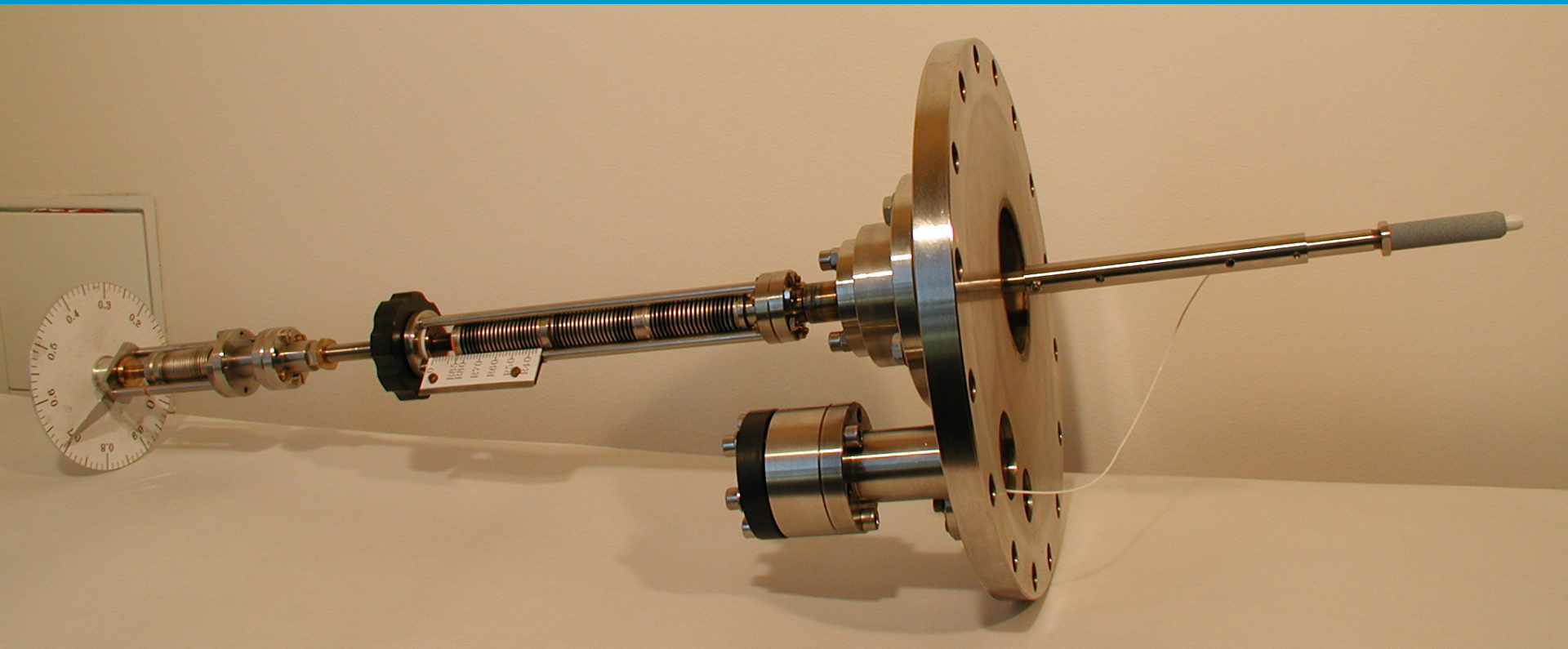

PROBE DIAGNOSTICS IN HIGH-TEMPERATURE PLASMA

Ball-pen probe – comparative measurements of plasma potential in CASTOR tokamak

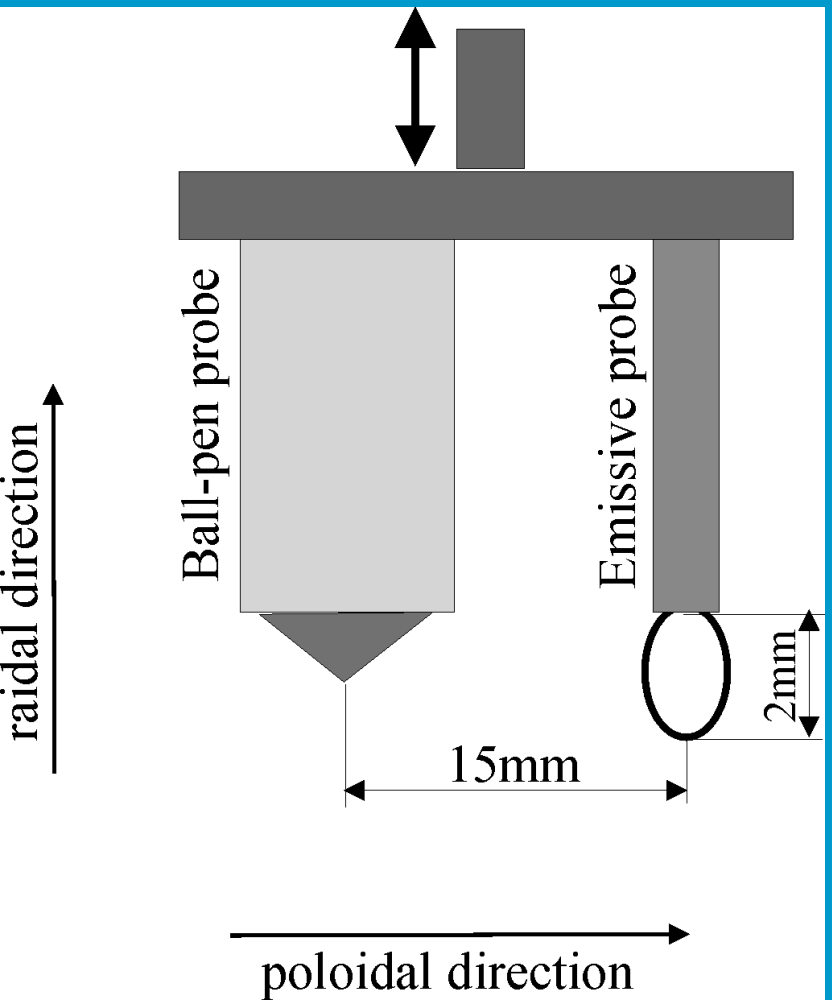

Schematics of the construction of combined emissive and ball-pen probe for comparative measurements of plasma potential.

J. Adámek et al., Czech.J.Phys. 54(2004)C95

PROBE DIAGNOSTICS IN HIGH-TEMPERATURE PLASMA

Characteristics of ball-pen and emissive probes in CASTOR tokamak edge plasma

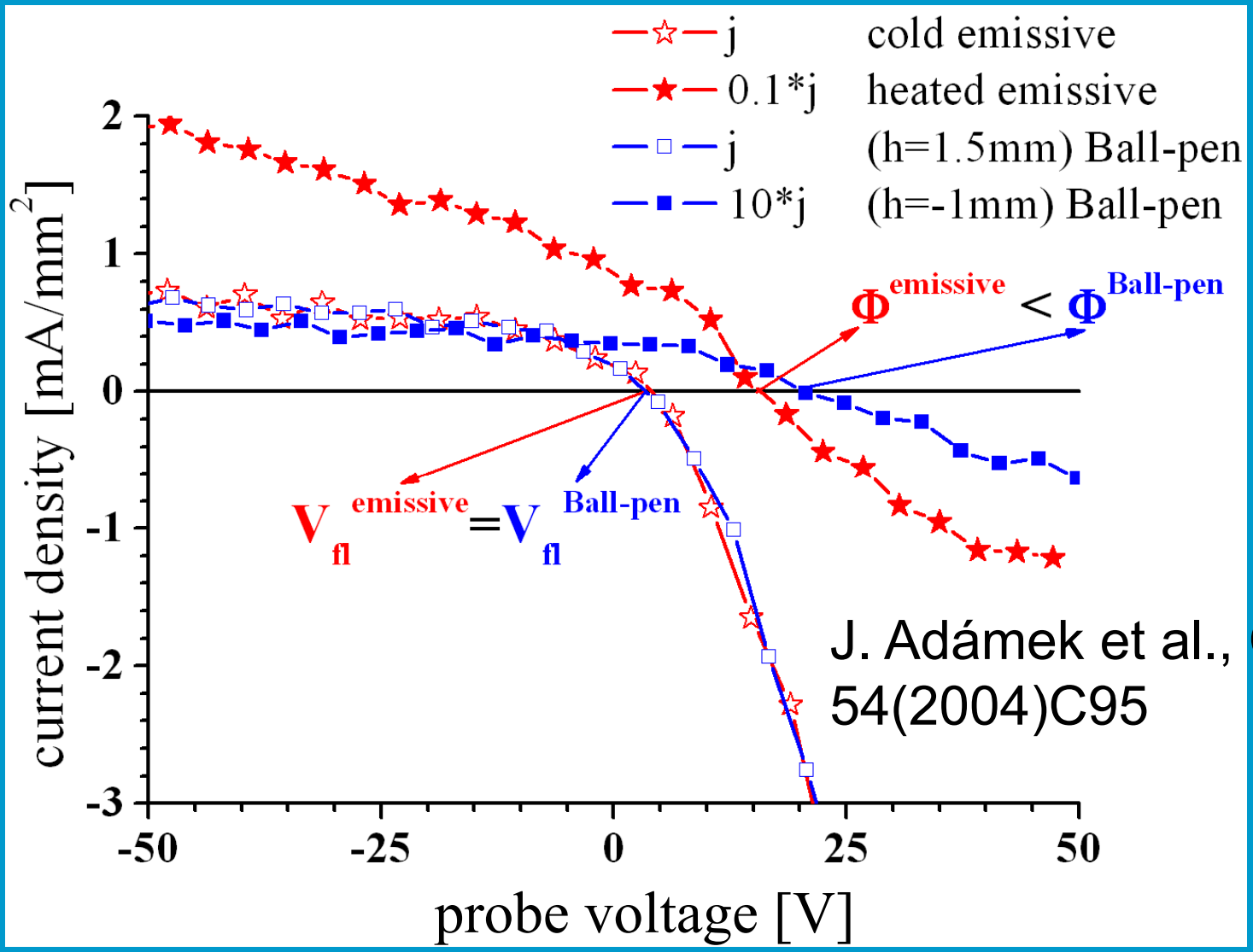

J. Adámek et al., Czech.J.Phys. 54(2004)C95

PROBE DIAGNOSTICS IN HIGH-TEMPERATURE PLASMA

Floating potential of ball-pen (red) and emissive probe (blue) in CASTOR tokamak edge plasma

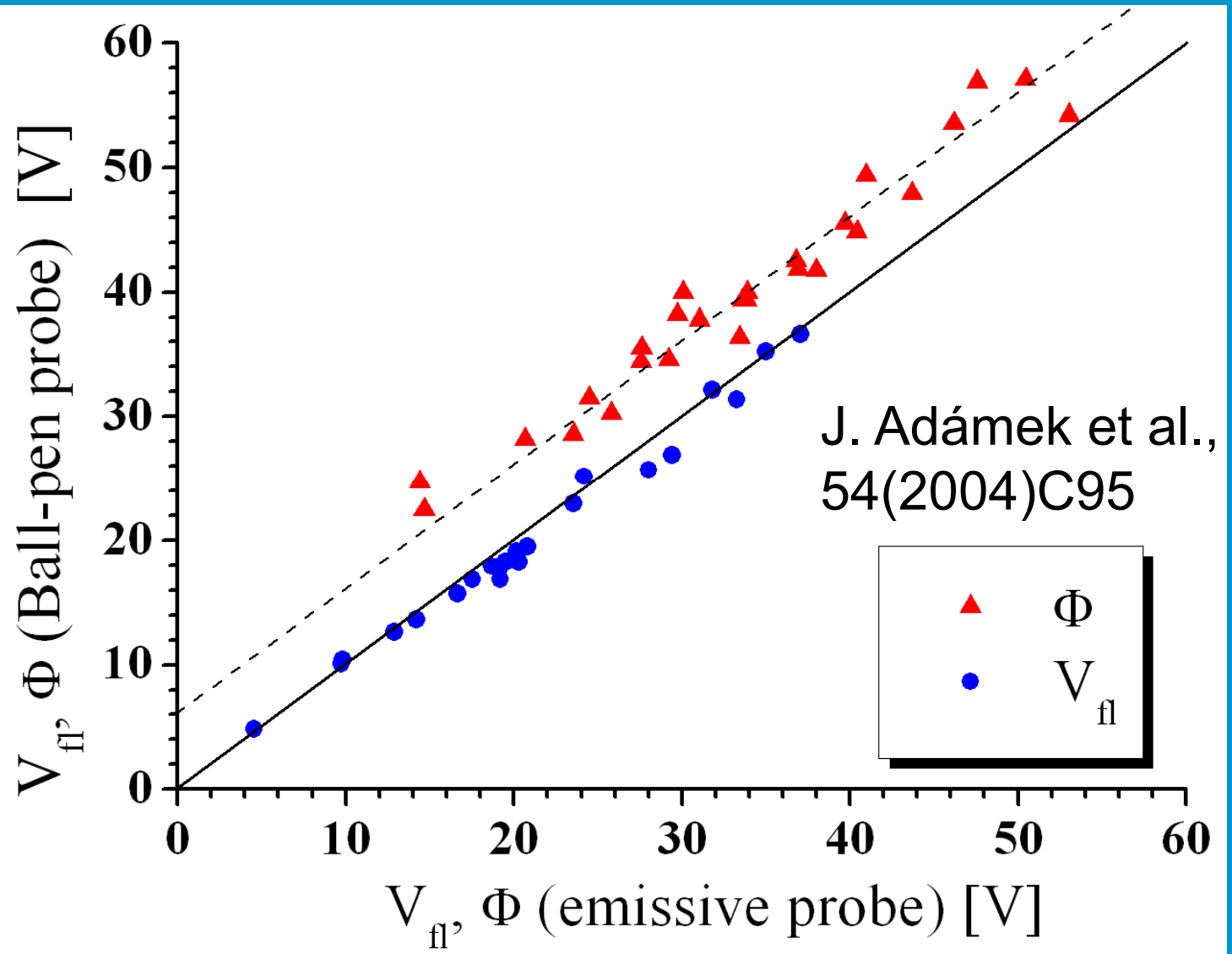

J. Adámek et al., Czech.J.Phys. 54(2004)C95

Conclusion

- Langmuir probe and the probe in general is an indispensable diagnostics also for the fusion relevant plasma.

Mass-spectrometer principles

FTMS, Fourier-transform mass-spectrometers

Gyroradius $r_c = mv / q_0 B$

Cyclotron frequency $f_c = q_0 B / \pi m$

Ions with different m / q absorb energy from RF field and emit „their“ cyclotron frequency. Frequency „mix“ is analysed by FFT hence yielding mass-spectrum of ions in the cell.

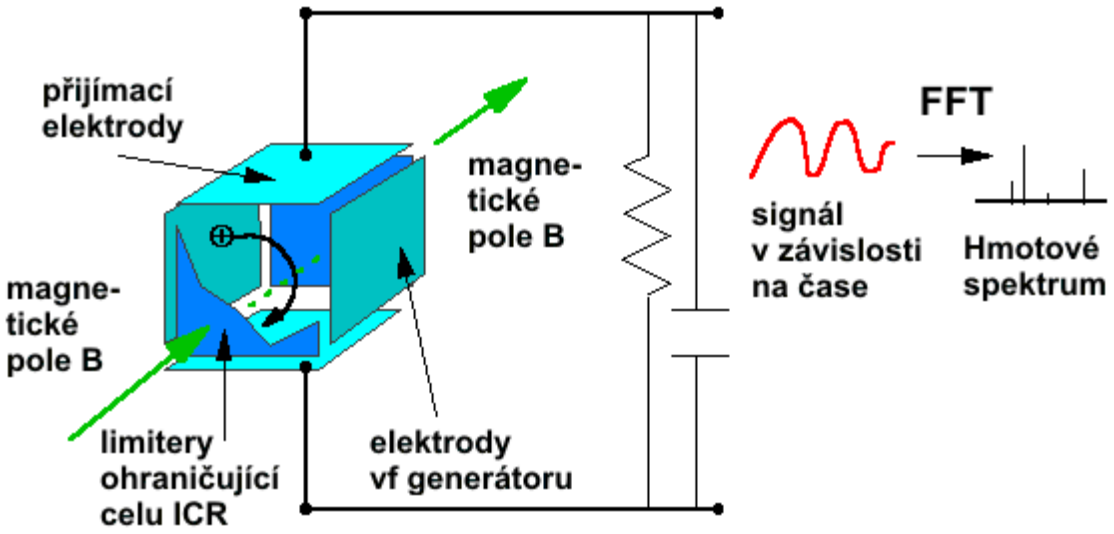

FTMS features and advantages (1)

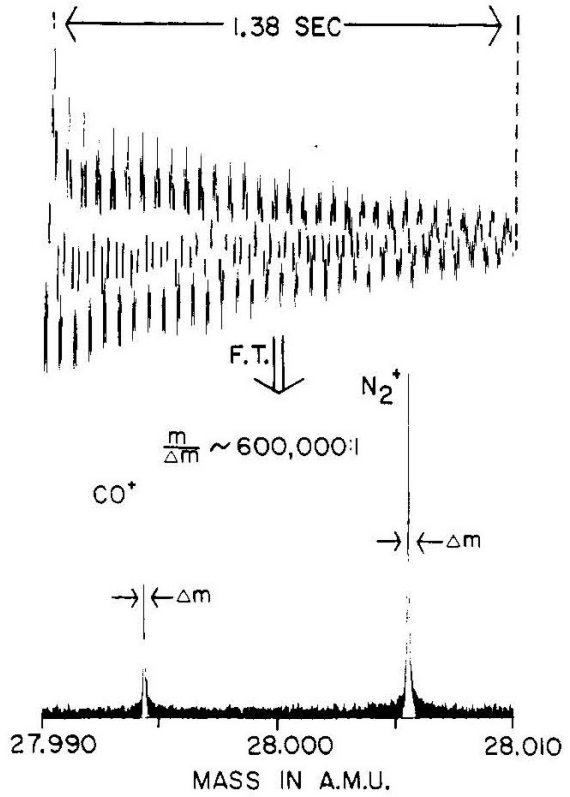

Time-domain (top) and frequency-domain (bottom) ion cyclotron signals for ions of two m/q ratios. Note that the slow oscillation due to ions of higher mass and the rapid oscillation due to ions of lower mass are seen simultaneously in the time-domain heterodyne "beat pattern" (left). Thus, digitization followed by discrete Fourier transform of the time-domain data gives a frequency-domain representation in which the whole mass spectrum is obtained at once (right). Note that FT/ICR performed at a modest magnetic field strength (3.0 T) can produce both high sensitivity (sample pressure was only 6×10^{-9} torr) and high mass resolution (N_2^+ and CO^+ differ in mass by only about 0.011 amu) simultaneously. (Data obtained by T.-C. L. Wang.)

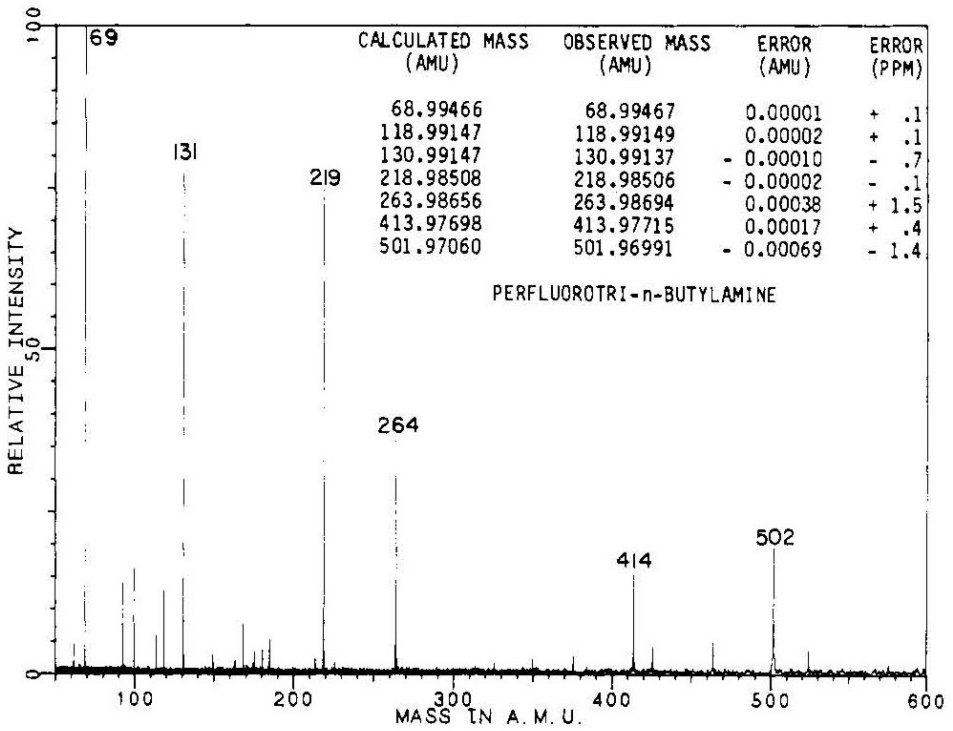

Fourier transform mass spectral calibration over approximately one decade in mass, for time-domain data obtained in approximately 0.1 s, using a Nicolet FT/MS 1000 instrument with 1-in. rectangular cell. For observed peak frequencies, ν, mass calibration was based on least-squares best-fit to an equation of the form $m = (A/\nu) + B/(\nu^2)$. The calculated mass for each singly charged positive ion peak was obtained by subtracting the mass of an electron from the total mass of the most abundant isotopes for each peak. [Reprinted with permission from Marshall, A. G. Texas A&M ICCP Symp., April 1985 (Texas A&M University Press).]

FTMS features and advantages (2)

FT/ICR Features for Analytical Mass Spectrometry

sample pressure	(0.1–1000) × 10^{-9} torr
mass resolution	to 4 000 000 at m/z 131
speed	0.01 –1 s/scan
EI/CI/laser/Cs^+	one source
chemical ionization	no reagent gas
MS/MS/...	one spectrometer
+/− ions	one switch
upper mass limit	ca. 100 000 amu
slits	none
high voltage	none
GC/MS	high dynamic mass resolution
automation	

Source (1 and 2):
AG Marshall,
Acc. Chem. Res. **1985,** *18,* 316-322

Advantages of Fourier Transform over Continuous-Wave Spectrometry

feature	improvement factor	applicable to
speed	10 000	IR, NMR, MS
signal-to-noise	100	IR, NMR, MS
automation		IR, NMR, MS
double resonance	no. of coupled spins or ions	NMR, MS
resolution	10 000	MS
upper mass limit	30	MS

FTMS features and advantages (3)

Product	apex-Qe	Explorer, QFT, ProMALDI	LTQ FT
Company	Bruker Daltonics, Inc. 978-663-3660 www.bdal.com	IonSpec Corp. 800-438-3867 www.ionspec.com	Thermo Electron 408-965-6000 www.thermo.com
Price (U.S.D.)	>$750,000	$380,000–1,400,000	>$830,000
MS types	Qq and FTICR	Explorer and QFT: Qq and FTICR; ProMALDI: FTICR	Linear ion trap and FTICR
Ionization sources	ESI, MALDI, APCI, APPI	ESI, nanoESI, MALDI, AP-MALDI, APCI, EI/CI	ESI, nanoESI, MALDI, AP-MALDI, APCI, APPI
Magnets available (T)	7.0, 9.4, 12.0	4.7, 7.0, 9.4, 12.0	7.0
Mass range (*m/z*)	90–10,000	15–18,000	50–4000
Mass resolving power (*m*/Δ*m*, fwhm)	600,000 for $[M + 10H^+]^{10+}$ charge state of ubiquitin, *m/z* 857 (7.0 T)	ESI broadband mode: 1,130,000 at *m/z* 195 (9.4 T); MALDI broadband mode: 80,000 at *m/z* 8567 (9.4 T)	100,000 at *m/z* 400 (7.0 T)
Mass accuracy (ppm)	Internal: <1 External: <2	Internal: <0.5 External: <2	Internal: <1 External: <2 with automatic gain control
Fragmentation methods	CAD (in collision cell and in ICR cell), ECD, IRMPD	SORI-CAD, CID, ECD, IRMPD, nozzle skimmer dissociation	CID (in linear ion trap), ECD, IRMPD
			1 at a resolving power of 100,000 at *m/z* 400
			Parallel processing on a chromatographic timescale with 100,000 resolution every second in ICR cell and up to 5 concurrent MS/MS scans in linear ion trap

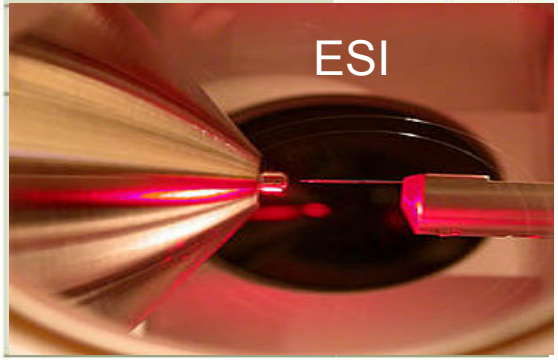

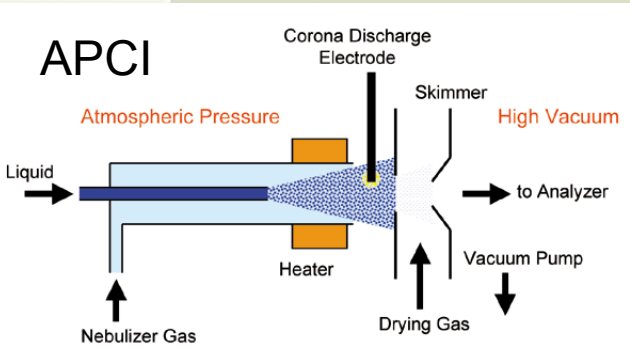

FTMS features and advantages (4)

sample spectrum

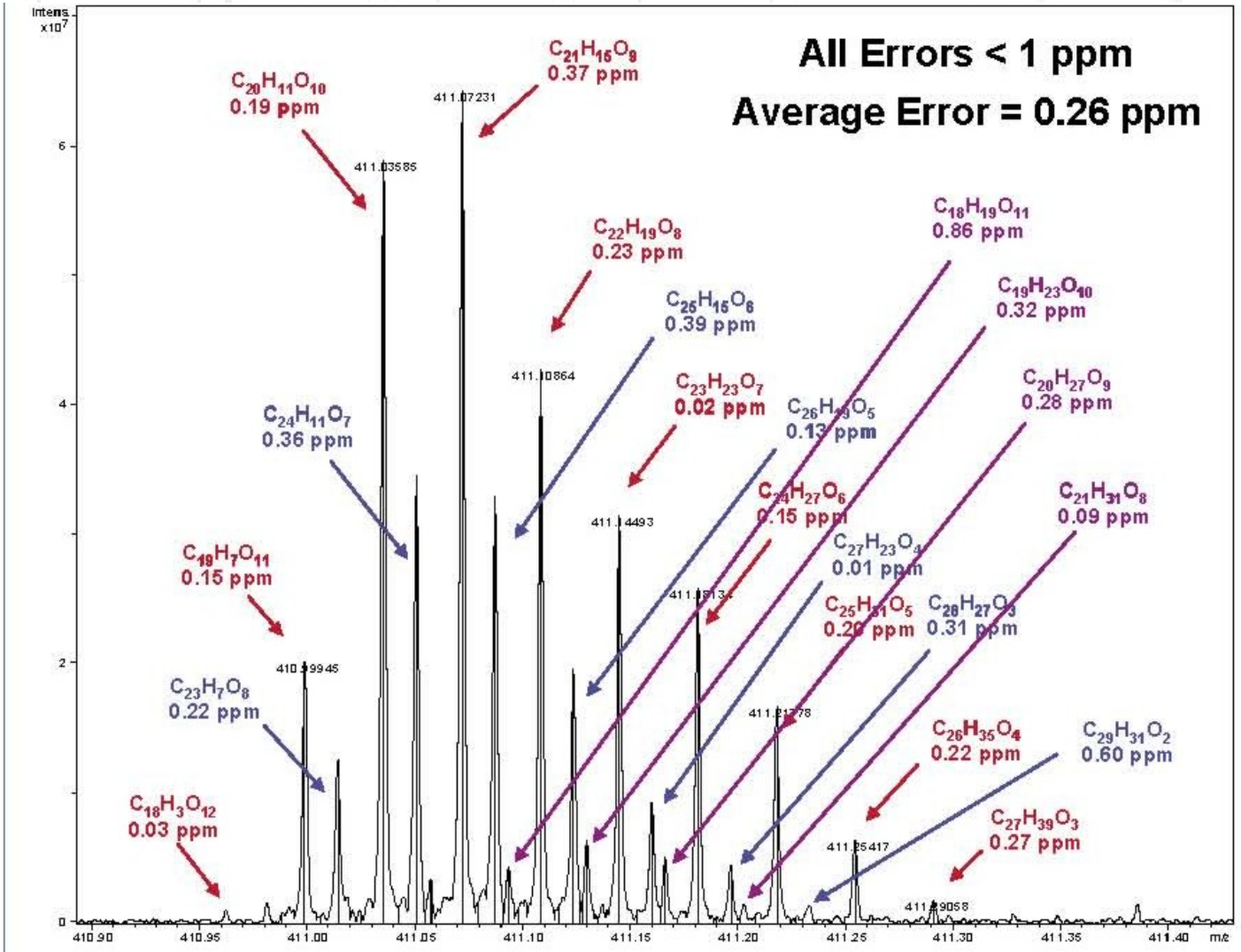

Source (3 and 4): Bruker Daltonics white papers

Mass-spectrometer principles

Magnetic-sector mass-spectrometers

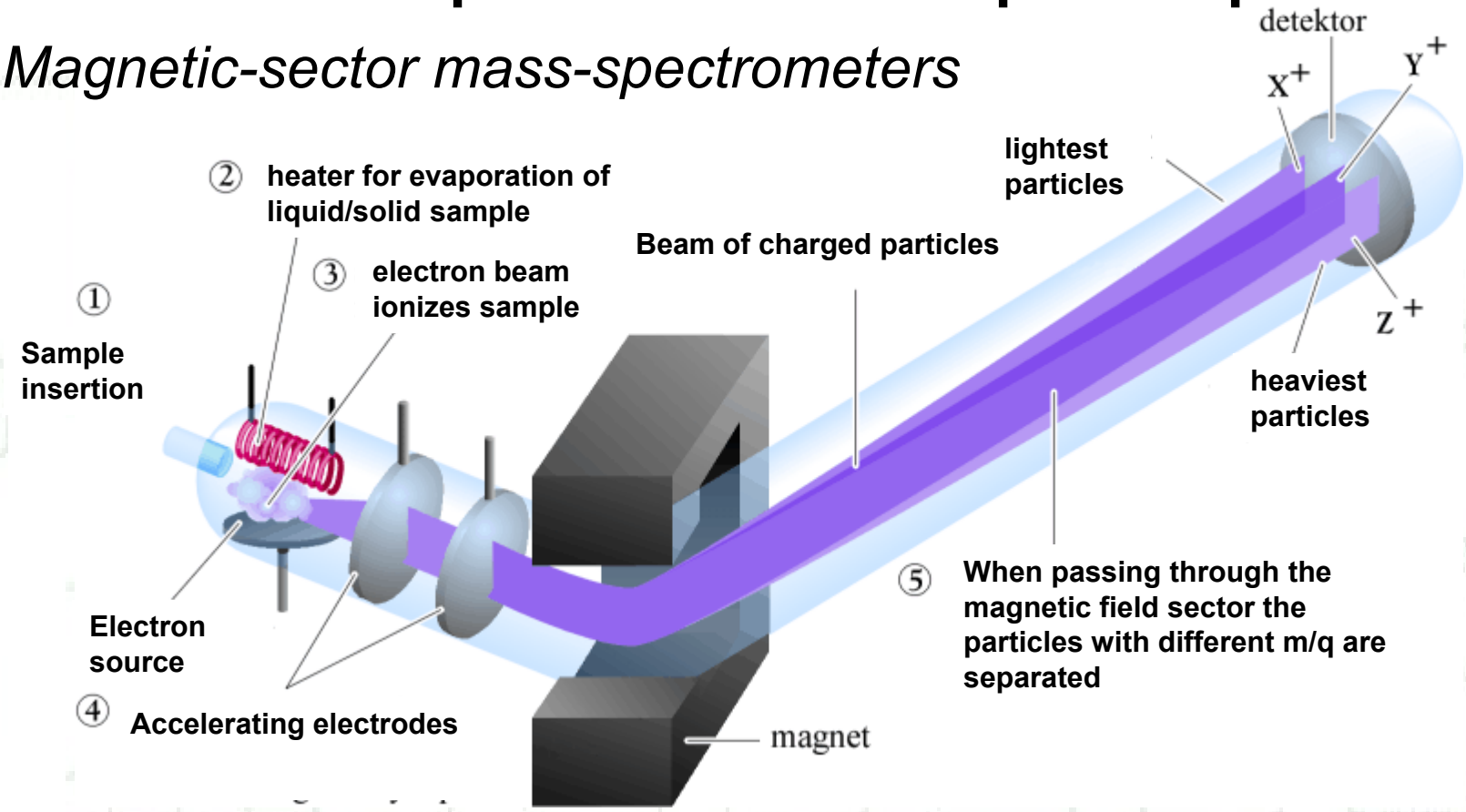

Ions are accelerated to energy $T=qV$ => have velocity $v=\sqrt{\frac{2qV}{m}}$.
Magnetic sector incurves their trajectories with radius r given by relation

$$qvB=\frac{mv^2}{r} \quad \Rightarrow \quad \frac{m}{q}=\frac{B^2r^2}{2V}$$

Mass-spectrometer principles

TOFMS, time-of-flight mass-spectrometers

Ions are accelerated to energy $T=qV$ => have velocity $v = \sqrt{\frac{2qV}{m}}$.

They pass the same route L, mass-indicator is time t.

Since $t = L / v$, hence $t = L\sqrt{\frac{m}{q}\frac{1}{2V}}$ and $\frac{m}{q} = \frac{2Vt^2}{L^2}$.

Removal of thermal velocity spread – reflectron.

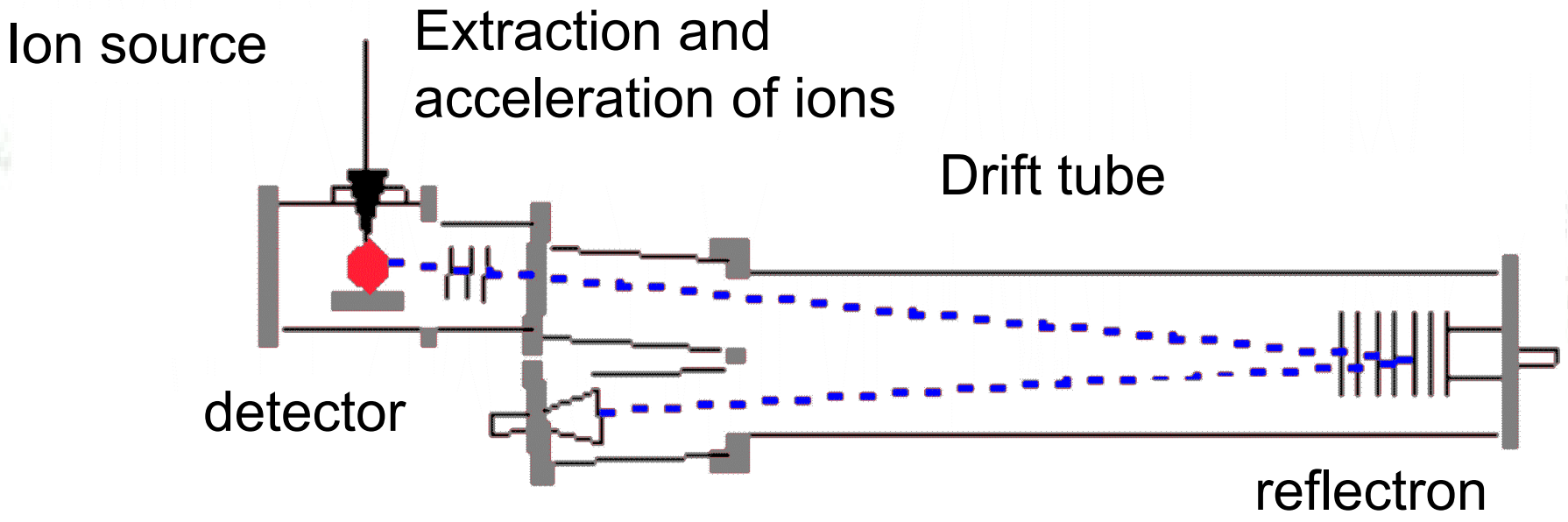

MALDI-TOF variants

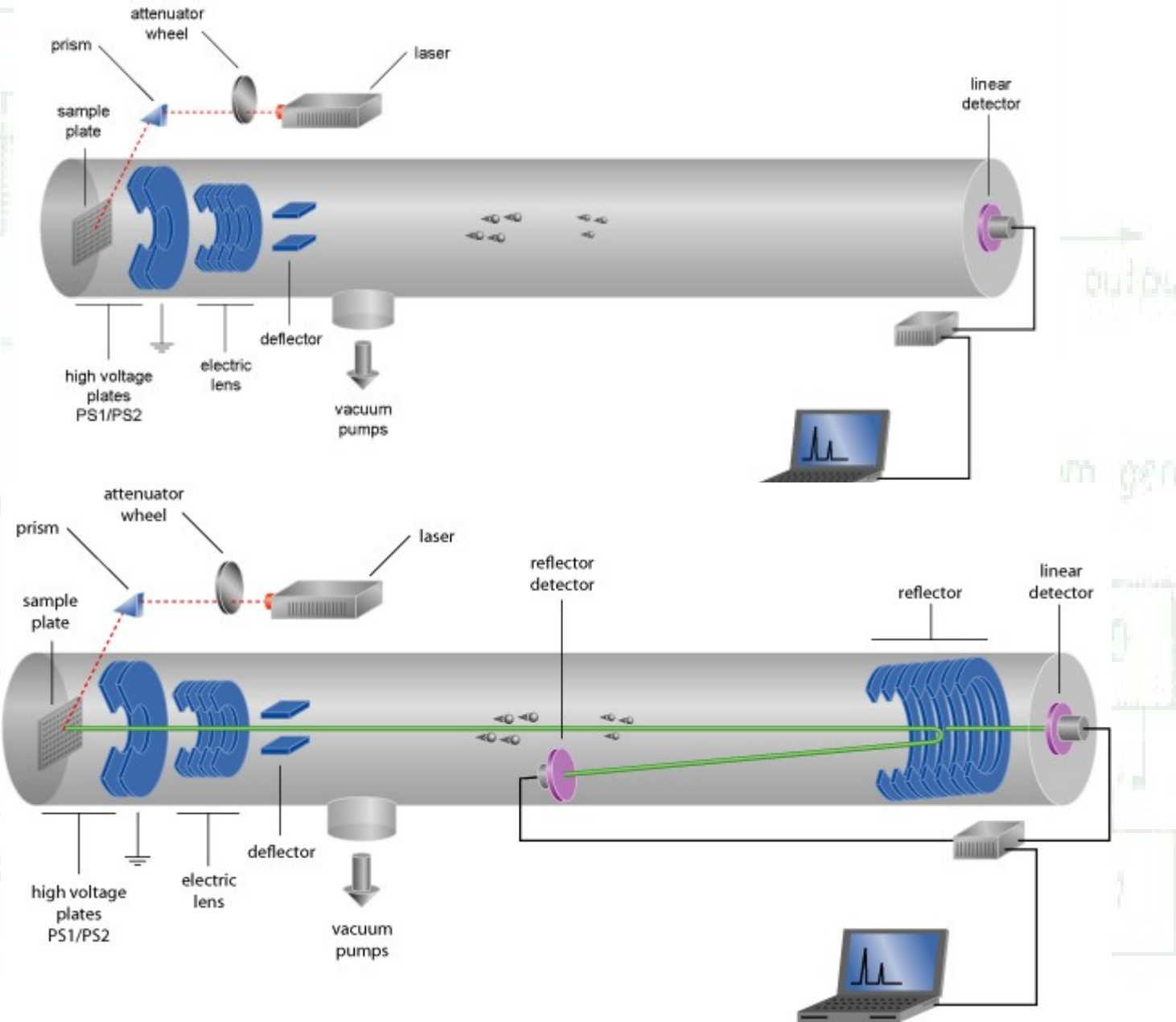

MALDI-TOF principle

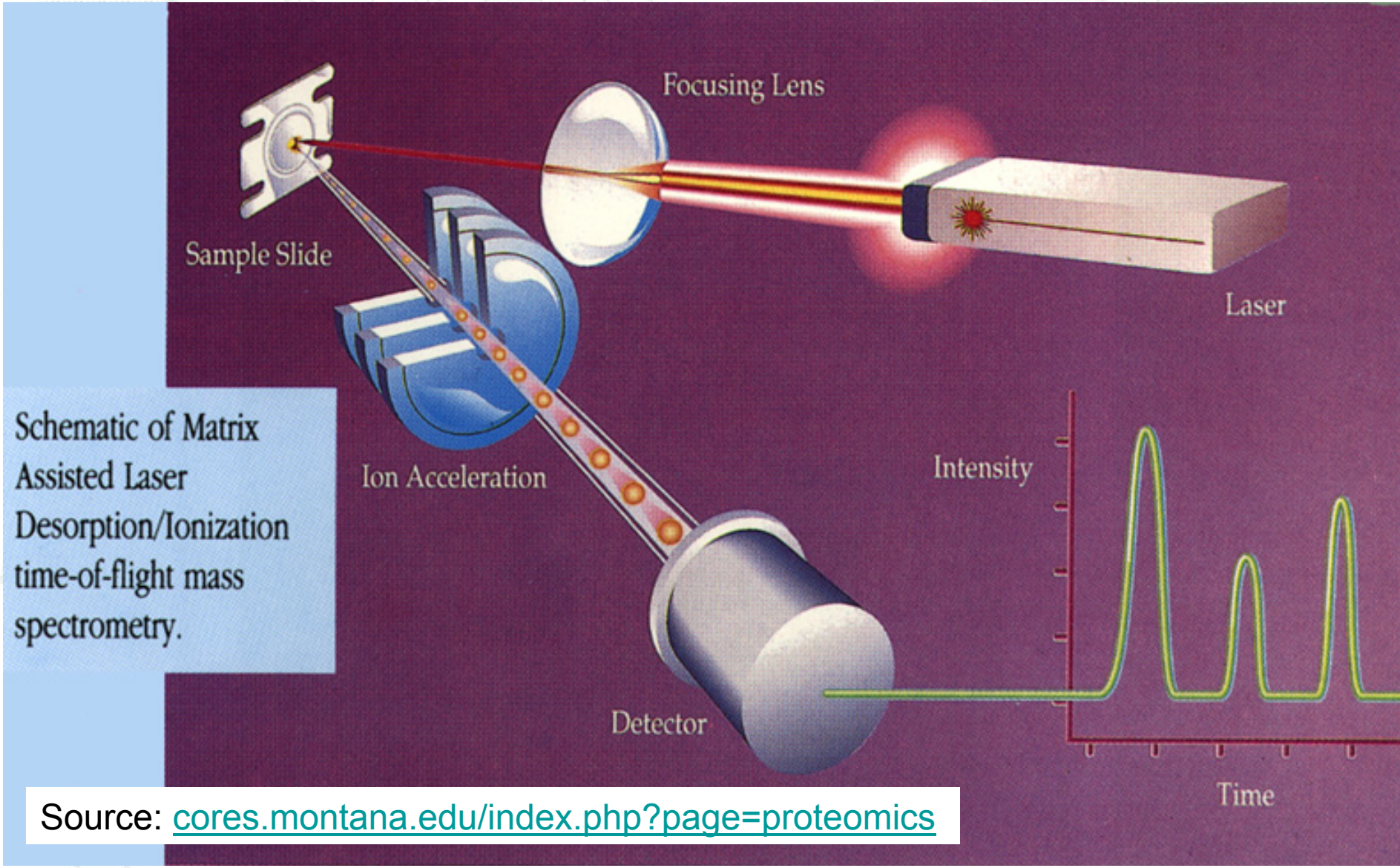

Schematic of Matrix Assisted Laser Desorption/Ionization time-of-flight mass spectrometry.

Source: cores.montana.edu/index.php?page=proteomics

Mass-spectrometer principles

Quadrupole mass-spectrometer

Mass spectrum is typically measured by varying amplitudes *U* (*dc* component) and *V (ac* component*)* while keeping constant the ratio *U*/*V* at constant frequency.
Mass resolution – stability diagram: A~U/m, Q~V/m.
Quadrupole transparency decreases with increasing resolution power (adjustable by varying the ratio U/V).

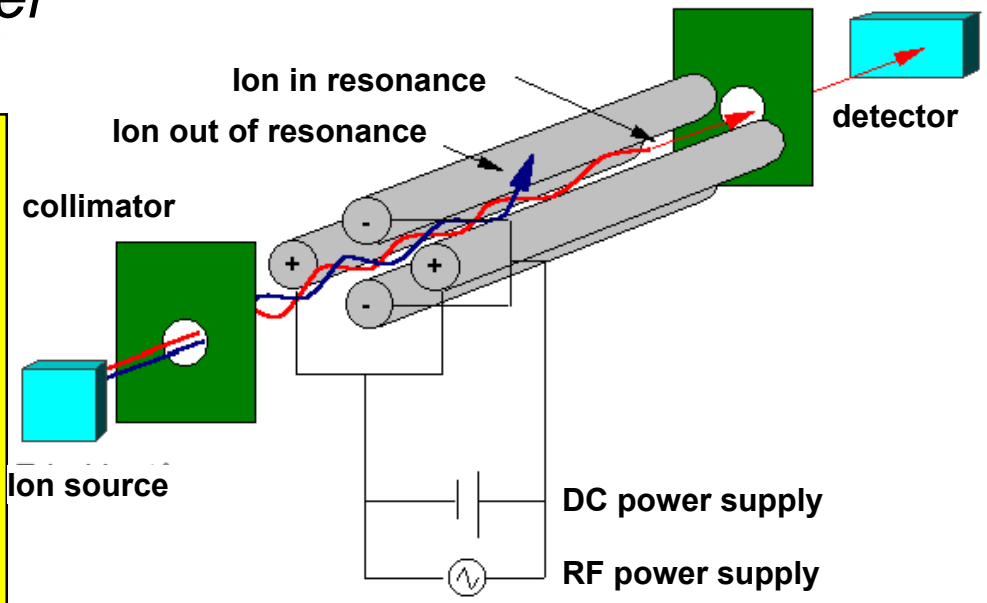

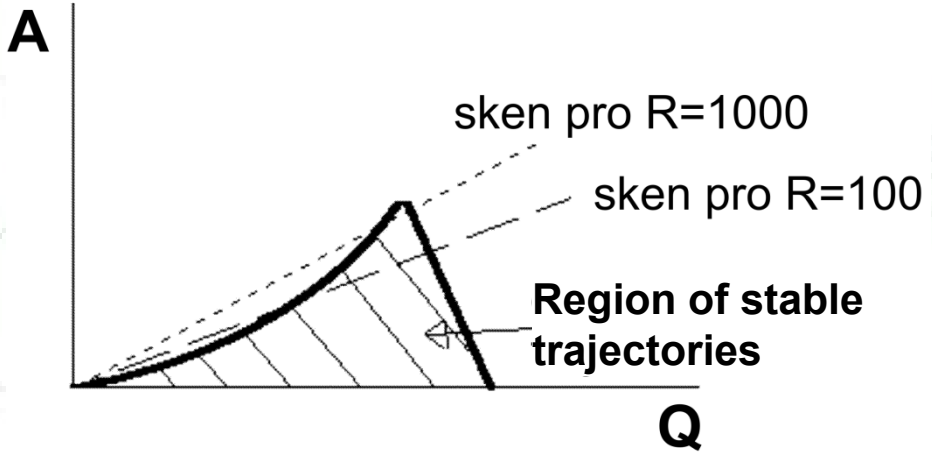

Detectors for mass-spectrometers

Channeltron

Channeltron mouth is polarized negatively with respect to its tail by approx. 2,5 kV. For positive ions – plus pole of HT supply grounded => negative mouth attracts positive ions.

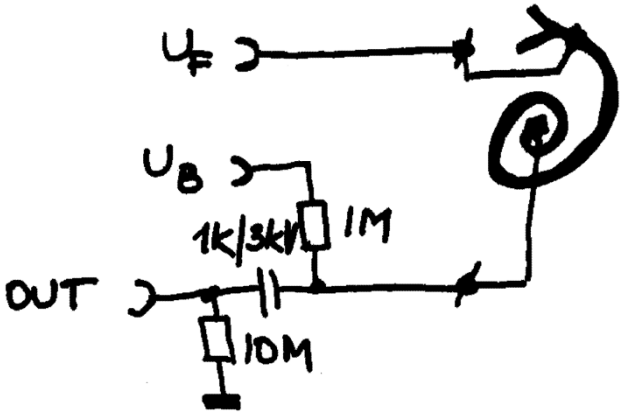

For negative ions – minus pole of HT supply grounded. Positive „attracting“ voltage is created by voltage divider 40MΩ/6.25Ω.

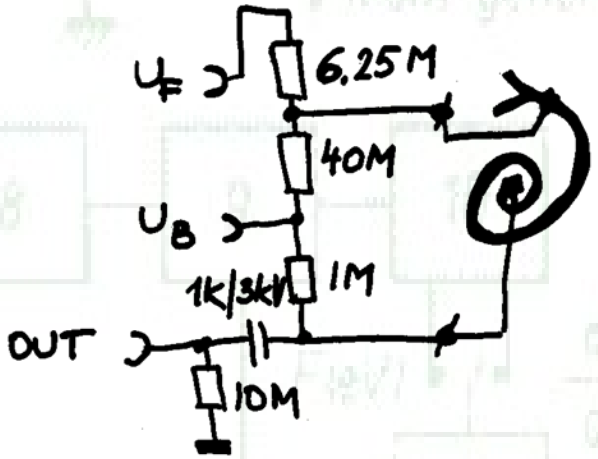

Working resistor approx. 1 MΩ.

Photomultiplier – similar operation, more bulky, more stable.

Detectors for mass-spectrometers

Microchannel plate
Matrix of small straight channeltrons arranged in parallel. Every channel has inner diameter 10-25 μm and length 1-2 mm.

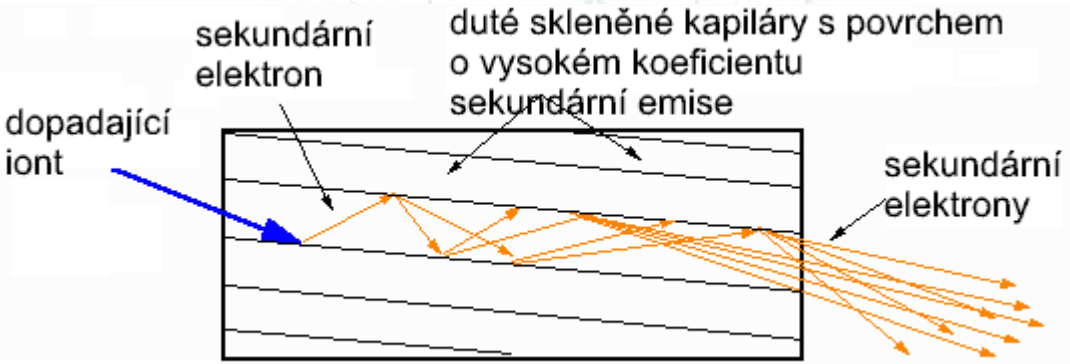

Microchannel plates have usually round shape with diameter several cm.
In order to minimize the effect of ion feedback the microchannel plates are usually in „chevron“ arrangement, i.e. the channeltron axes include obtuse angle. Voltage of a magnitude similar to channeltron is applied between the microchannel plate surfaces.

Application of mass-spectrometers for low-temperature plasma diagnostics

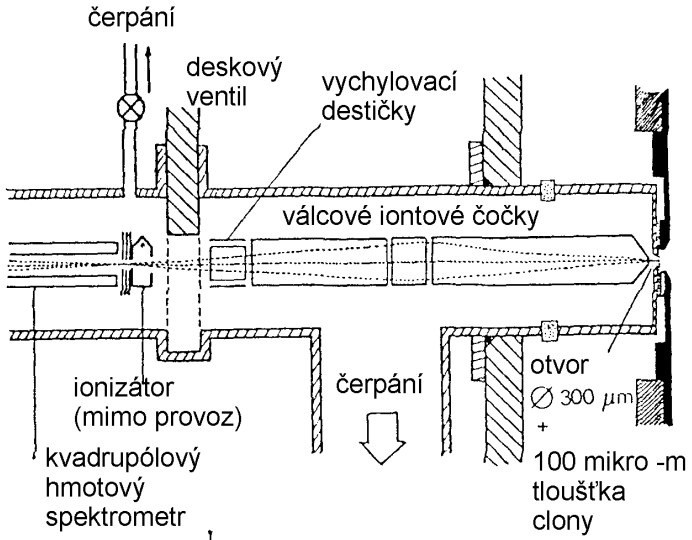

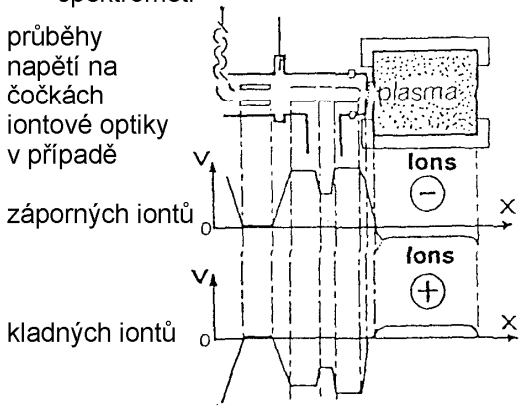

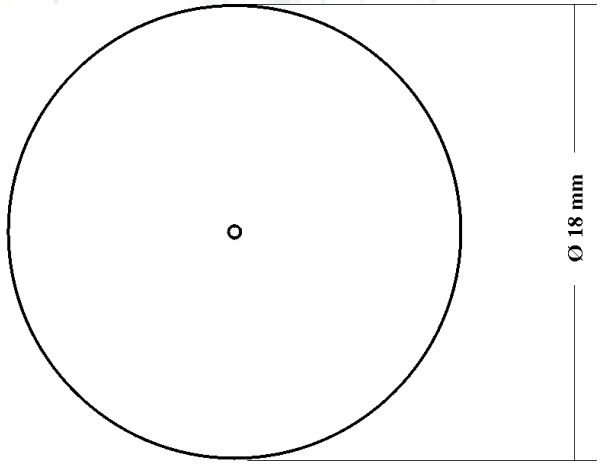

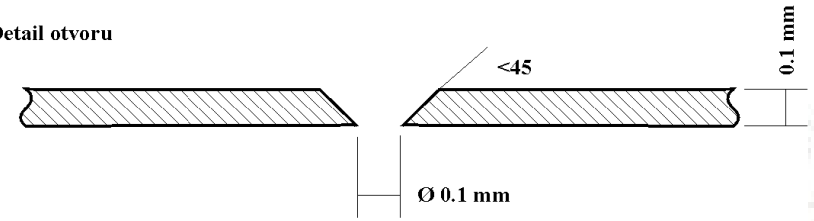

Materiál: molybden

Mass spectra interpretation

Discharge in nitrogen (traces of impurities)

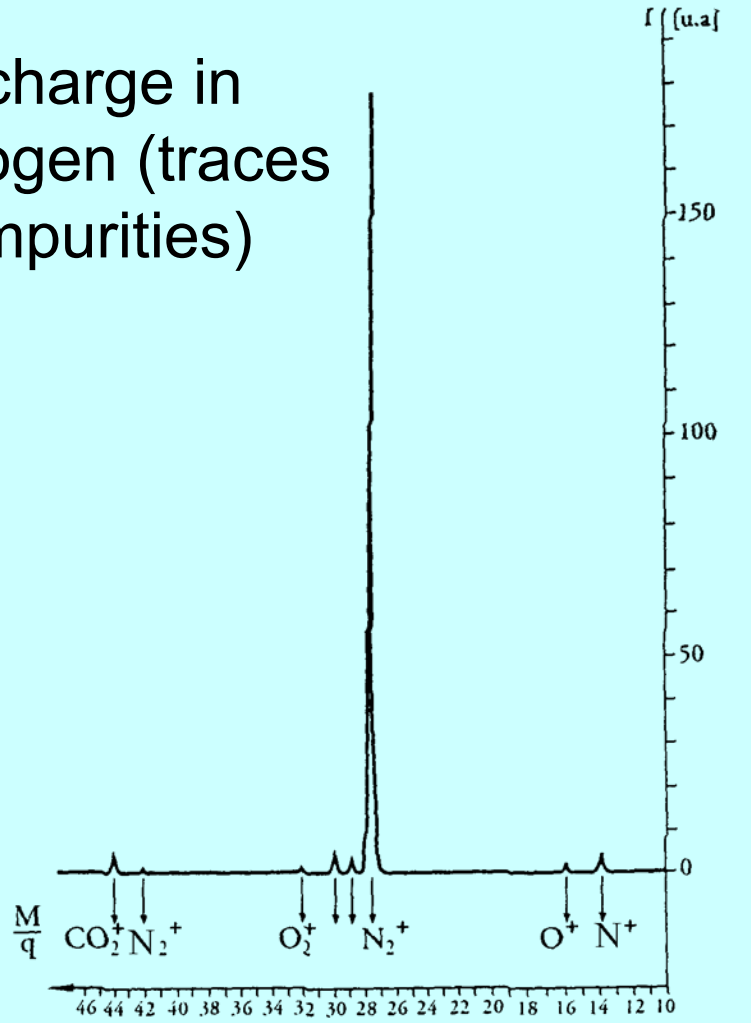

ions	N^+	O^+	N_2^+	O_2^+	Ar^+	N_3^+	$(CO_2)^+$
c_i	1,57%	0,17%	93,5%	0,89%	0,06%	1%	2,79%

Discharge in H_2, He and mixtures of H_2, He with silane (SiH_4)

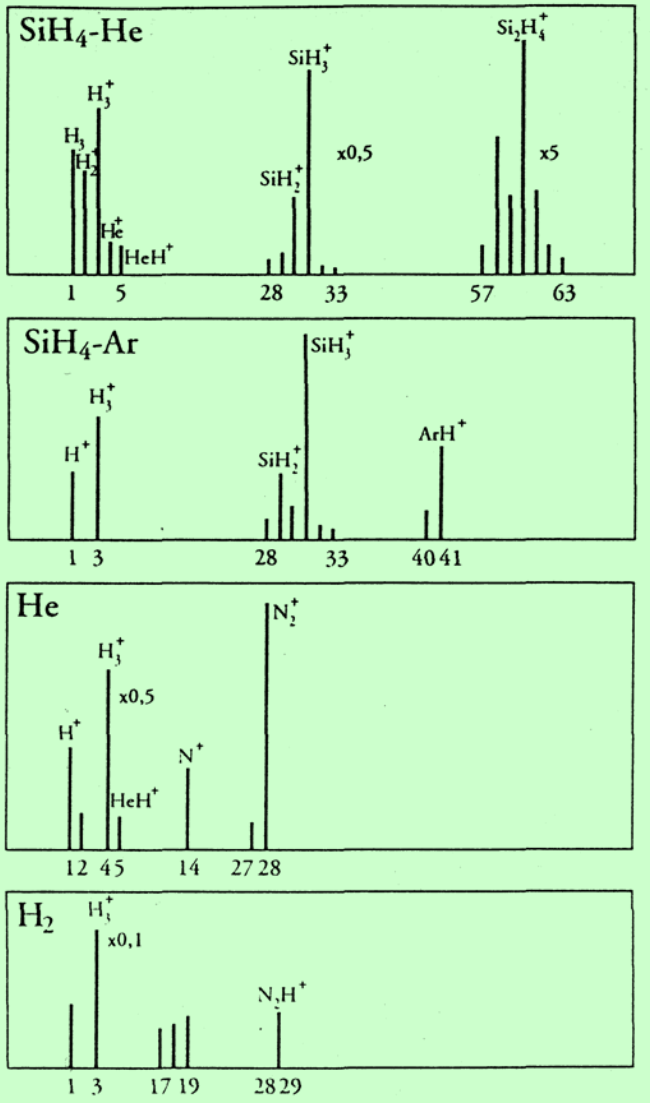

Mass spectra interpretation

Monitoring complex neutral substances
(which would be easily fragmented in the ion source)
by attaching proton or electron:

PTR-MS (proton-transfer reaction mass-spectrometry)
proton donor most often H_3^+

A. Hansel, A. Jordan, R. Holzinger, P. Prazeller, W. Vogel, W. Lindinger, Proton-transfer reaction mass-spectrometry - online trace gas-analysis at the ppb level, International Journal of Mass Spectrometry 149 (1995) 609

EA-MS (electron attachment mass-spectrometry)
uses hot-filament energy-controlled electron source

E. Stoffels, W. W. Stoffels, and K. Tachibana, Electron attachment mass spectrometry as a diagnostics for electronegative gases and plasmas, Rev. Sci. Instrum. 69 (1998) 116.

Conclusion

- At the study of ion-molecule chemical reactions and at optimization of technological processes in low-temperature plasma the mass-spectrometer appears to be indispensable equipment.
- It is advantageous to combine the probe and the mass-spectrometer diagnostics together with other types of diagnostics, e.g. optical emission/absorption spectroscopy, microwave diagnostics, LIF, etc.

Thank you for your attention